ABSTRACT

MOHAN, SIBIN. Exploiting Hardware/Software Interactions for Analyzing Embedded Systems. (Under the direction of Associate Professor Frank Mueller).

Embedded systems are often subject to real-time timing constraints. Such systems require determinism to ensure that task deadlines are met. The knowledge of the bounds on worst-case execution times (WCET) of tasks is a critical piece of information required to achieve this objective.

One limiting factor in designing real-time systems is the *class of processors* that may be used. Contemporary processors with their advanced architectural features, such as out-of-order execution, branch prediction, speculation, and prefetching, cannot be statically analyzed to obtain WCETs for tasks as they introduce non-determinism into task execution, which can only be resolved at run-time. Such micro-processors are tuned to reduce average-case execution times at the expense of predictability. Hence, they do not find use in hard real-time systems. On the other hand, static timing analysis derives bounds on WCETs but requires that *bounds on loop iterations be known statically*, *i.e.*, at compile time. This limits the class of applications that may be analyzed by static timing analysis and, hence, used in a real-time system. Finally, many embedded systems have communication and/or synchronization constructs and need to function on a wide spectrum of hardware devices ranging from small microcontrollers to modern multi-core architectures. Hence, any *single analysis technique (be it static or dynamic) will not suffice* in gauging the true nature of such systems.

This thesis contributes *novel techniques that use combinations of analysis methods and constant interactions between them to tackle complexities in modern embedded systems*. To be more specific, this thesis

(I) introduces of a new paradigm that proposes minor enhancements to modern processor architectures, which, on interaction with software modules, is able to obtain tight, accurate timing analysis results for modern processors;

(II) it shows how the constraint concerning statically bound loops may be relaxed and applied to make dynamic decisions at run-time to achieve power savings;

(III) it represents the temporal behavior of distributed real-time applications as colored graphs coupled with graph reductions/transformations that attempt to capture inherent “meaning” in the application.

To the best of my knowledge, these methods that utilize interactions between different sources of information to analyze modern embedded systems are a first of their kind.

Exploiting Hardware/Software Interactions for Analyzing Embedded Systems

by
Sibin Mohan

A dissertation submitted to the Graduate Faculty of
North Carolina State University
in partial fullfillment of the
requirements for the Degree of
Doctor of Philosophy

Computer Science

Raleigh, North Carolina

2008

APPROVED BY:

Dr. Alex Dean	Dr. Purush Iyer
Dr. Frank Mueller Chair of Advisory Committee	Dr. Tao Xie

DEDICATION

to ammumma, mom, dad and rads

BIOGRAPHY

Sibin Mohan was born on March 20, 1979 to Mrs. T. Shobhana and Mr. B. M. C. Kumar in Kozhikode (Kerala, India), but has lived mostly in the lovely city that is Bangalore. He completed his schooling at the Frank Anthony Public School (FAPS), Bangalore. He received his Bachelor of Engineering (B.E.) undergraduate degree in Computer Science and Engineering from PES Institute of Technology which is a part of Bangalore University, India. He then worked at Hewlett-Packard India Software Operations, Bangalore, as a Software Engineer for one year.

Sibin joined the graduate program in the Dept. of Computer Science at North Carolina State University in Fall 2002 where he has been since, working with Dr. Frank Mueller. He obtained his Masters degree in Computer Science in Fall 2004. Sibin is the recipient of the “Preparing the Professoriate” fellowship from the Graduate School at North Carolina State University. Since Fall 2004 he has been pursuing his Ph.D. in Computer Science at North Carolina State University, mainly in the Systems area.

ACKNOWLEDGMENTS

This dissertation is the culmination of many years of work, all of which have been extremely rewarding. I have been able to reach this goal largely due to the belief, support and wisdom imparted by many people I have had the honour of interacting with over the years. While I try to acknowledge every single one of them, I realize that being only human, I might miss a few names.

To Dr. Frank Mueller, my advisor, I offer sincere thanks and appreciation for having the patience to shepherd me through the journey that was this Ph.D. As the ancient Chinese proverb states, "a journey of a thousand miles begins with a single step." I realize that this Ph.D., that first important step, would not have been possible without his insight, advice, critique and support. His counsel on research methodology, teaching, presentation skills, writing skills, *etc.* have all been instrumental in shaping me as a researcher. His management style, dedication towards research and attention to detail is something that I can only hope to emulate. He has also guided and actively assisted me through the long process of searching for future career opportunities.

Some of the best courses I took during my time at NC State was courtesy of Dr. Matt Stallmann. His courses challenged and excited me at the same time and often made me see the field of Computer Science in a new light. He was also gracious enough to mentor me through the process of navigating my way through my first comprehensive teaching assignment.

Comments and questions raised by Dr. Alex Dean, Dr. Purush Iyer and Dr. Tao Xie helped me focus on important issues and avoid pitfalls during the course of my research. I would like to thank them for being a part of my dissertation committee and guidance provided thus.

Dr. Purush Iyer, Dr. Peng Ning, Dr. Nagiza Samatova and Dr. Tao Xie took time off their busy schedules to examine and provide valuable feedback on my job application materials. I am thankful for their feedback and the knowledge that they imparted during the whole process. I am also grateful to Dr. Becky Rufty for her valuable advice on this and related topics. I would also like to thank Dr. David Whalley and Dr. John Regehr for writing reference letters for me.

I would also like to thank Dr. Eric Rotenberg as many of the ideas in this dissertation would not have come up if not for the deep understanding of computer architecture he instilled in me via his courses. I would also like to thank him for making his architecture simulator and toolset available for use in my research. Aravind Anantaraman and Vimal Reddy were always willing to help me to understand and solve problems related to the simulator framework and for that I am grateful.

Graduate school can never be complete or pleasant without the administration that silently

moves the great machinery in the background. Dr. David Thuente as the Director of Graduate Programs has been very helpful in directing me through the administrative details that go along with being a student. I would also like to thank the Computer Science staff members, Margery Page, Carol Allen, Ginny King and Susan Peaslee, to name but a few.

Not a day goes by that I don't remember, or feel grateful towards, Mr. Vijayan. His teachings on C++, programming paradigms, operating systems, *etc.* coupled with quick philosophical insights often drew parallels with slices of real life. I attempt to emulate his remarkable teaching style every time I step in front of a classroom full of students. I would also like to thank Dr. Krishna Rao and Mr. Joye Joseph whose teaching had a profound effect on me.

Johannes Helander took a chance on a graduate student he met at a conference and has been a mentor and friend ever since. That was the start of a great opportunity for me; an opportunity to work on some really exciting research ideas. Conversations with him range over a diversity of topics, from cutting-edge research ideas to varieties of beer, all of which ensures that every time I talk to him I come back having learned something new.

Jaydeep, Nirmit, Yifan, Kaustubh, Kiran, Anita, Harini, Anubhav, Nik, Ravi, Chao, Arun, Vivek, Raghuveer and Heshan have all been great lab-mates over the years. Interactions with them resulted in my learning a great deal and often made me look forward to coming in to work every day. I would also like to thank my various room-mates (Salil, Ajit, Rahul, Ishdeep, Sharath) who have had to put up with me and my cooking over the years!

No person is complete without his friends and I consider myself lucky to have some amazing people as close friends. Nisha, whose thought processes resemble mine in uncanny ways, provides a mirror to the inner workings of my mind. I consider myself lucky to have her alongside as one of my closest friends, right from our childhood days. Ayush, Biju, Chatt, Cherry, David, Ramesh and Palani ensured that school and everything else that followed was memorable. Meeting and/or talking to them is still something I eagerly look forward to. Cohan, always has the ability to surprise me, albeit in a pleasant way. He is brimming with ideas that he loves to share, is extremely helpful and is one of the nicest, smartest and best read people I have come across. Mrin, Sudheer, Chinmoyee and their family ensured that I never missed home and were always ready to welcome me into their family moments. Hema, a very dear friend, was the first person to take the effort to instruct me on the meaning of my own name. She is a terrific companion for attending concerts, reminiscing about bygone days, you name it. Folks that I met while working in various voluntary organizations on campus have also helped me achieve a well-rounded outlook on life.

To Cup-A-Joe, without which I might have graduated sooner, albeit a little poorer as a

human being. Discussions, debates, encouragement, queries, plans, dreams, all originating from a close circle of friends that used to meet there often helped ground me on some very basic realities in everyday life and provided a valuable sounding board for my thoughts and ideas. Salil, Sarat, Meeta, DC, SK, Milind, Ajit, Nik and Sally have, over the years, been instrumental in ensuring that I keep my sanity intact and helped pass many afternoons and evenings in an enjoyable manner.

I would also like to thank Dr. Appaji Gowda for being, literally, a life-saver. I would not be here today, doing what I am, without him.

My family. At some point or the other, I have been the recipient of love, guidance and aid from every one who is a part of it. To name but a few, Bindu, Vasu and their family, Deepa, Sashi and their family, Shyju, Sreekala, Raju and their families have all been most supportive through the various ups and downs in my life. Dinesh was the brother that I never had, and then lost.

To Rupa, her parents Usha and K.S. Venkatagiri, and Manu, I have the utmost love, respect and admiration. They welcomed me into their family and treat me as one of their own.

If I have the confidence to move forward in life, it is due to the unwavering support and dedication of my parents. They are the backbone to my flesh. Their trust, confidence and love have always been showered upon me. They believed in me when the chips were down and helped me stand up again. They completely back every decision I make, no matter how risky. They always tried to make my life better while making sacrifices in their own. I hope that they can truly believe that their efforts and labour have been fruitful.

My grandmother, Padmavathy Amma, was one of the most important people in my life. She raised me from when I was born, catered to my every whim, and instilled in me values that constitute the core of what I am today. She molded my belief system, my thinking abilities, my interactions with other people, and even instilled culture and ethics in me. I hope that she is watching over me and will be happy with what I have achieved so far.

If my grandmother nurtured me during the early part of my life, then my wife, Radha, is the person that seems to have taken over the mantle to back me the rest of the way. She is the most caring, loving and thoughtful person that I have ever met. I cannot be thankful enough that she agreed to be my wife. My fondest memory at NC State has been meeting her and getting married to her. Time spent with her is simply put, joyous. I can have an intelligent conversation with her on any topic under the sun. Her superb ability to play the part of the devil's advocate on any topic, technical or not, has helped me understand, rethink and shape many of my decisions and beliefs. I am glad that she has infinite patience that allows her to put up with my idiosyncrasies. She is the muse to my flights of fancy and inspiration for the ideas that make it to the real world.

TABLE OF CONTENTS

LIST OF TABLES ..... **xi**

LIST OF FIGURES ..... **xii**

1 Introduction **1**
- 1.1 Real-Time Systems 1
- 1.2 Worst-Case Execution Time (WCET) 2
- 1.3 Timing Analysis 2
- 1.4 Tackling the Complexity of Contemporary Processors 4
  - 1.4.1 CheckerMode 4
- 1.5 Relaxing Constraints on Embedded Software 5
  - 1.5.1 ParaScale 6
- 1.6 Analysis of Distributed Embedded Systems 7
- 1.7 Organization 7
- 1.8 Hypothesis 8

2 *CheckerMode* – Tackling the Complexity of Modern Processors **9**
- 2.1 Summary 9
- 2.2 Introduction 9
  - 2.2.1 Plausibility of the approach 11
  - 2.2.2 Processor Vendor Limitations 11
  - 2.2.3 Assumptions 12
  - 2.2.4 Organization 12
- 2.3 CheckerMode 12
  - 2.3.1 Processor Enhancements 14
  - 2.3.2 Software Overview 16
  - 2.3.3 Driver/Analysis Controller and Tuning 16
  - 2.3.4 False Path Identification and Handling 17
  - 2.3.5 Loop Analysis Overhead 17
  - 2.3.6 Input Dependencies 17
  - 2.3.7 Analysis Overhead 18
- 2.4 Experimental Framework 18
- 2.5 Results 20
  - 2.5.1 C-Lab Benchmark Results 21
- 2.6 Conclusion 23

3 Merging State and Preserving Timing Anomalies in Pipelines of High-End Processors 24
3.1 Summary . . . 24
3.2 Introduction . . . 24
3.3 Snapshots . . . 25
3.4 Analysis Model . . . 26
3.5 Snapshot Capture using Pipeline Drain-Retire (DR) Technique . . . 27
3.6 Capturing Structural and Data Dependencies using Reservation Stations . . . 28
3.6.1 Structural Dependencies . . . 28
3.6.2 Data Dependencies . . . 30
3.7 Snapshot Usage . . . 31
3.8 Merging Pipeline Snapshots . . . 33
3.8.1 Merging Two Snapshots . . . 33
3.8.2 Incorrect Merge Technique . . . 35
3.8.3 Merging Reservation Stations . . . 36
3.8.4 Merge for More than Two Snapshots . . . 37
3.9 Proof of Correctness . . . 38
3.10 Merging Register Files . . . 45
3.11 Implementation . . . 46
3.12 Conclusion . . . 46

4 Fixed Point Loop Analysis for High-End Embedded Processors . . . 48
4.1 Summary . . . 48
4.2 Introduction . . . 48
4.3 Reduction of Analysis Overhead for Loops . . . 49
4.3.1 Fixed Point Timing and Out-of-order Execution . . . 49
4.3.2 Fixed point Pipeline State Analysis using Reservation Stations . . . 52
4.4 Experimental Framework . . . 55
4.5 Time Dimension Analysis Results . . . 56
4.5.1 Partial Analysis of Loops . . . 56
4.5.2 CLab Benchmarks: SRT benchmark . . . 57
4.5.3 Composing longer benchmark paths using loop WCEC bounds . . . 61
4.5.4 Other CLab Benchmark results . . . 63
4.6 Pipeline State Analysis Results . . . 64
4.7 Conclusion . . . 65

5 Parametric Timing Analysis and Its Application to Dynamic Voltage Scaling . . . 66
5.1 Summary . . . 66
5.2 Introduction . . . 66
5.3 Numeric Timing Analysis . . . 69
5.4 Parametric Timing Analysis . . . 70
5.5 Creation and Timing Analysis of Functions that evaluate Parametric Expressions . 77
5.6 Using Parametric Expressions . . . 79
5.7 Framework . . . 80
5.8 Experiments and Results . . . 84
5.8.1 Overall Analysis . . . 87

5.8.2 Leakage/Static Power 88
5.8.3 WCET/PET Ratio, Utilization Changes and Other Trends 90
5.8.4 Comparison of ParaScale-G with Static DVS and Lookahead 92
5.8.5 Overheads 94
5.9 Conclusion 95

6 Temporal Analysis for Adapting Concurrent Applications to Embedded Systems 96
6.1 Summary 96
6.2 Introduction 97
6.2.1 Awareness of Hardware Capabilities 97
6.2.2 Model-based Development 98
6.2.3 Limitations of Analysis Techniques 99
6.2.4 Contributions 99
6.3 Saving Memory through Sequential Execution 101
6.3.1 Futures 102
6.4 The Timing Graph 103
6.4.1 Representation of the Timing Graph 103
6.4.2 Graph Invariants 105
6.5 Information Sources and Graph Creation 106
6.5.1 Information Gathering Techniques 106
6.5.2 Graph Creation 108
6.6 Timing Graph Transformations 109
6.6.1 Assumptions 110
6.6.2 Graph Pruning and Reduction 110
6.7 Outcome of Timing Graph Transformations 114
6.7.1 Futures and Program Modifications 116
6.7.2 False Parallelism and Hot Spots 117
6.8 Experimental Framework 118
6.9 Results 120
6.9.1 Graph Results 120
6.9.2 Temporal Timing Analyzer Results 121
6.10 Conclusion 122

7 Related Work 124
7.1 WCET Requirements 124
7.2 Static Timing Analysis 125
7.3 Dynamic and Stochastic Timing Analysis 127
7.4 Timing Anomalies 127
7.5 CheckerMode Related Work (Hybrid Techniques) 129
7.6 ParaScale Related Work 131
7.7 Temporal Timing Analysis Related Work 133

8 Future Work **135**
8.1 CheckerMode Future Work 135
8.2 ParaScale Future Work 136
8.3 Future Work for Analysis of Distributed Embedded Systems 137
8.4 Combination of Hardware and Software Analysis Techniques 137

9 Conclusion **139**
9.1 Analysis Techniques for Modern Processors 139
9.2 Reducing Constraints on Embedded Software 140
9.3 Analysis of Distributed Embedded Systems 141
9.4 Correctness of the Dissertation Hypothesis 142

Bibliography **143**

LIST OF TABLES

Table 2.1 C-Lab Benchmarks 19

Table 2.2 Averaged WCECs for C-Lab Benchmarks 21

Table 2.3 Path-Aggregate Cycles (3 Iterations) for the Synthetic Benchmark 22

Table 4.1 Path-Aggregate Cycles (3 Iterations) 56

Table 4.2 Path-Aggregate Cycles (2 Iterations) for the bubblesort function of SRT. 58

Table 4.3 Path-Aggregate Cycles (3 Iterations) for the bubblesort function of SRT. 59

Table 4.4 Loop WCEC formulae for loops in SRT benchmark 60

Table 4.5 Loop WCEC formulae for loops in ADPCM benchmark 61

Table 4.6 Path-Aggregate Cycles (2 Iterations) for the FFT benchmark 62

Table 4.7 Path-Aggregate Cycles (3 Iterations) for the FFT benchmark 63

Table 4.8 “long” Synthetic benchmark 64

Table 4.9 “short” Synthetic benchmark 64

Table 5.1 Instruction Categories for WCET 69

Table 5.2 Examples of Parametric Timing Analysis 75

Table 5.3 WCECs for inter-task and intra-task schedulers for various DVS algorithms. 82

Table 5.4 Task Sets of C-Lab Benchmarks and WCETs (at 1 GHz) 83

Table 5.5 Parameters Varied in Experiments 84

Table 5.6 Periods for Task Sets 84

Table 6.1 Graph edges based on static/dynamic information 121

LIST OF FIGURES

Figure 1.1 Static and dynamic analysis compared to actual execution time . . . 3

Figure 2.1 CheckerMode in Action . . . 14

Figure 2.2 CheckerMode Design . . . 15

Figure 2.3 Control Flow Graph of Toy Benchmark and Measured Cycles . . . 19

Figure 2.4 Measured Cycles (Aggregate Technique) for Synthetic Benchmark . . . 20

Figure 2.5 Timing Results for the ADPCM Benchmark . . . 21

Figure 2.6 Measured execution cycles for C-Lab Benchmarks . . . 22

Figure 3.1 Model used for description and capture of Snapshots . . . 27

Figure 3.2 Snapshot Captured using the DR Technique . . . 28

Figure 3.3 Definition of a Snapshot, based on the “Drain-Retire” mechanism . . . 29

Figure 3.4 Mechanism to Capture/Handle Structural Hazards . . . 30

Figure 3.5 Snapshot Merge Algorithm (DRM) . . . 34

Figure 3.6 Merging using the DRM Algorithm . . . 35

Figure 3.7 Incorrect Merge . . . 36

Figure 3.8 Merging Reservation Stations . . . 37

Figure 3.9 Merge for Multiple Snapshots . . . 37

Figure 3.10 Anomaly Effects on Merge . . . 38

Figure 3.11 Case 1 (a) (i) t'_k is greater than $t^R_{\{i\}}$ . . . 40

Figure 3.12 Case 1 (a) (ii) t'_k is less than $t^R_{\{i\}}$ . . . 40

Figure 3.13 Case 2 (a) (i) t'_k is less than $t^R_{\{i\}}$ . . . 41

Figure 3.14 Case 2 (a) (ii) t'_k is greater than $t^R_{\{i\}}$ . . . 42

Figure 3.15 Case 3 (a) neither t'_k nor $t^R_{\{i\}}$ change 42

Figure 4.1 Counter example against use of only fixed point timing 50

Figure 4.2 Execution of counter example through the pipeline 50

Figure 4.3 A Second Fixed Point 53

Figure 4.4 Alternative Execution Scenario for counter example 54

Figure 4.5 Synthetic Benchmark for Analyzing Stable state of Reservation Stations 55

Figure 4.6 CFG 56

Figure 4.7 Measured execution cycles for loop path compositions (SRT *bubblesort* function) 57

Figure 4.8 Complete execution cycles for C-Lab Benchmarks – including loop WCECs 61

Figure 4.9 δ's for two and three level compositions for nine loops in ADPCM benchmark ... 62

Figure 5.1 Static Timing Analysis Framework 69

Figure 5.2 Numeric Loop Analysis Algorithm 70

Figure 5.3 Use of Parametric Timing Analysis 71

Figure 5.4 Parametric Loop Analysis Algorithm 71

Figure 5.5 Syntactic and Semantic specifications for constraints on analyzable loops. 73

Figure 5.6 Example of an outer loop with multiple paths 74

Figure 5.7 WCET Bounds as a Function of the Number of Iterations 76

Figure 5.8 Flow of Parametric Timing Analysis 77

Figure 5.9 Example of using Parametric Timing Predictions 78

Figure 5.10 Experimental Framework 81

Figure 5.11 Energy consumption for PCG Wattch Model – Dynamic Energy consumption 87

Figure 5.12 PCGL-W – Leakage Consumption from the Wattch Model 88

Figure 5.13 PCGL – Leakage Consumption from the Wattch Model 89

Figure 5.14 Energy Consumption Trends for increasing WCET Factors for ParaScale-G 91

Figure 5.15 Comparison of Dynamic Energy Consumption for ParaScale-G and Lookahead . . 93

Figure 6.1 Edges and Nodes in the Timing graph 104

Figure 6.2 Synchronization constructs 105

Figure 6.3 Deadlocks in Timing Graphs 105

Figure 6.4 Sample code to illustrate creation of the Timing Graph 106

Figure 6.5 Timing graph created by application of various information gathering techniques . 108

Figure 6.6 Two Point-of-View Simplifications 111

Figure 6.7 Remove direct red edges 112

Figure 6.8 Move outgoing red edges to successor 113

Figure 6.9 Move incoming red edges to predecessor 114

Figure 6.10 Outcome of graph transformations 115

Figure 6.11 Multiple producer-consumers 115

Figure 6.12 Converting Blue edges to Red – creating futures 116

Figure 6.13 Options for the Future 117

Chapter 1

Introduction

Every year, *billions* of microprocessors are sold for use in embedded systems [120]. This is in sharp contrast to a few hundred million desktop processors that are sold in the same time-frame. From automobiles to medical equipment, thermostats to space shuttles, embedded systems are all around us. Moreover, the use of embedded systems is increasing, if anything, with the advent of "*Cyber-Physical Systems*" (CPS), which can be described as "*integrations of computation with physical processes*." Hence, cyber-physical systems affect and are affected by the physical world and the environment that they operate in. The modern automobile and even *smart homes* fall into this category. They are typically comprised of networks and combinations of smaller embedded systems that perform specific tasks.

1.1 Real-Time Systems

The software and hardware used for embedded and cyber-physical systems, in general, must be validated, which traditionally amounts to checking the correctness of the input/output relationship. Many such systems also impose timing constraints on the execution times of constituent tasks. Violations of these constraints (often referred to as "*deadlines*") could lead to fallouts that are dangerous to users, the environment or both. Such systems are commonly referred to as "*real-time systems*", and they impose temporal constraints on computational tasks to ensure that results are available on time. Often, approximate results supplied in time are preferred to more precise results that may become available late, *i.e.*, after the passage of deadlines.

Consider the case of the Anti-lock Braking System (ABS) [135] found in most modern automobiles. It consists of a rotating road wheel that prevents a locked wheel or a "*skid*" under

heavy braking. The driver is able to maintain control by the ABS as it allows the wheel to roll forward. In fact, recent versions not only perform the ABS functionality but also Electronic Brakeforce Distribution (EBD), Traction Control System (TCS), Electronic Stability Control (ESC), *etc.*. The ABS system is a classic example of a *real-time, embedded system* that we encounter in everyday life. If a driver must hit the brakes of a car in an emergency, then the ABS must kick in and function *correctly* in the *milliseconds (perhaps even microseconds) time-frame*. It is absolutely useless if it functions correctly, say *ten seconds* after the brakes have been pressed – in fact, a failure to operate in the short, required duration might result in a loss of human life and/or damage to property. Nuclear reactor controls, electronic engines, modern avionics – all of these applications fall under the purview of real-time systems and have stringent design criteria. They require advance knowledge of the properties of and guarantees on the behavior of the system, the most critical of which is that *no task in the system misses its deadline.*

1.2 Worst-Case Execution Time (WCET)

Schedulability analysis [77] is used to guarantee that a given system of real-time tasks will be able to meet its deadlines on a particular hardware system. One critical piece of information required for such analysis is the "**worst-case execution time**" (WCET) of each task, which is defined as

> "the *guaranteed* worst-case time taken by the task to execute on a *specific* hardware platform."

The process of determining the WCET of a task is known as "*timing analysis*" and is often characterized as being either *(a) static* timing analysis or *(b) dynamic* timing analysis.

1.3 Timing Analysis

Timing analysis has become an increasingly popular research topic. This can be attributed in part to the problem of increasing architectural complexity, which makes applications less predictable in terms of their timing behavior, but it may also be due to the abundance of embedded systems that we have recently seen. Often, application areas of embedded systems impose stringent timing constraints, and system developers are becoming aware of a need for verified bounds on execution times. The *tighter* these bounds relative to the true worst-case times, the greater the value of

the analysis. Of course, even a tight bound has to be a *safe bound* in that it must not underestimate the true WCET; it may only match or exceed it.

Static timing analysis [14, 15, 26, 27, 34, 36, 49, 52, 53, 59, 73, 74, 82, 84, 89, 94, 97, 103, 119, 126, 133] techniques suffer from the drawback that they are either overly pessimistic or impose severe constraints on the types of code that may be analyzed (*e.g.*, known upper bounds on loops, absence of function pointers and no heap allocation). If such an analysis is pessimistic, as shown in Figure 1.1, then system resources may be wasted. Bounds on execution times require constraints to be imposed on the tasks (timed code), the most striking of which is the requirement to statically bound the number of iterations of loops within the task. Complex architectural features, such as out-of-order (OOO) processing [96] and branch prediction [113], are often beyond the reach of static analyses, mainly due to the fact that they introduce non-determinism into the task code. These issues cannot be resolved at compile time, thus forcing real-time system designers to completely avoid the use of such processors.

Dynamic timing analysis methods [14, 15, 19, 119, 125, 127], on the other hand, are either trace-driven, experimental or stochastic in nature. They are unable to guarantee the safety of WCET values obtained [126]. Architectural complexities, difficulties in determining worst-case input sets and the exponential complexity of performing exhaustive testing over all possible inputs are also reasons why dynamic timing analysis methods are unsafe and, hence, infeasible in general. The threat of dynamic methods is that the execution time of tasks might actually be *underestimated* (as shown in Figure 1.1), which can result in serious errors during system operation, implying potentially dangerous fallouts.

The objective of any timing analysis technique is to approximate the worst-case *actual* execution time of a task, *i.e.*, the longest possible execution time considering all inputs and hardware complexities, deterministic or not. The more closely this value is approximated, the easier it is to design the system in an accurate, safe and efficient manner in terms of resource usage. Determination of the WCET bounds of a task is a non-trivial process due to a variety of reasons, broadly classified into:

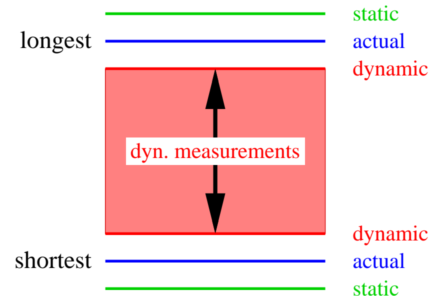

Figure 1.1: Static and dynamic analysis compared to actual execution time

1. **hardware complexities**: non-determinism of modern architectural features, process variations during the manufacturing of microprocessors, *etc.*; and

2. **software complexities**: non-determinism of inputs, complexity of task code, *etc.*

This work addresses these shortcomings on both fronts – *hardware* as well as *software*. Section 1.4 briefly discusses novel techniques to tackle hardware and architectural complexity while Section 1.5 introduces techniques to relax constraints imposed on task code. Section 1.6 introduces techniques aimed at analyzing complex embedded software – containing multiple threads that could potentially be *distributed* in nature. It also demonstrates applications where timing analysis techniques could be utilized to analyze complex systems. All of these techniques utilize the interactions and passing of information between hardware and software to increase the accuracy of the analysis. The main idea is that a single source of information (such as only static or only dynamic analysis methods) is not sufficient for analyzing modern embedded systems that are inherently complex. **Thus, novel methods that utilize information from multiple sources is required for a more complete analysis.**

1.4 Tackling the Complexity of Contemporary Processors

A serious handicap in performing static timing analysis is the complexity of modern processors and their functional units. Various features that decrease *average* execution times for tasks are often detrimental for worst-case timing analysis. Out of order (OOO) processing [96] and branch prediction [113] are two important features in modern processors that introduce non-determinism to task execution, which cannot be resolved at compile time [12, 23, 35]. Other issues that increases the complexity of the analysis are the presence of *statically indeterminate loops* in task code and *timing anomalies* [13, 79, 81, 109]. Hence, designers of real-time systems are often forced to use less complicated, older and inherently less powerful processors. While this guarantees determinism, it neglects performance. The following section (1.4.1) introduces the concept of "*hybrid*" timing analysis that utilizes interactions between a software timing analyzer and run-time information from the actual microprocessor to obtain tight WCET estimates on contemporary processors.

1.4.1 CheckerMode

The task of obtaining accurate timing analysis results for modern, out-of-order processors is achieved by the use of the *CheckerMode* infrastructure. Minor enhancements to the micro-architecture of future processors are proposed. These will aid in the processes of obtaining tight WCET bounds. A "checker mode" is added to processors that will, on demand, capture varying

details as checkpoints of the processor state, also called “snapshots”. This information is then communicated to a software module. The software module stores the various checkpoints (“snapshots”) and also drives the execution of the processors along statically determined paths to capture accurate timing information for each of them. The checkpoints are used to track back along the various execution paths and to restart along a different path if necessary. The execution times obtained for each of the paths is analyzed and combined by the software driver to calculate an accurate WCET for the entire module/program.

Decisions on where to obtain snapshots, the details required for a snapshot, *etc.* are made by the software driver. The timing results for each straight-line path are fed back to the software module. The software module, similar to a static (numeric) timing analyzer, then combines the timing results for individual paths to obtain a bound on WCET for the entire task. The cache states, the state of the branch predictor, the pipeline, *etc.*, for each of the paths, are also considered while performing these calculations. To time an alternate path, the information from the previous checkpoint is then restored onto the processor function units to reflect the state of the system when the choice between the paths was made.

The ability to capture these snapshots is **disabled** during normal execution, so as to not interfere with regular program execution. The approach is evaluated by implementing additional micro-architectural functionality (the ability to capture snapshots, to restore a previous snapshot on to the processor function units and to obtain accurate timing results for parts of the program) on a customized SimpleScalar [22] framework that is configured in a manner similar to modern processor pipelines. Techniques to reduce the complexity of analysis for loops to ensure that the analysis overhead is independent of the number of loop iterations are also introduced. The ability of this analysis to correctly account for “timing anomalies” that could occur during out-of-order execution is also shown. To the best of my knowledge, this method of using a hardware/software co-design technique to obtain accurate WCETs for modern out-of-order processors is a first of its kind.

1.5 Relaxing Constraints on Embedded Software

The requirement for static knowledge of loop bounds addresses the halting problem, *i.e.*, without these loop bounds, WCET bounds cannot be derived. The programmer must provide these upper bounds on loop iterations when they cannot be inferred by program analysis. Hence, these statically fixed loop bounds may present an inconvenience. They also restrict the class of programs

that can be used in real-time systems. This type of timing analysis is referred to as *numeric* timing analysis [49, 52, 53, 94, 132, 133] since it results in a single numeric value for WCET given the upper bounds on loop iterations. The constraint on the known maximum number of loop iterations is removed by *parametric* timing analysis (PTA) [124], which is used in the *ParaScale* infrastructure, introduced in Section 1.5.1.

1.5.1 ParaScale

Parametric timing analysis permits variable-length loops. Loops may be bounded by n iterations as long as n is known prior to loop entry during execution. Such a relaxation widens the scope of analyzable programs considerably and facilitates code reuse for embedded/real-time applications. This work describes (a) the application of static timing analysis techniques to dynamic scheduling problems and (b) assesses the benefits of PTA for dynamic voltage scaling (DVS). This work contributes a novel technique that allows PTA to interact with a dynamic scheduler while discovering actual loop bounds during execution prior to loop entry. At loop entry, a tighter bound on the WCET can be calculated on-the-fly, which may then trigger scheduling decisions synchronous with the execution of the task.

The benefits of using PTA to analyze code sections is evaluated by measuring power savings in the system. Power savings are typically achieved by means of dynamic voltage scaling (DVS) or dynamic frequency scaling (DFS) techniques. The *ParaScale* infrastructure utilizes a combination of inter, and intra-task DVS techniques to achieve power savings. ParaScale uses the results of PTA by using parametric formulae, evaluated at run-time, to make dynamic decisions on the amount of execution completed, amount of slack left, and frequency/voltage scaling to reduce power consumption. An intra-task scheduler is used for this purpose. Hence, ParaScale provides the ability to evaluate the benefits of PTA on a system.

The ParaScale approach utilizes online intra-task DVS to exploit parametric execution times resulting in much lower power consumptions, *i.e.*, even without any scheduler-assisted DVS schemes. Hence, even in the absence of dynamic priority scheduling, significant power savings may be achieved, *e.g.*, in the case of cyclic executives or fixed-priority policies, such as rate-monotone schedulers [76]. Overall, parametric timing analysis expands the class of applications for real-time systems to include programs with dynamic loop bounds that are loop invariant while retaining tight WCET bounds and uncovering additional slack in the schedule.

1.6 Analysis of Distributed Embedded Systems

Cyber-physical systems operate on a variety of embedded hardware ranging from 8-bit microcontrollers to sophisticated multicores. Knowledge of the temporal behavior of an application is hidden inside the application logic, where it is extremely difficult to extract, analyze and model for any given hardware. While static and dynamic timing analyses are used to obtain the worst-case execution times (WCETs) for real-time applications, they may not be able to provide a complete picture of a program. This is particularly true in the case of larger, more complex programs. Programs that contain function pointers are typically out of reach of static analyzers. Dynamic analyzers are unable to gauge the true nature of the program and have shown to be unsafe – *i.e.*, they may underestimate the WCET of the program, which could lead to dangerous effects. If the application uses concurrency constructs, such as signals, locks or mutexes, then neither of these techniques can fully analyze the application.

The work presented here studies the use of combinations of a variety of techniques to form the complete picture of the structure and execution characteristics of a distributed embedded application. The results obtained are collected to create *timing graphs*, the topology of which can be studied to extract *meaning* about the application. This information can then be used to

- provide information to the designers of the system to be used to identify problematic areas in the application and to
- tailor the amount of parallelism in the system so that the same application can execute on small embedded microcontrollers as well as large, modern multicore processors.

1.7 Organization

The remainder of this dissertation is loosely split into three parts:

1. **CheckerMode**: Chapter 2 describes the overall design for the CheckerMode framework to tackle the complexities of modern architectures (first published at RTAS 2008 [86]). Chapter 3 contains the analysis of how the CheckerMode framework is able to handle timing anomalies that occur during OOO execution (*accepted* for publication at RTSS 2008 [87]). Chapter 4 explains the analysis techniques that are able to accurately analyze statically indeterminate loops without enumerating all iterations.

2. **ParaScale**: Chapter 5 describes the ParaScale infrastructure used to relax constraints on embedded software, the results from which are used to attain power savings (published in RTSS 2005 [89] and the TECS journal [88]).

3. **Distributed Embedded Systems**: Chapter 6 discusses techniques used to analyze distributed embedded systems (published in ECRTS 2008 [85]).

Chapter 7 presents the related work. Chapter 8 presents ideas for future work while Chapter 9 presents the conclusion.

1.8 Hypothesis

Modern embedded systems with timing constraints are too complex to be analyzed by any single technique alone due to the non-determinism introduced by hardware features as well as complexities in software. Hence, the hypothesis of this dissertation is that

> *by employing a combination of multiple analysis techniques, multiple sources of information and constant interactions between hardware and software it becomes feasible to gauge the worst-case behavior of modern embedded systems that utilize contemporary processors and complex software constructs.*

The analysis presented is constrained to

1. analyzing *out-of-order processor pipelines*, correct handling of *timing anomalies* and *loops* around them; to

2. providing power savings by removing constraints that enforce *statically determinate loop bounds*; and to

3. reason about *distributed real-time embedded systems* that have basic *communication and synchronization constructs*.

Chapter 2

CheckerMode – Tackling the Complexity of Modern Processors

2.1 Summary

A limiting factor for designing real-time systems is the class of processors that can be used. Typically, modern, complex processor pipelines cannot be used in real-time systems design. Contemporary processors with their advanced architectural features, such as out-of-order execution, branch prediction, speculation, prefetching, *etc.*, cannot be statically analyzed to obtain **tight** WCET bounds for tasks. This is caused by the non-determinism of these features, which surfaces in full only at runtime. This chapter introduces a new paradigm to perform timing analysis of tasks for real-time systems running on modern processor architectures. Minor enhancements to the processor architecture are proposed to enable this process. These features, on interaction with software modules, are able to obtain tight, accurate timing analysis results for modern processors.

2.2 Introduction

Static timing analysis [15, 27, 34, 59, 84, 89, 94, 103, 119] provides bounds on the WCET of tasks. The *tighter* that these bounds are relative to the actual worst-case times, the greater the value of the analysis. Of course, even tight bounds must be *safe* in that the true WCET must *never* be underestimated; the WCET bound may at most match or otherwise overestimate the true WCET.

A serious handicap in performing static timing analysis is the complexity of modern processors and their functional units. Various features that decrease *average* execution times for tasks

are often detrimental for worst-case timing analysis. Out of order (OOO) processing [96] and branch prediction [113] are two important features in modern processors that introduce non-determinism to task execution, which cannot be resolved at compile time [12, 23, 35]. Hence, designers of real-time systems are often forced to use less complicated, older and inherently less powerful processors. In this chapter, techniques to bridge this gap by means of the *CheckerMode* infrastructure are presented. CheckerMode combines the best features of both, static and dynamic analysis, to create a novel hybrid mechanism for WCET analysis.

Minor enhancements to the micro-architecture of future processors are presented that will aid in the process of obtaining accurate WCET bounds. A "checker mode" is added to processors that will, on demand, capture varying levels of information as "*snapshots*" of the processor state. This information is communicated to a software module that stores the various snapshots and also drives the execution of instructions in the processor along statically determined paths. Accurate timing information for each path is then captured. These snapshots are also used to backtrack to an earlier state and then restart along a different path. Execution times obtained for each path are analyzed and then combined by the software driver to calculate an accurate WCET for the entire program/function.

Decisions on where to obtain snapshots, the level of detail required for each snapshot, *etc.* are made by the software controller ("driver"). Timing results for each straight-line path are then fed back to the software module. The software module (similar to a static/numeric timing analyzer), then combines the timing results for individual paths to obtain a bound on WCET for the entire task. The cache states, the state of the branch predictor, the pipeline, *etc.*, for each of the paths, are also considered while performing these calculations. To time an alternate path, the information from the previous snapshot is restored onto the processor function units to reflect the state of the system when the choice between the paths was made.

The ability to capture these snapshots is disabled during normal execution, so as to not interfere with regular program execution. The approach is evaluated by implementing additional micro-architectural functionality (the ability to capture snapshots, to restore a previous snapshot on to the processor function units and the ability to obtain accurate timing results for parts of the program) on a customized SimpleScalar [22] framework that is configured in a manner similar to modern processor pipelines.

To the best of my knowledge, this method of using a hardware/software co-design technique to obtain accurate WCETs for modern out-of-order processors is a first of its kind.

2.2.1 Plausibility of the approach

The proposed hardware enhancements are realistic. The support for speculative execution due to dynamic branch prediction, precise exception handling and precise hardware monitoring, and even most of the internal buffers required by the CheckerMode design already exist in modern high-end embedded processors. For example, the ARM-11 features out-of-order execution, dynamic branch prediction, and precise traps, which requires shadow buffers (for registers, branch history tables *etc.*) [28] in order to recover to a prior execution state. In addition to these features, the Intel x86 architecture supports Precise Event Based Sampling (PEBS) with user access to selected shadow buffers [114]. Future processor extensions also make heavy use of checkpoint buffers [29, 30, 66]. CheckerMode's design will make such buffers uniformly available to the user. Enhancements to the ALU and branch logic to handle the new semantics for NaN (Not-A-Number) operands are required by CheckerMode (see Section 2.3), which are minor modifications compared to the space and complexity of the already existing shadow buffers. In fact, most processors already implement a NaN representation for floating point values (and an equivalent bottom value for integers), which is generated when undefined arithmetic (*e.g.*, divide-by-zero) is performed and results in an exception (trap). The sole modification suggested would be to gate the exception, *i.e.*, suppress it in CheckerMode, and proceed with arithmetic operations in the presence of NaN values.

2.2.2 Processor Vendor Limitations

One other shortcoming of static timing analysis approaches developed so far is given by their targeting of a generic processor type based on vendor-supplied design details. In such an approach, each new processor design requires that the timing model be manually adapted while the CheckerMode technique automatically adapts with changing processor details. Furthermore, such timing models are only as good as the information provided by the vendor, which may not reveal all details of the design. For example, Intel's CPU stepping index indicates subtle processor modifications within the same CPU family but does not reveal all details.

In fact, fabrication variability due to smaller feature sizes in the smallest production processes used to date already result in timing variability between two processors originating from the same batch [16–18, 61]. Taken to the extreme, access latencies within a cache may actually *differ* from one line to another or equivalent functional units may have different micro-timing characteristics. Hence, generic timing analysis of a processor line becomes meaningless in such a setting. The CheckerMode infrastructure avoids this detailed level of processor modeling and allows vendors to

protect their IP while providing a method to obtain highly accurate timing. Since CheckerMode observes the execution time on an actual processor, such variability is captured.

CheckerMode widens the scope of processors that may be used in a real-time system. Contemporary processors with state-of-the-art functionality and performance may subsequently be used in real-time systems. This also changes the landscape for timing analysis in that more accurate results can be obtained on modern pipelines without risk of losing functionality. In a world of increasingly specialized components, the idea that some processors could be designed specifically for use in real-time and embedded systems has already caught on, *e.g.*, with designs that customize generic core, such as the ARM-7/9/11 licensed by Qualcomm and many others. This is especially true in the design and testing phases for the real-time systems being created. These processors would not behave any differently during normal execution but would only have the additional characteristic that more information can be gathered from them during the analysis phase. Hence, there is an assurance that the additional features will not further complicate the analysis.

2.2.3 Assumptions

CheckerMode, in its current state only addresses the unpredictable nature of out-of-order instruction execution in contemporary high-end embedded processor pipelines. Other complexities, such as memory hierarchies, including caches, and dynamic branch prediction are beyond the scope of this initial work and will be addressed in the future. Tasks are analyzed in *isolation*. Preemptions and cache-related preemption delays, handled by orthogonal work [105], could be incorporated in the future and should not require any changes to the CheckerMode approach since their analysis occurs at a higher level.

2.2.4 Organization

This chapter is organized as follows. Section 2.3 introduces the CheckerMode infrastructure. Section 2.4 explains the experimental setup. Section 2.5 enumerates the results from the experiments while Section 2.6 summarizes the high-level contributions.

2.3 CheckerMode

The *CheckerMode* infrastructure, detailed in this section, provides the means to obtain accurate WCET values for modern processor pipelines. It encompasses enhancements/additions to

the microarchitecture while closely interacting with software to obtain WCET bounds. The idea is to design embedded processors, that in addition to executing software normally (in a so-called *deployment mode*), are capable of executing in a novel *CheckerMode* that supports timing analysis.

CheckerMode provides cycle-accurate bounds on the WCET by assessing alternate execution paths in a program. In deployment mode, a processor executes along just one path following a conditional branch; which path is executed may depend on the input data. In CheckerMode, a processor no longer proceeds with conventional data-driven execution. Instead, it executes all alternate paths, one at a time, following each conditional branch in order to find the path with the largest execution time. Before the execution of each alternate path, the original execution context (including caches, branch history tables etc.) is restored to correctly simulate the effect of alternations in isolation from one another. These low-level WCET results are propagated inter-procedurally in a bottom-up fashion (over the combined control-flow and call graphs) until the WCET for an entire task has been computed.

Consider a task that consists of a number of feasible execution paths. The execution times for these paths are obtained by actual execution in CheckerMode through the processor pipeline. The execution time for each path is then captured and stored. When conditional execution arises, all alternate paths are timed separately on the pipeline. The timing information as well as the "state" of the processor (determined by the cache state, branch predictor state, register state, *etc.*) are combined when alternate paths join. The combination is performed such that the state that results from the combination must not underestimate the execution time of the alternate paths or even the future execution of the task. A set of timing schemes for individual paths as well as combinations of paths, derived from this methodology, is discussed in the results section.

Prior to the execution of alternate paths, a "snapshot" of the processor state is obtained and stored. After the execution of one of the alternate paths, its state is recorded for later combination with other paths. Then, the state of the processor is restored to the one that existed before the path started executing. This is achieved by restoring the state (*e.g.*, of each of the parts of the pipeline) from the previously captured snapshot.

Consider the simple control-flow graph (CFG) in Figure 2.1. The CFG contains two possible paths – if the branch is taken, it follows path $1 \rightarrow 2 \rightarrow 4$; if it is not taken, it follows path $1 \rightarrow 3 \rightarrow 4$. When CheckerMode execution reaches basic block 1, a snapshot (snapshot 0) of the processor state is captured and stored. The amount of information to be captured can vary depending on the type of analysis required and can be made configurable. Execution then proceeds down one side of the CFG – say, the taken path. When execution of the path is complete, at basic

block 4, another snapshot (snapshot 1) of the processor state is captured and stored. The time taken to execute this path is also measured and sent to the timing analyzer. The program counter is then reset to basic block 1 (the branch condition) to trace execution down the other side (not-taken) and to subsequently capture the execution time for that path. Before execution proceeds along the not-taken path, the state of the processor is *restored* to the previously saved snapshot (snapshot 0). This isolates the effects of execution of one path from that of another. Once the processor state from snapshot 0 is written back, execution from basic block 1 proceeds down the not-taken path ($1 \rightarrow 3 \rightarrow 4$) before the processor state (snapshot 2) and execution time are captured once again. Only then can the CheckerMode unit shift its focus to the code that follows basic block 4. For execution to proceed from basic block 4, the processor must be set to a consistent state. At this point, it is necessary to perform a *merge* of the snapshots from the two paths. The merge must be performed such that the worst-case behavior of the subsequent code is preserved. Hence, we must merge the state of all processor units captured in preceding snapshots. Once a merge has been performed, the new state must be written back to the processor and execution continues from that point on.

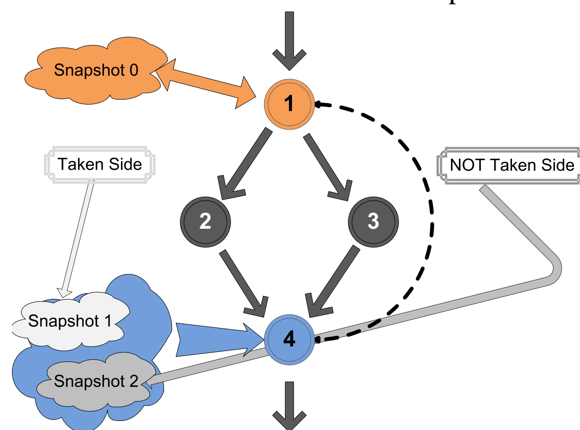

Figure 2.1: CheckerMode in Action

The hardware-supported CheckerMode is complemented by software analysis to govern checker execution (see Figure 2.2). The *analysis controller (or driver)* steers checker execution along distinct execution paths, *i.e.*, it indicates which direction a branch along the path should take till all paths have been traversed. The timing information and the states of the processor obtained for each possible path are then used by a "timing analyzer" to obtain the WCET for the entire task (or even certain code sections). Each of these is explained in the following sections.

2.3.1 Processor Enhancements

In this work, the embedded hardware is enhanced to support explicit access to the unit-level context of hardware resources, which can be saved and restored. The analysis phase restores a context prior to examining a path and then saves the newly composed context at the end of a path,

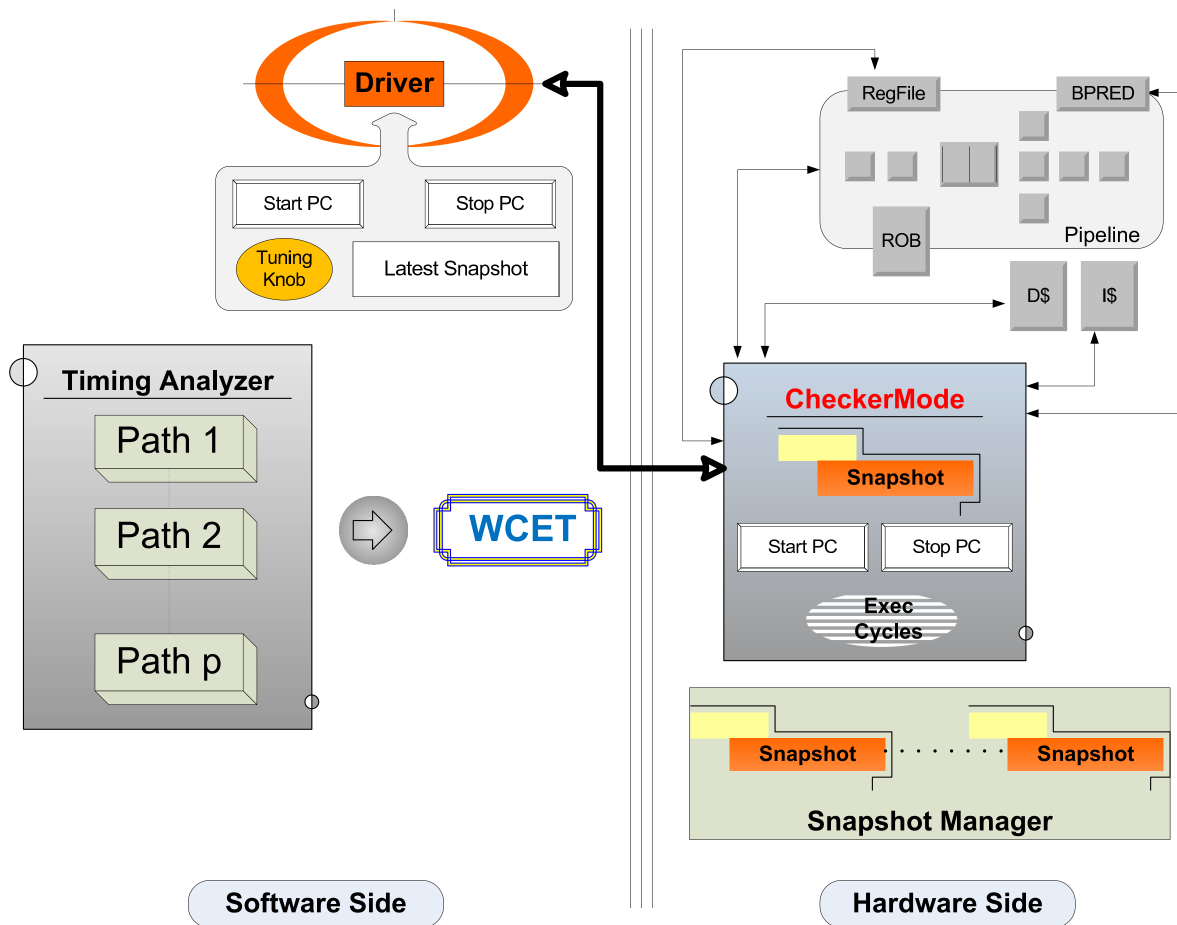

Figure 2.2: CheckerMode Design

together with the timing for the path.

Hence, the novel **CheckerMode** unit of the processor supports the following functions:
(a) Capture *snapshots* of the processor state and communicate them to the software controller. A snapshot captures the current state of the processor pipeline, associated functional units and caches, ROB, etc.
(b) Reset the processor to a previously saved state. Given an earlier snapshot, the state of the processor pipeline, caches, functional units, *etc.*, is overwritten with information from the stored snapshot.
(c) Start and stop execution between any two program counter (PC) values. This includes support to calculate the number of cycles elapsed between the execution of the given start and stop PCs.

The right-hand side of Figure 2.2 shows the details of the hardware side of the design. The

CheckerMode unit must be able to read and write to the various functional units of the processor. The CheckerMode unit is controlled by the driver (or controller) on the software side.

2.3.2 Software Overview

The left-hand side of Figure 2.2 illustrates the various components that make up the software side of the design. It consists of the following components:

Timing Analyzer (TA): The TA breaks down the task code into a control-flow graph (CFG) and then extracts path information from it. Using this information, the TA is able to determine the start of alternate execution flows – points where snapshots must be obtained. It also provides the start and stop PCs to the driver and obtains the WCET and processor state for that particular path from the driver.

Snapshot Manager (SM): The SM maintains various snapshots that have been captured as well as the PCs at which they were obtained. SM abstractions can be integrated into the processor as depicted in Fig. 2.2, or, alternately, into the driver within the software controller.

Driver: The driver controls the hardware side of the system. It instructs the hardware on when to start and stop execution, when snapshots must be captured, and when the state of the processor must be reset to a previous snapshot, as detailed below.

The input to the TA is the executable of a task. Assembly information is extracted (with PCs) from an executable and then converted to internal representations as combined control-flow and call graphs. The start and stop PCs provided by the TA encapsulate a single path. The TA, the driver, and the SM interact to decide which snapshot corresponds to which path, which PC, *etc.*, and thereby control program execution.

The TA is responsible for obtaining the final WCET for the entire program as well as various program segments (functions/scopes). It "combines" the information from various paths (execution time, pipeline state, *etc.*) for this purpose. The driver, also part of the software system, is described in more detail below.

2.3.3 Driver/Analysis Controller and Tuning

The driver is responsible for controlling processor operations. Besides directing the execution of the code on the pipeline, it relays instructions from the TA such as when to capture/restore snapshots. The driver represents the interface between the hardware and software components of the CheckerMode design. The driver contains information about the start and stop PCs that define

the start/end points of the path to be timed. It also stores the latest captured snapshot. The driver maintains information about which instruction is a branch and where snapshots need to be captured. It also relays information in the other direction – from the hardware to the timing analyzer – *e.g.*, the path execution time.

2.3.4 False Path Identification and Handling

A principal component of the analysis controller is a queue of saved processor contexts guiding path exploration. In some cases, not all paths need to be considered, as implied by these contexts. For example, a path can be dropped if static analysis concludes that this execution path cannot be executed (*i.e.*, it is a "false path"). Similarly, if a path can be shown to be shorter than some other paths that have already been explored, then again this path can be dropped from the queue.

2.3.5 Loop Analysis Overhead

We can reduce the complexity of determining the WCET by *partial execution of loops* such that the analysis overhead is independent of the number of loop iterations. The approach of a fix-point algorithm from prior work [10] is used to determine a stable execution time for the loop body. Now loop executions can be steered such that paths of a loop body are repeatedly executed till a stable value is reached. This technique is explained in detail in Chapter 4.

2.3.6 Input Dependencies

In CheckerMode, input-dependent register values are deemed *unknown*, which is internally represented in a manner similar to NaN (not-a-number) values already existing in floating point units (and similarly for integer ALUs). Operations on unknown values are straightforward: if *any* input is unknown then the output is also unknown. It is necessary to represent the known/unknown status of condition codes at the bit level. A branch condition based on an unknown value then indicates a need to consider alternate paths. Conversely, concrete (known) values are evaluated as always and input-invariant branches will result in timing of only the taken execution path.

The semantics of execution in CheckerMode must be altered to include this NaN value. *E.g.*, the addition operation will now be redefined as:

$$r_{result} = \begin{cases} \mathbf{NaN} & if\ r_a = \mathbf{NaN} \bigvee r_b = \mathbf{NaN} \\ r_a + r_b & otherwise \end{cases}$$

Hence, any operation with NaN as one of the operands will result in NaN (unless the result is independent of that particular operand, *e.g.*, multiplication with 0 will always result in 0). Similar enhancements are developed for other instructions that depend on input-dependent or memory-loaded operands.

2.3.7 Analysis Overhead

The process of timing analysis now amounts to timing sequences of paths by saving and restoring snapshots of processor state in a coordinated fashion. While this process can be lengthy, it still remains independent of the input to the program, and in the worst-case, can be run overnight. Since this is an **offline** task to be performed during system design and validation, the cost is secondary and does not affect the dynamic, run-time behavior of the system. Sometimes such a full verification of WCET bounds is generally only warranted after extensive code changes during development and for each software deployment, including system upgrades. In practice though, safety requirements of hard real-time systems demand that this level of verification be carried out for even the smallest changes. During system development, it could be performed after larger changes from time to time but must finally be performed fully at least once before the final deployment.

2.4 Experimental Framework

The key components of the CheckerMode design were implemented in the SimpleScalar processor simulator [22]. This cycle-accurate simulator can be configured for the various processor and branch prediction schemes. SimpleScalar was used in three configurations:

1. *Simple-IO (SimIO)* simulates a simple, in-order (IO) processor pipeline (pipeline width 1, instruction issue in program order)

2. *Superscalar-IO(SupIO)* with a pipeline width (from fetch to retire) of 16 and in-order instruction execution

3. *Out-of-order (OOO)* execution with the same pipeline width as in Superscalar-IO.

Table 2.1: C-Lab Benchmarks

Benchmark	Function
ADPCM	adaptive pulse code modulation
CNT	Sum and count of positive and negative numbers in an array.
FFT	Finite Fourier Transform
LMS	Least Mean Square Filter
MM	Matrix Multiplication
SRT	Implementation of Bubble Sort.

The C-Lab benchmarks [25] (enumerated in Table 2.1) were used for the experiments. Experiments were also conducted on a synthetic benchmark whose control-flow structure is depicted in Figure 2.3(a). Execution time for paths is measured using four different techniques, extending from the use of basic blocks (BB) [5] to paths (sequences of consecutive BBs):

1. *Short* measures the execution time of a single BB, starting from the time that **any** instruction in the BB/path moves into the *execute* stage of the pipeline and finishing when the last instruction of the BB/path exits from the *retire* stage.

2. *Path-Short* captures the execution time for paths (concatenated BBs) using the "short" technique so that timing starts at the first BB and ends with the last BB in the path.

3. *Path-Aggregate* captures the time for concatenated paths so that timing starts at the first BB of the first path and ends with the last BB of the last path.

4. *Program-Aggregate* includes the time from the start of the execution (main function) to the end of a BB in the path being timed, starting when the first instruction in the main function is *fetched* and finishing when the last of the path exits from the *retire* stage.

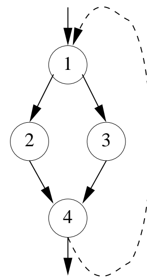

(a) CFG

Path	Cycles		
	SimIO	SupIO	OOO
bb 1	36	20	20
bb 2	8	4	20
bb 3	38	13	29
bb 4	15	5	22
bb 4'	15	5	16

(b) Cycles (Short Technique)

Figure 2.3: Control Flow Graph of Toy Benchmark and Measured Cycles

2.5 Results

The results obtained for the “short” technique (Figure 2.3(b)) show that timings for the processor modes SimIO and SupIO accurately reflect the actual WCET bounds, both for single BBs and paths. However, the OOO results exceed those of SupIO, due to early out-of-order execution of some instructions in parallel with other instructions from prior BBs in the path. Timing is started when any instruction in the relevant path comes into the execute stage of the pipeline, which could very well happen even when the previous path is not complete due to the inherent nature of out-of-order execution. Since timing only stops when the last instruction in the current path retires, the total execution time includes some time from execution of instruction in the previous path. Hence, the observed execution time includes cycles for instructions from earlier paths, which were not supposed to be timed. Even timing multiple BBs of a path in sequence (“path-short” technique) does not alleviate this problem. bb4 and bb4’ represent the same code – the difference is the path taken to get to basic block 4. In the first case, the “then” case of the branch was selected and in the second case, then “else” case was followed.

In contrast, the “aggregate” technique (Figure 2.4) reflects the time from instruction fetch (instead of execute) and also times longer paths. This addresses the above problem of early execution by some instructions because in the long run, timing longer paths reduces the inaccuracies from interactions between individual instructions . Results show a strict ordering of execution cycles for $SimIO \geq SupIO \geq OOO$, as expected by the amount of instruction parallelism, since time is measured from the first fetch of an instruction. The differences between paths (“delta”) provide a bound on the number of cycles for the tail BB in the path, thus excluding any pipeline overlap with prior BBs. Hence, these delta values can be used to assess the amount of cycles attributed to specific BBs alone. They also adhere to the same strict ordering. In general, such timing results are only valid in the same execution context/path, *i.e.*, different BB sequences of one path may influence subsequent BBs in the control flow.

Path	SimIO	delta	SupIO	delta	OOO	delta
BB1	82	BB1-BB0=56	66	BB1-BB 0=4	47	BB1-BB0=1
BB1,2	114	BB1,2-BB1=32	94	BB1,2-BB1=28	59	BB1,2-BB1=12
BB1,3	241	BB1,3-BB1=159	131	BB1,3-BB1=65	92	BB1,3-BB1=45
BB1,2,4	151	BB1,2,4-BB1,2=37	97	BB1,2,4-BB1,2=3	61	BB1,2,4-BB2=2
BB1,3,4	278	BB1,3,4-BB1,3=37	134	BB1,3,4-BB1,3=3	94	BB1,3,4-BB1,3=2

Figure 2.4: Measured Cycles (Aggregate Technique) for Synthetic Benchmark

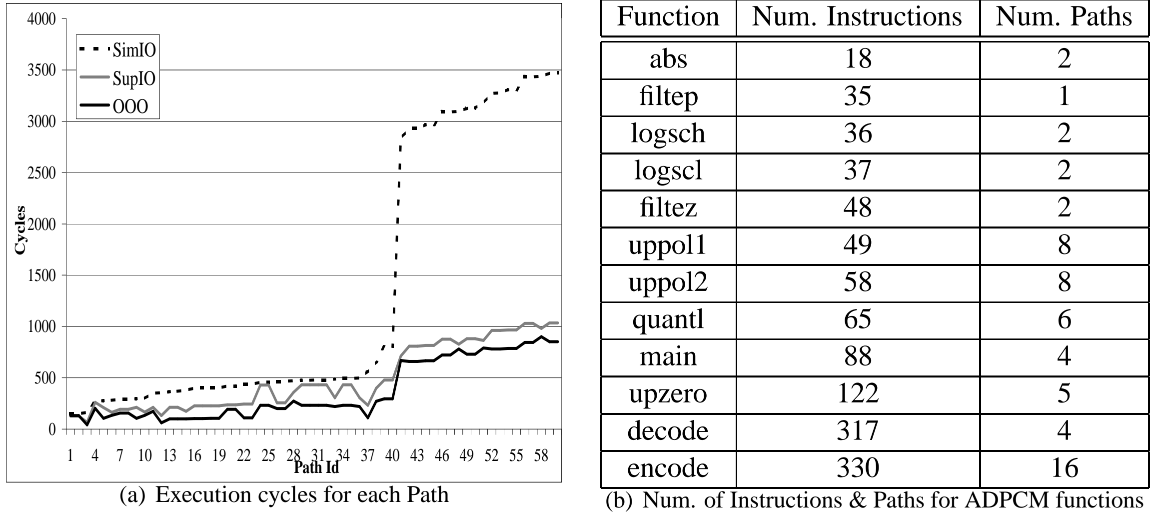

(a) Execution cycles for each Path

Function	Num. Instructions	Num. Paths
abs	18	2
filtep	35	1
logsch	36	2
logscl	37	2
filtez	48	2
uppol1	49	8
uppol2	58	8
quantl	65	6
main	88	4
upzero	122	5
decode	317	4
encode	330	16

(b) Num. of Instructions & Paths for ADPCM functions

Figure 2.5: Timing Results for the ADPCM Benchmark

2.5.1 C-Lab Benchmark Results

All paths from each of the C-lab benchmarks were extracted and then timed independently using the CheckerMode framework in each of the three configurations (SimIO, SupIO and OOO). Figures 2.5 and 2.6 summarize the results for the ADPCM, LMS and SRT benchmarks, respectively. ADPCM is the largest benchmark in the C-lab suite, with 14 functions and 60 paths, while LMS and SRT are smaller benchmarks with 10 paths each. Results are sorted in ascending order based on the timing results for the SimIO configuration. All three graphs show the $SimIO \geq SupIO \geq OOO$ ordering except for one path in the SRT benchmark, the reason for which is explained later.

Table 2.2: Averaged WCECs for C-Lab Benchmarks

Benchmark	SimIO	SupIO	% Savings	OOO	% Savings
ADPCM	1340	486	63.7	367	72.6
CNT	356	197	44.6	76	78.7
FFT	1047	439	58.1	288	72.5
LMS	839	457	45.6	236	71.9
MM	161	144	10.6	58	64.0
SRT	330.2	198	40.1	93	71.8

Figure 2.5(a) shows the timing results for the ADPCM benchmark, while Table 2.5(b) lists the various functions in ADPCM as well as the number of instructions and paths in each function. These results show the strict ordering for the three configurations, with SimIO results being the largest and OOO being the smallest. The same graph shows that the timing results for SimIO increase significantly around path 42. This is because paths $42 - -61$ originate from the "encode" and "decode" functions of the ADPCM benchmark and contain a larger number of instructions and,

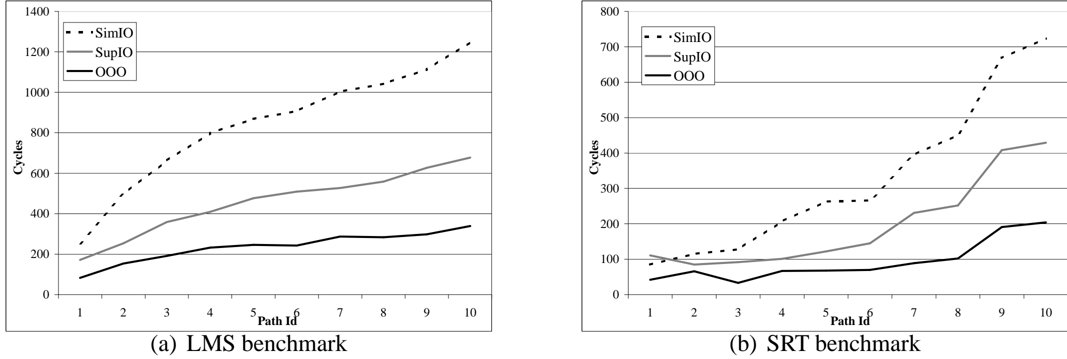

(a) LMS benchmark (b) SRT benchmark

Figure 2.6: Measured execution cycles for C-Lab Benchmarks

in the case of *encode*, a large number of paths as well. While there is enough parallelism in the code for SupIO and OOO to exploit, the SimIO configuration, with its in-order behavior and single width pipeline, is unable to scale as well as the other two configurations. This also shows that the number of dependencies between instructions in the two functions is not very high, as OOO is able to scale well to handle the larger instruction load.

The graph for LMS (Figure 2.6(a)) shows that all three configurations scale in a similar fashion for larger paths. It is interesting to note that the timing results for SupIO are approximately half of that for SimIO. Similarly, the timing results for OOO are approximately half that of SupIO. Similar results are seen for the SRT benchmark as well (Figure 2.6(b)), except for the shortest path (path 1). This path is so short that the effects described at the beginning of Section 2.5 become apparent – *i.e.*, timing is started when the first instruction of the program is fetched and stopped when the final instruction is retired. Hence, the first instruction has to wait for a while before it is dispatched. When the paths are very short, the pipeline contains a large number of instructions that do not belong to the particular path being timed, hence bloating the results for pipelines with larger width. The single width SimIO configuration does not suffer from this problem as the instruction is

Table 2.3: Path-Aggregate Cycles (3 Iterations) for the Synthetic Benchmark

Path	SimIO			SupIO			OOO		
	$+$	o	δ	$+$	o	δ	$+$	o	δ
LLL	453	443	10	291	193	98	183	123	60
LLR	580	570	10	328	230	98	216	156	60
LRL	580	570	10	328	230	98	216	156	60
LRR	707	697	10	365	267	98	249	189	60
RLL	580	570	10	328	230	98	216	156	60
RLR	707	697	10	365	267	98	249	189	60
RRL	707	697	10	365	267	98	216	189	60
RRR	834	824	10	402	304	98	282	222	60

dispatched immediately after being fetched.

The FFT and MM benchmarks also show similar results. The results of all six benchmarks are summarized in Table 2.2. The second, third and fifth columns are the *worst-case* number of cycles for each benchmark averaged across all paths. The fourth and the sixth columns show the average savings for each benchmark for the preceding configuration (preceding row in the table) as compared to SimIO (column 2). Specifically, the fourth column shows the average savings for SupIO over SimIO, and the sixth column shows the average savings for OOO over SimIO. These savings are based on the averages across all paths.

2.6 Conclusion

This chapter outlined a "*hybrid*" mechanism for performing timing analysis that utilizes interactions between hardware and software. The *CheckerMode* concept provides the foundation to make contemporary processors predictable and analyzable so that they may be safely be used in real-time systems. Current trends in microprocessor features indicate that the proposed hardware modifications are realistic [114]. Once fully implemented within the SimpleScalar simulator, the CheckerMode unit will have the ability to not only drive execution along given program paths but also to capture and write back processor state to/from snapshots. This will provide the ability to accurately gauge the execution time for a given program path. This work will enhance the design choices available to real-time systems engineers. The CheckerMode concept will provide them with the ability to use current and future state-of-the-art microprocessors in their systems and utilize a hybrid of static and dynamic timing techniques to validate WCETs.

Chapter 3

Merging State and Preserving Timing Anomalies in Pipelines of High-End Processors

3.1 Summary

This chapter provides further insights into the CheckerMode idea presented in Chapter 2 by introducing novel pipeline analysis techniques for accurately capturing the worst-case behavior of real-time tasks, *i.e.*, methods to capture (“snapshot”) pipeline state and to subsequently perform a “merge” of previously captured snapshots. This chapter also includes proofs that the pipeline analysis correctly preserves worst-case timing behavior on OOO processor pipelines. It also specifically shows that anomalous pipeline effects, effectively dilating timing, are preserved by these methods.

3.2 Introduction

Chapter 2 introduced the notion of “hybrid” timing analysis [86] called the *CheckerMode* infrastructure which combines the best features of both static and dynamic analysis to obtain accurate WCET estimates for real-time tasks running on modern microprocessors. This chapter,

1. presents a more formal definition of the semantics of a snapshot;

2. explains how the information in a snapshot is obtained;

3. illustrates how two or more snapshots are "merged", which occurs when multiple control paths "join" together;

4. *prove* that the mechanisms for capturing and merging snapshots are correct in that they retain all worst-case pipeline effects;

5. explains how the mechanisms to capture and merge snapshots are able to correctly handle "timing anomalies" [13, 79, 81, 109].

The remainder of this chapter is organized as follows: Section Section 3.3 introduces the notion of snapshots while Section 3.4 explains the models used for the analysis in this Chapter. Section 3.6 explains the techniques to capture the behavior of instructions in the pipeline. This is mainly aimed at capturing structural and data dependencies in an accurate manner. Section 3.5 details how a snapshot is captured while Section 3.7 provides the context on how these snapshots can used. Section 3.8 discusses how two or more snapshots are merged (before a join point in the control flow) so that the processor are reset to a consistent state for the following instructions. Section 3.9 proves that pipeline effects that modify timing will be retained post-merge. Section 3.10 develops a simple mechanism to merge register files. Section 3.11 discusses the details of the implementation. Finally, the conclusions are presented in Section 3.12.

3.3 Snapshots

Snapshots describe the state of the processor captured while performing timing analysis using the "hybrid" CheckerMode technique [86] to obtain the worst-case execution time for modern processor architectures. It typically consists of the state of each functional unit of the processor at a given point in time (t). This state includes, but is not limited to:

I pipeline state: in a generic sense, the state of instructions in the pipeline. Ideally, this state includes a description of *which* instructions are at *what* stage in the pipeline at time t. It also includes the contents of the register file.

II cache state: the contents of the instruction and data caches at t. This information could be either *(a)* the complete cache contents or *(b)* incremental difference compared to the last snapshot. It could also be a combination of the two, where periodically the state of the entire cache is captured, but in between store only the incremental differences (so-called deltas).

III branch predictor state: similar to the cache state above: *(a)* complete branch history register and branch table contents; *(b)* delta from previous snapshot; or *(c)* a combination of the two.

IV your favorite processor unit: state from any additional/future processor units that needs to be captured to accurately characterize the worst-case behavior of the processor.

This chapter focuses on capturing the **pipeline** information of the processor for snapshots and not on caches, branch predictors, *etc.* Analysis of instruction caches is a solved problem, and any such analysis can be plugged into the CheckerMode framework to obtain better worst-case results. Analysis of data caches is a hard problem but some analysis does exist [93, 104, 123, 131], results from which can also be inserted into the CheckerMode framework to tighten the WCET results. Branch Predictor analysis is left for future work.

While capturing fine-grained details of instruction flow through the pipeline (defined above as "pipeline state") would be ideal, practical difficulties prevent the process. Many changes to the design and implementation of the processor will have to be carried out to attain the ability to observe every single stage of the pipeline, instructions in flight, data forwarding, etc. Hence this chapter presents a novel technique devised to capture pipeline information, which, in essence, achieves the effect of characterizing the state of the pipeline at the given instant. This technique is named, the "drain-retire" (DR) technique. The DR technique is based on the idea that the only point of predictability in an out-of-order pipeline is at the retire stage. Since retire happens *in-order*, one can be sure that the retire order of instructions is deterministic. The DR technique is discussed in more detail in Sections 3.5 and 3.7.

3.4 Analysis Model

Figure 3.1(a) shows a section of the instruction stream that is executing through the pipeline. Let S_n be the last snapshot that was captured. Let "max" be the maximum number of instructions that can fit into the pipeline assuming that there are no dependencies between any of them. This is the theoretical upper bound for the pipeline capacity and is typically never achieved in practice – due to the existence of dependencies between instructions, which introduce bubbles in the pipeline.

If r is the most recent instruction that was fetched into the pipeline, then let p be the instruction that was issued max cycles earlier in the instruction stream. Hence, p is the farthest instruction in the stream that can directly affect r's flow through the pipe. Instructions before p have

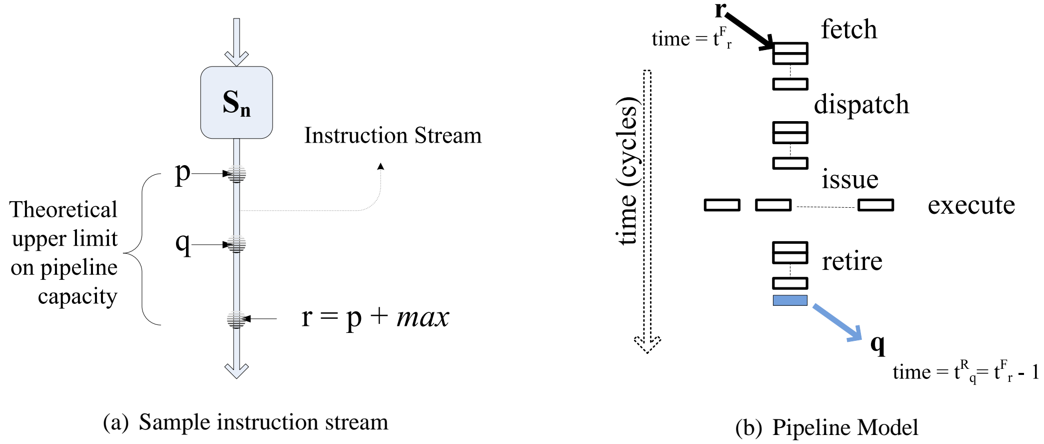

Figure 3.1: Model used for description and capture of Snapshots

retired, and any resulting state changes have been committed.

Figure 3.1(b) shows the pipeline model that is used for this work. Fetch happens in-order, but multiple instructions can be fetched in the same cycle. Similarly, retire also happens in-order and multiple instructions can retire in the same cycle. Hence, when a fetch of instruction r occurs at time t_r^F (*i.e.*, the fetch time for instruction r), let q be the last instruction that retired one cycle earlier at time t_q^R (*i.e.*, the Retire time for instruction q). Figure 3.1(a) shows that q must lie between:

$$p \leq q < r \tag{3.1}$$

Note that q is no longer in the pipeline when r is being fetched. Hence:

$$t_q^R = t_r^F - 1 \tag{3.2}$$

3.5 Snapshot Capture using Pipeline Drain-Retire (DR) Technique

Ideally, capturing a snapshot at r would involve capturing information about which instructions are in what stage of the pipeline and how long they have been/will be there. This resembles a *step curve* of the instructions that are in the pipeline. This is not practical as are unable to capture the precise information in a pipeline without significant changes in silicon. Instead, this chapter presents a novel "*drain-retire*" mechanism to characterize the flow of instructions in the pipeline. It takes advantage of the fact that in an out-of-order pipeline the only point where determinism can be *guaranteed*, is at the *retire* stage (instructions *must* retire in-order). The algorithm to capture a snapshot using the DR mechanism is as follows:

1. Stop fetching after r.

2. Store t_q^R, the time when q retired.

3. Let execution proceed through the pipeline until r retires (*i.e.*, the pipeline drains completely).

4. Track the retire time of every instruction from q up until, and including r (*i.e.*, t_r^R).

Figure 3.2 shows the results of applying the above algorithm to the model and instructions described in Section 3.4. This figure shows the step curve obtained by tracking the retire times of all instructions following q until r retires.

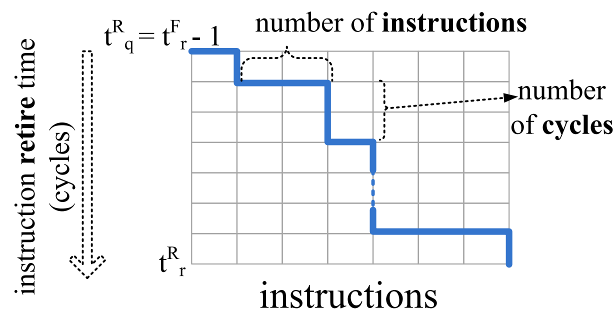

Figure 3.2: Snapshot Captured using the DR Technique

The vertical axis represents time while the horizontal axis represents the instructions that retire. Hence, the curve is bounded, in the time domain, by t_q^R and t_r^R with upper bound max. Unlike similar step curves for in-order pipelines, this curve is *multi-dimensional*. The horizontal axis now encodes information about groups of instructions that retire together. As the figure shows, the horizontal parts of the "step" directly represents the order and the number of instructions retiring at that particular point in time (*i.e.*, multiple instructions retiring in the same cycle). *Note*: the *exact* order of instruction retirement at any given level must also be tracked. All of this information, combined with the "state" of the reservation stations (Section 3.6), now forms a pipeline *snapshot*, which is formally defined in Figure 3.3.

3.6 Capturing Structural and Data Dependencies using Reservation Stations

3.6.1 Structural Dependencies

Consider the situation shown in Figure 3.4(a). "a_1" and "a_2" are two *multi-cycle* instructions that require the same execution unit (for *e.g.*, the "floating point multiply" unit). Assume that there is only one instance of this type of execution unit in the pipeline. Now there exists a *structural*

$$\mathbf{S_n} = \left\{\mathbf{q}, \mathbf{t_q^R}, \left\{\mathbf{t_{\{i\}}^R}, \{\mathbf{i}\}\right\}, \mathbf{RES}, \mathbf{RF}, \mathbf{S_{<q}}\right\}$$

$where,$

$$S_n \quad : \quad snapshot\ at\ instruction\ \mathbf{n}$$

$$q \quad : \quad last\ instruction\ to\ retire\ before\ \mathbf{n}\ was\ fetched$$

$$t_q^R \quad : \quad retire\ cycle\ for\ q$$

$$\left\{t_{\{i\}}^R, \{i\}\right\} \quad : \quad set\ of\ tuples\ where,$$

$$t_{\{i\}}^R : retire\ cycle$$

$$\{i\} : all\ instructions\ that\ retire\ at\ t_{\{i\}}^R$$

$$RES \quad : \quad state\ of\ the\ reservation\ stations\ immediately\ \mathbf{after}\ instruction\ \mathbf{n}\ has\ retired$$

$$RF \quad : \quad state\ of\ the\ register\ file\ immediately\ \mathbf{after}\ instruction\ \mathbf{n}\ has\ retired$$

$$S_{<q} \quad : \quad link/pointer\ to\ last\ snapshot\ before\ q\ (= \emptyset\ if\ S_n\ is\ first\ snapshot)$$

Figure 3.3: Definition of a Snapshot, based on the “Drain-Retire” mechanism

dependency between a_1 and a_2. Hence, a_2 cannot obtain access (be issued) to the execution unit before a_1 vacates it. This dependency must be retained across the join point (where alternate paths meet) because it could affect the worst-case behavior of execution that proceeds beyond it. Assume that path “D”’s execution time is affected by the fact that a_2 has to wait. Also assume that the WCET for path “D” ($wcet_D$) increases or decreases by a factor δ depending on whether a_2 is made to wait or not, respectively. Let $wcet_E$ be the worst-case execution time for path “E”. The following pathological situation now occurs:

$$wcet_D - \delta < wcet_E < wcet_D + \delta$$

Hence, even though “E” becomes the longer path (among “D” and “E”), it is *not* the worst-case path for the combination. The worst-case effects are seen when a_2 experiences a delay due to structural dependencies with a_1, thus delaying path “D” to exhibit a WCET of $wcet_D + \delta$. A mechanism is required to capture these structural dependencies among instructions, especially those

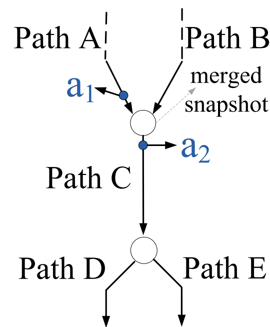

(a) Example to show hazards affecting worst-case behavior

Exec Unit	Instruction	Entry Cycle	Exit Cycle
integer add	a	103	104
integer mult	b	104	110
float add	m	123	129
float mult	x	136	150

(b) Reservation Stations

Figure 3.4: Mechanism to Capture/Handle Structural Hazards

that lie on either sides of snapshots. The concept of of *reservation stations* is introduced precisely for this purpose.

Reservation stations, for tracking structural dependencies (Figure 3.4(b), are implemented as tables with one entry per execution unit. It stores three values per execution unit:

1. the **instruction** using that execution unit;
2. **entry cycle**: cycle/time when the instruction was issued the particular execution unit;
3. **exit cycle**: cycle/time when the instruction exited from the execution unit.

3.6.2 Data Dependencies

Most modern pipelines use data-forwarding techniques (bypass) to reduce the wait times for instructions that are waiting on data (register values) to become ready. When data is produced, at the end of the execution stage of certain instructions, it can immediately be forwarded to instructions that are waiting on it. These data values are available to waiting instructions even *before* they are written into the register file. Such data forwarding techniques and their effects must be characterized correctly, if the CheckerMode architecture is to correctly capture the worst-case behavior of tasks.

From Figure 3.4(a), let us now assume that a_1 and a_2 have *only* a data dependency among them(and not structural dependency as explained in the previous section) such that a_2 must wait for a_1 to write a result into a register (say r_1) that is a source register for a_2. If another instruction (say a_3) on path “B” also writes to r_1, but earlier than when a_1 would have written to it. Since a_1 and a_3 resides on the opposite side of a join point when compared to a_2, the latter can gain access to the register value (r_1) earlier than it would have otherwise on the “A” path, and can execute earlier. Hence, the worst-case behavior of the program is not correctly preserved.

Reservation stations are also used for the register file to correctly track the data dependencies between instructions and the time(s) when data becomes available and when they can be used by dependent instructions. Each register now has an associated “reservation station” which stores the *latest* cycle when the register value was available (*i.e.* after the execution stage of the instruction that produced that value).

Note: The process of writing information into the reservation stations is *not* on the critical path. Hence, it does not affect the execution of instructions in the pipeline.

3.7 Snapshot Usage

A snapshot captured using the DR technique in the previous section consists of information about:

1. instructions
2. their order of retirement
3. cycles between retirement of instructions
4. the last instruction that retired (q) before the snapshot instruction (r).

This section elaborates the use of this information.

When execution must be restarted from a snapshot, instruction fetching must from instruction q because instructions that preceded it cannot directly affect the execution of r. While fetch can start from q, there is no information about the processor state at q. Hence, the last snapshot before q, which is S_n, must be restored, as seen in Figure 3.1(a). To account for the worst case, the start must actually be from the snapshot that precedes instruction p. Instruction p is the instruction that is at the theoretical bound for the capacity of the pipeline, max, relative to r. If there exists a snapshot between p and q, then the pessimism may be reduced by starting at the snapshot that *immediately* precedes q since it is known that instruction q defines the *realistic* capacity of the pipeline. Now information from this snapshot can be restored to bring the processor into a consistent state. Fetching is restarted from the instruction that immediately follows S_n and execution is allowed to proceed until the new/current snapshot, S_r (at instruction r), is reached. Once instruction q retires, information about subsequent instructions is looked up from S_r to see how much time elapses, if any, between their retirement. Each instruction starting from r can now retire only after the requisite number of cycles has elapsed, as determined by the information in S_n. Hence, instructions can retire

at or after the number of cycles recorded *for it* in the snapshot, but *never before*. From Figure 3.2, it is seen that two instructions following q can retire at the same time, but no earlier than 1 cycle after q. The next instruction can only retire 2 cycles after the previous 2 instructions have retired, and so on.

A similar process is employed for the *issue* stage of the pipeline. The reservation stations are used to control what instructions are issued, when and into what execution unit. Figure 3.4(b), shows that an instruction that wishes to use an execution unit (say the integer multiplier), cannot gain access to it before cycle 104, and once it has been given access, another instruction cannot obtain it until the previous instruction exits (which, in this case, will be cycle 110). This process ensures that structural dependencies between instructions on either side of the snapshot are still retained.

Similarly, instructions that depend on certain register values to be ready cannot proceed with their execution until the cycle stored in that register's reservation station comes to pass. This ensures that instructions that have data dependencies among them still retain the correct dependency information post-merge.

Hence, the semantic meaning associated with snapshots, initially constrained to static aspects only, has been enhanced by dynamic information. This has an effect on the instruction flow through the pipeline. Hence, a snapshot is now defined as information that affects the flow of instructions through the pipeline when the "snapshot instruction" (r in the above case) is fetched. Snapshots are able to affect the pipeline behavior by allowing instructions captured in them to retire only with predetermined delays (*i.e.*, at or after the retire times captured in the snapshot) or gain access to execution units based on constraints enforced by the reservation stations, *etc.*. Modifications to the retire stage, mentioned in Section 3.5, as well as the issue stage (to look up the reservation stations) are useful in aiding the process of restoring snapshots by providing the ability to exercise fine control on when certain instructions (captured in the snapshot) are allowed to be issued or to retire.

Note: This method of using snapshots and constraining instruction flow through the pipeline can be achieved in one of two ways:

1. by enhancing the *fetch* stage of the pipeline so that finer control can be exercised on *when* instructions are to be fetched and from *where* in the program flow

2. by inserting nop instructions to cover "bubbles" in the program flow.

The latter technique is less invasive and requires hardly any changes at the micro-architectural level. Since the driver in the CheckerMode infrastructure has overall control of the framework, it could periodically inject nops to maintain the correctness of the analysis.

3.8 Merging Pipeline Snapshots

When alternate paths meet, snapshots from both sides must be *merged* so that instructions that follow see a consistent state of the pipeline. Also, the merged state must inherit the worst-case behavior from either side. Another requirement is that pipeline effects resulting from anomalous behavior [79, 81] must still be retained post-merge. In this section, we present a merge technique that handles all of the above effects correctly. This merge technique is referred to as "*drain-retire merge*" (DRM). Section 3.9 will present a proof showing that timing anomalies are retained after applying DRM.

3.8.1 Merging Two Snapshots

Merging more than two snapshots is a simple extension of the same techniques. The algorithm to perform a merge of two snapshots (DRM) is illustrated in Figure 3.5. It proceeds by simultaneously retrieving snapshots from the top of each stack, extracting information and comparing it pairwise before composing a merged state and storing it in a new snapshot (S_m).

Remark: The older "starting point" (q) is picked from the two snapshots and also the older "last snapshot" ($S_{<q}$). This is to ensure that the state of the processor is correct when the merged snapshot state is restored within the processor.

To understand how this algorithm works, consider examples of snapshots shown in Figure 3.6(a). Snapshot "A" has three instructions (a, b, c) while snapshot "B" has four (f, g, h and i). Instructions d and j are not part of the snapshot. They are the first instructions that follow the snapshot. The following steps are used to perform the merge:

1. Start from the first (earliest) instruction in both snapshots.
2. Combine all instructions at the same cycle (level) into the new, merged snapshot. Hence, a, f, g and h will be combined so that they retire during the same cycle.
3. Compare instructions in both snapshots to find the snapshot with the longer number of cycles until the next retire occurs. The figure shows that b and c from "A" retire later than i from "B".

```
// DRM Algorithm to merge two snapshots

drm_merge ( snapshot S_a, snapshot S_b ){
    S_m ← NULL; // merged snapshot
    do {
        t_1 ← get next retire cycle in S_a ;
        I_1 ← get instructions retiring at t_1 in S_a ;
        t_2 ← get next retire cycle in S_b ;
        I_2 ← get instructions retiring at t_2 in S_b ;

        S_m ← { max( t1, t2 ), I_1 ∪ I_2 };
    } while( not_empty(S_a) and not_empty(S_b) );

    S_m ← remaining retire times and instructions from non-empty snapshot;
    S_m ← older( S_a.q, S_b.q );
    S_m ← older( S_a.prev_snapshot, S_b.prev_snapshot );

    S_m ← merge_reservation_stations( S_a.RES, S_b.RES ) ;

    S_m ← merge_reg_file_state( S_a.RF, S_b.RF ) ;

    return S_m;
}
```

Figure 3.5: Snapshot Merge Algorithm (DRM)

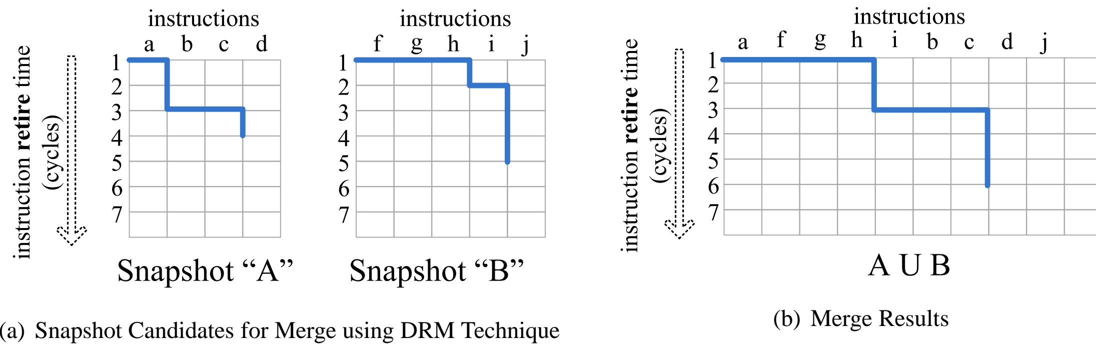

(a) Snapshot Candidates for Merge using DRM Technique

(b) Merge Results

Figure 3.6: Merging using the DRM Algorithm

4. Set the retire time for all instructions on both paths to the longer delay. Hence, b, *c and* i will now retire at cycle 3.

5. Repeat for all remaining instructions/retire times in both snapshots.

Figure 3.6(b) shows the results of applying the DRM merge algorithm. After the merged snapshot is restored instruction stream immediately after the join point is followed. Also, for the sake of obtaining the WCET of the program the longer path and its WCET are picked for the analysis. If the path that provided snapshot "B" (P_B) is longer, then its instructions and WCET are used. The problem of finding the WCET for the entire program is then reduced to finding the longest path in short sections of code and using their WCETs for future calculations.

As explained in Section 3.7, restarting execution at a snapshot means restarting from an instruction that originates from before the particular snapshot (*e.g.*, instruction q in Figure 3.3). If P_B is the longer path, then q belongs to the mix of instructions that constitutes P_B. Even if P_B is very short and q happens to lie before the branch condition the longer path must be picked to execute through the pipeline to reach the merged state, which will eventually pass through P_B in this case. Hence, at any point in time, only instructions from one path (P_A or P_B) will execute through the pipeline.

3.8.2 Incorrect Merge Technique

Figure 3.7(b) shows an incorrect way of performing the merge. In contrast to Figure 3.6(b), each instruction now retires at its original time. If the information from Figure 3.7(b) was used instruction i would always retire at cycle 2 and not account for the fact that "A" could carry over some worse behavior where instructions b and c retire one cycle later.

While this alternate method may result in fewer cycles for the WCET, it does not safely capture effects due to the execution of alternate paths and the influence they may have on each

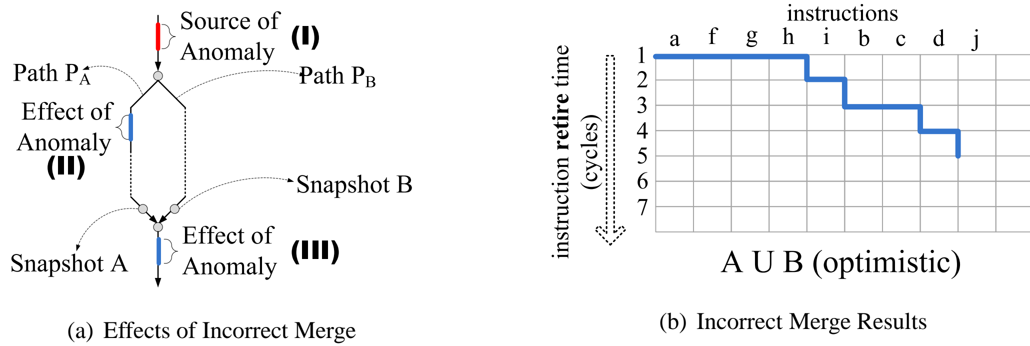

Figure 3.7: Incorrect Merge

other. The problem arises because of the search for paths that show worst-case behavior *locally*. If effects from one part of the program affect the worst-case behavior of instructions that are at a large distance, then using this incorrect merge technique will result in wrong WCET estimates.

Consider the situation shown in Figure 3.7(a). Let paths P_A and P_B be the paths that produced snapshots "A" and "B", respectively. Let the result of merging them be as depicted in Figure 3.7(b). Let us further assume that P_B has the larger WCET. As explained before, only instructions from P_B will exist in the pipeline when this newly merged snapshot is encountered. Now let us assume that there exists a timing anomaly in this section of the program and the source of this anomaly is at point (I). Let us also assume that only certain instructions in path P_A (point (II) in the figure) depend directly on the instructions that form the anomaly. Instruction b in Figure 3.7(b) has its retire time increased due to this anomaly. Let other instructions following the merge (point (III) in the figure) depend indirectly (due to instructions at (II)) on the anomaly. Path P_B is not affected by the anomaly. *If the retire times shown in Figure 3.7(b) are used, then the effects of the anomaly will not be felt post-merge, because the time dilation effects that resulted in an increase in (say) b's retire time are not carried over.* This would have otherwise dilated the execution/retire times for instructions at point (III). Hence, the overly aggressive, incorrect merge may not result in a correct handling worst-case pipeline effects (in particular timing anomalies). There exists a distinct possibility that future instructions (post-merge) will not execute based on the worst-case behavior. Such incorrect merge techniques can result in an underestimation of the WCET estimates.

3.8.3 Merging Reservation Stations

The steps to perform a merge for reservation stations are shown in Figure 3.8. While merging reservation stations for the execution units, pick the later of the two entry cycles as well as the later exit cycle. This ensures that the worst-case behavior of the program is carried forward

post-merge.

```
merge _reservation_stations( Sa.RES, Sb.RES ) {
        for   each  ( execution_unit_entry E ){
              E_merged_res_station_entry_cycle = max(Ea.entry_cycle,Eb.entry_cycle);
              E_merged_res_station_exit_cycle = max(Ea.exit_cycle, Eb.exit_cycle);
        }

        for each ( register_entry R ){
              R_merged_register_cycle = max(Ra.cycle,Rb.cycle);
        }

        return merged_res_station ;
}
```

Figure 3.8: Merging Reservation Stations

The merge for register reservation stations is similar in that a $\max$ of the reservation station entries from both paths is stored as the new value for that particular register. This ensures that instructions that execute post-merge cannot gain access to the register values until the cycle which is stored in the reservation station for that particular register. While the register values might be written (generated) earlier (from an alternate path), they cannot be used until the reservation station allows it.

3.8.4 Merge for More than Two Snapshots

```
merge _n(S1...Sn) {
        if ( only two snapshots Sx, Sy )
                return drm_merge( Sx, Sy ) ;
        return merge_n( merge_n(S1...Sn-1), Sn ) ;
}
```

Figure 3.9: Merge for Multiple Snapshots

The DRM algorithm can be extended to merge more than two snapshots. In such situations, it is called recursively, as shown in Figure 3.9. Two snapshots are merged at a time, and each of these merged snapshots can then be merged with other single or merged snapshots.

3.9 Proof of Correctness

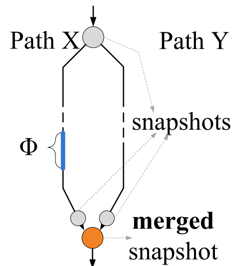

Figure 3.10: Anomaly Effects on Merge

The term "timing anomaly" refers to an anomaly in the execution of code in dynamically scheduled processors [79]. It was later generalized by others [13,81,109]. It denotes counter-intuitive results in timings, *e.g.*, a cache hit may result in longer execution times than a miss for a given path due to overlapped structural resource conflicts. These anomalous effects show up as pipeline effects, where execution times for instructions are dilated in ways that cannot be predicted easily. They prevent accurate modeling of out-of-order processors and thus prevent the process of obtaining accurate estimates of worst-case execution times for such processors. Instead, this chapter shows how such effects can be safely bounded. Hence, any pipeline state merge algorithm must ensure that the effects in the pipeline due to such anomalies are retained, *i.e.*, the merge must not remove these anomalies from the pipeline and subsequent analysis.

Assumptions: This work only addresses pipeline effects. Hence, any architectural/execution artifact that results in changes to the passage of instructions through the pipeline is considered. The reasons could be internal (*e.g.*, data dependencies) or external (*e.g.*, cache hits/misses) to the pipeline. The origins and causes for the effects could have occurred at a much earlier stage or just immediately before time dilation in the pipeline. Effects on other parts of the processor, including caches and branch predictors, are not yet considered here as they are subject to future work.

Theorem 3.9.1. *Correctness of Merging Two Snapshots: The DRM merge algorithm (Figure 3.5) retains all worst-case pipeline timing effects, including timing anomalies.*

Proof. **(I)** Consider the situation shown in Figure 3.10. It shows two alternate paths (X and Y with WCETs C_X and C_Y respectively), each of (possibly) different lengths. A snapshot is captured at the beginning (say S_{branch}) when the two paths diverge. Two snapshots are captured (say S_X and S_Y), one for each path, before the paths meet. These two snapshots are "merged" using the DRM algorithm to obtain the new, single snapshot (say S_m) that is used to initialize the state of the processor before execution proceeds. ϕ is the *potential* time dilation produced during the execution of path X due to pipeline effects (such as timing anomalies). Such dilation could lead to one of the following three cases related to the retire time of some instructions in X:

- **Case 1**: ϕ causes some instructions to retire *later*, *i.e.*, it increases the execution times for some (or all) instructions, thus resulting in an increase in C_X. These instructions also enter and leave their respective reservation stations later than they would have otherwise. They also produce results (and write them to register files) later.

- **Case 2**: ϕ causes some instructions to retire *earlier*, *i.e.*, it decreased the execution times for some (or all) instructions, thus resulting in a decrease in C_X. Hence, they are able to enter/exit reservation stations, as well as produce results (to be written into registers) earlier than before.

- **Case 3**: ϕ does affect the retire times or reservation station usage for any instructions in the snapshot, *i.e.*, it neither increased nor decreased C_X.

(II) Consider the case of an arbitrary instruction k (part of path X) with its *original* reservation station times ([Entry, exit]) denoted as $[E, e]_k$, its retire time t_k^R which is part of snapshot S_X. Let RF_k be the time when the instruction writes its results (if any) into the register. Hence, RF_k is the time stored in the reservation station associated with the register that was written into by k. Let S_X also be affected by an anomaly. Hence, the time(s) of k and the WCET of X are now,

$$[E, e]'_k = [E \pm \phi, e \pm \phi]_k \quad (3.3)$$
$$t'_k = t_k^R \pm \phi \quad (3.4)$$
$$RF'_k = RF_k \pm \phi \quad (3.5)$$
$$C'_X = C_X \pm \phi \quad (3.6)$$

As part of the DRM process, k, its reservation station state and its retire time (t'_k) will be compared with instructions from the snapshot on the the alternate path (S_Y). Let $[E, e]_{\{i\}}$ and $RF_{\{i\}}$ be the state of the reservation stations and $t_{\{i\}}^R$ be the retire time that $[E, e]'_k$ and t'_k are being compared with (from the other snapshot), where $\{i\}$ represents the sequence of corresponding instructions from the other snapshot.

(III) Case 1: ***(a)*** ϕ increased the retire times for k. Hence,

$$[E, e]'_k = [E + \phi, e + \phi]_k \quad (3.7)$$
$$t'_k = t_k^R + \phi \quad (3.8)$$

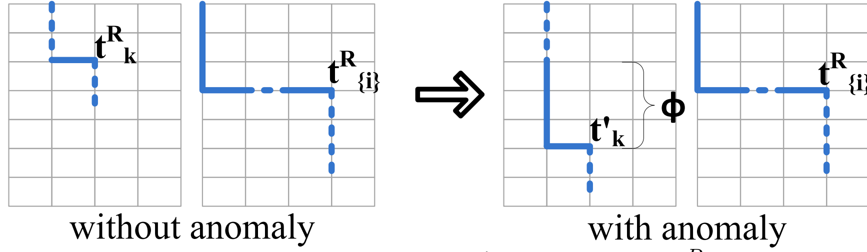

Figure 3.11: Case 1 (a) (i) t'_k is greater than $t^R_{\{i\}}$

(i) If $t'_k > t^R_{\{i\}}$ then the merged snapshot (S_m) will store t'_k as the retire cycle for all instructions $k \cup \{i\}$. Hence, Figure 3.11 shows that the increase in time to retire for an arbitrary instruction k results in changes to the snapshot (instructions retire later), thus ensuring that the pipeline effect propagates beyond S_m.

Remark: These effects on S_m will materialize regardless of whether $t^R_k < t^R_{\{i\}}$ (seen in Figure 3.11) or $t^R_k > t^R_{\{i\}}$.

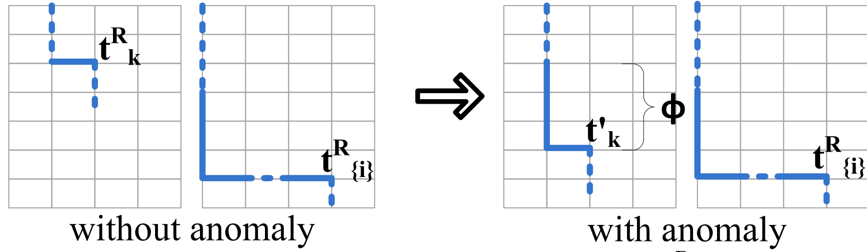

Figure 3.12: Case 1 (a) (ii) t'_k is less than $t^R_{\{i\}}$

(ii) If $t'_k < t^R_{\{i\}}$ then the merged snapshot (S_m) will store $t^R_{\{i\}}$ as the retire cycle for all instructions $k \cup \{i\}$. Figure 3.12 shows that the increase in the retire time for k did not affect the snapshot. The retire time for k (t^R_k) would *never* have affected the merged snapshot because the larger $t^R_{\{i\}}$ value would have been picked anyways. This is due to the fact that the aim is to estimate the worst-case behavior of the program. We can also conclude that the pipeline effect would be contained within S_{branch} and S_m in this case because the retire time for the instructions affected are not part of the worst-case behavior of the path.

Remark: This situation can only occur if $t^R_k < t^R_{\{i\}}$ to begin with as shown in Figure 3.12. If t^R_k was larger, then it would default to case III (a) (i).

Case 1: ***(b)*** ϕ increased the WCET of X. Hence,

$$C'_X = C_X + \phi \tag{3.9}$$

(i) If $C'_X > C_Y$ (Figure 3.11), then the WCET for the entire construct will now be C'_X. Hence, the effects of ϕ will be included in the estimation of the total, increased WCET of the program. Again, this is regardless of whether $C_X > C_Y$ or $C_X < C_Y$.

(ii) If $C'_X < C_Y$ (Figure 3.12) then the WCET for the entire construct will now be C'_Y. This result means that the effects of ϕ would never have affected the WCET estimation of the program anyways as Y was always the longer path.

Remark: This result is only possible if $C_X < C_Y$ to start with, else it would default to case III (b) (i).

(IV) Case 2: ***(a)*** ϕ decreased the retire times for k. Hence,

$$t'_k = t^R_k - \phi \tag{3.10}$$

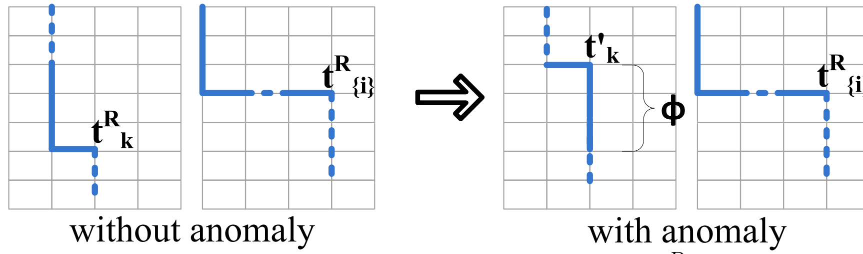

Figure 3.13: Case 2 (a) (i) t'_k is less than $t^R_{\{i\}}$

(i) If $t'_k < t^R_{\{i\}}$ then the merged snapshot (S_m) will store $t^R_{\{i\}}$ as the retire cycle for all instructions $k \cup \{i\}$. If $t^R_k < t^R_{\{i\}}$, then this change due to ϕ did not matter anyways, as k's retire time was not contributing to the worst-case state to be seen by future instructions. If, on the other hand, $t^R_k > t^R_{\{i\}}$ (as shown in Figure 3.13), then the effect of the anomaly is that it changed the worst-case behavior of instructions in path X. The significance of this effect is that instructions in the other path will contribute to the worst-case state that is carried forward beyond S_m, and the worst-case retire cycle is now $t^R_{\{i\}}$, which is less than the original t^R_k.

(ii) If $t'_k > t^R_{\{i\}}$, then the merged snapshot (S_m) will store t'_k as the retire cycle for all instructions $k \cup \{i\}$. Hence, the decrease in retire time for k results in changes to the snapshot. Instructions previously retired at t^R_k now retire earlier (at t'_k) as seen in Figure 3.14. Thus the pipeline effect will propagate beyond S_m.

Remark: This condition holds only if $t^R_k > t^R_{\{i\}}$; otherwise, it would default to case IV (a) (i).

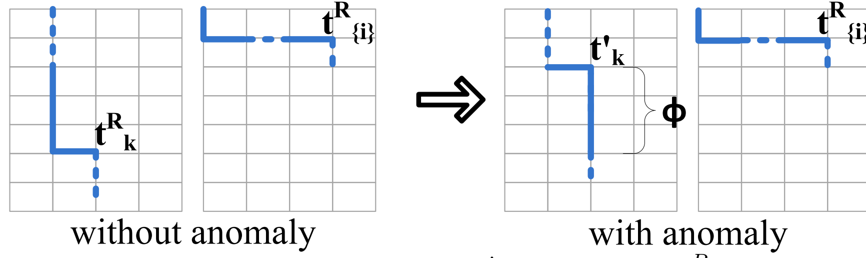

Figure 3.14: Case 2 (a) (ii) t'_k is greater than $t^R_{\{i\}}$

Case 2: ***(b)*** ϕ decreased the WCET of X. Hence,

$$C'_X = C_X - \phi \tag{3.11}$$

(i) If $C'_X < C_Y$ (Figure 3.13), then the WCET for the entire construct will now be C'_Y. If $C_X > C_Y$, then ϕ has already affected the WCET of the program. Where C_X would have been chosen originally for the WCET of the construct in Figure 3.10, C_Y is now chosen. Of course, if $C_X < C_Y$, then the anomaly limits its effects between S_{branch} and S_m. It does not affect the WCET for the two alternate paths because C_Y would have been chosen anyways.

(ii) If $C'_X > C_Y$ (Figure 3.14), then the WCET for the entire construct will now be C'_X. Hence, ϕ has resulted in a reduction of the WCET of the program from the original C_X.

Remark: This condition is true only if $C_X > C_Y$, else it reverts to the situation in IV (b) (i).

(V) Case 3: ***(a)*** ϕ did not affect the retire times of any instructions in the snapshot. Hence,

$$t'_k = t^R_k \tag{3.12}$$

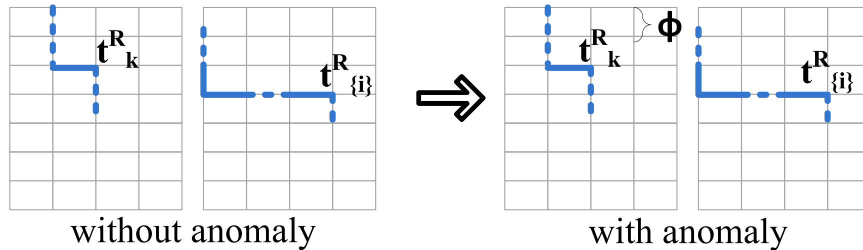

Figure 3.15: Case 3 (a) neither t'_k nor $t^R_{\{i\}}$ change

The effects of ϕ are completely encapsulated within the boundary between the two snapshots (*i.e.*, between S_{branch} and S_X). Hence, it is not necessary to consider the anomaly as it will not affect the execution of future instructions (beyond the merge point) because the effects of the anomaly on the pipeline have been dissipated/absorbed before the instructions in snapshot S_X reach

the retire stage (Figure 3.15).

Case 3: ***(b)*** ϕ did not change the execution time of X (Figure 3.15). Hence,

$$C'_X = C_X \tag{3.13}$$

(VI) Case 1: ϕ increased the [Entry,exit] for k. Hence,

$$[E, e]'_k = [E + \phi, e + \phi]_k \tag{3.14}$$

(i) If $e'_k > e_{\{i\}}$, then the merged reservation station state will have an entry cycle of $\max(E'_k,\ E_{\{i\}})$ and an exit cycle of $\max(e'_k,\ e_{\{i\}}) = e'_k$. Hence, although instructions may gain access to the execution unit later than they would have (if $E'_k > E_{\{i\}}$), they are not allowed to vacate the unit until later (e'_k). These effects are due to the increase in time by ϕ.

(ii) If $e'_k < e_{\{i\}}$, the merged reservation station state will have an entry cycle of $\max(E'_k,\ E_{\{i\}})$ and an exit cycle of $\max(e'_k,\ e_{\{i\}}) = e_{\{i\}}$. Hence, the exit times for the merged state is not affected by this change. This is similar to the situation in II, Case (1)(a)(ii) where the effects of the anomaly would not have propagated since the reservation station state of the path comprising k does not reflect the worst-case behavior. Depending on whether E'_k or $E_{\{i\}}$ is greater, the instruction may or may not gain access to the reservation station earlier.

Case 2: ϕ decreased the [Entry,exit] for k. Hence,

$$[E, e]'_k = [E - \phi, e - \phi]_k \tag{3.15}$$

(i) If $e'_k < e_{\{i\}}$, the merged reservation station state will have an entry cycle of $\max(E'_k,\ E_{\{i\}})$ and an exit cycle of $\max(e'_k,\ e_{\{i\}}) = e_{\{i\}}$. If $e_k < e_{\{i\}}$, then the change did not matter since k's reservation station state was not contributing to the worst-case state of the merged snapshot. If, on the other hand, $e_k > e_{\{i\}}$, then the effect of the anomaly was to modify the worst-case behavior of instructions in the path. Instructions from the other path (with their corresponding state of reservation stations) will contribute to the worst-case behavior for the task. Hence, the effect of the anomaly is seen. Instructions that execute post-merge gain access to execution units earlier than they would have, thus reducing overall execution time and, hence, retaining the original effect of the anomaly.

Instructions that are a part of the snapshot also gain access to the reservation stations at a later time, depending on whether E'_k or $E_{\{i\}}$ is greater.

(ii) If $e'_k > e_{\{i\}}$, the effect of the anomaly was to reduce the time taken for instructions to be issued to execution units. The state of the merged reservation station will be, $[\max(E'_k,\ E_{\{i\}}),\ e'_k]$. Without reservation stations, instructions would have been able to exit from the execution units at e_k. Due to the presence of reservation stations, they now exit at time $e'_k < e_k$. Hence, the effect of the anomaly in reducing the execution time is carried forward beyond the merge.

(VII) Case 1: ϕ increased the RF entry for k. Hence,

$$RF'_k = RF_k + \phi \tag{3.16}$$

(i) If $RF'_k > RF_{\{i\}}$, then the merged register reservation station state will store the value, RF'_k. Hence, instructions that depend on the register corresponding to RF will gain access to the execution unit *later* than they would have due to the increase in time by ϕ.

(ii) If $RF'_k < RF_{\{i\}}$, the merged register reservation station state will will store the value $RF_{\{i\}}$. This is similar to the situation in II, Case (1)(a)(ii) and VI Case (1) (a) (ii), where the effects of the anomaly would not have propagated since the register reservation station state of the path comprising k does not reflect the true worst-case behavior.

Case 2: ϕ decreased the RF for k. Hence,

$$RF'_k = RF_k - \phi \tag{3.17}$$

(i) If $RF'_k < RF_{\{i\}}$, the merged register reservation station state will have a cycle of $RF_{\{i\}}$. If $RF_k < RF_{\{i\}}$, then the change did not matter since k's register reservation station state was not contributing to the worst-case state of the merged snapshot. If, on the other hand, $RF_k > RF_{\{i\}}$, then the effect of the anomaly was to modify the worst-case behavior of instructions in the path. Instructions from the other path (with their corresponding state of reservation stations) will contribute to the worst-case behavior for the task. Hence, the effect of the anomaly is seen. Instructions that execute post-merge are allowed to access the data written into the register file earlier than they would have, thus reducing overall execution time hence retaining the original effect of the anomaly.

(ii) If $RF'_k > RF_{\{i\}}$, the effect of the anomaly was to reduce the time taken for instructions to gain access to the data (they depend on) from the register file. The state of the merged

register reservation station will be, RF'_k. Without register reservation stations, instructions would have been able to read the required data values at RF_k. Due to the presence of reservation stations, they now get the required inputs (from the register) at $RF'_k < RF_k$. Hence, the effect of the anomaly in reducing the execution time is carried forward beyond the merge.

Cases (I) – (VII) proved that pipeline effects due to timing anomalies (or other pipeline effects) will be retained post-merge if the merge is based on the DRM algorithm. If the pipeline effects resulted in increases or decreases (execution time/retire cycles/*etc.*), then these effects are carried over if these effects changed the worst-case behavior of the path. Hence, this proof holds for merging any *two snapshots*. □

Theorem 3.9.2. *Correctness of Merging Multiple Snapshots: The algorithm in Figure 3.9 is correct with respect to preserving worst-case timing effects in the pipeline when merging multiple snapshots.*

Proof. The DRM algorithm is effectively applied recursively to perform merges on multiple snapshots. The "drm_merge" algorithm is called on *two* snapshots at a time to obtain a merged state, which is then merged with the next snapshot and so on. This chapter has shown above that pipeline effects are not lost when merging two snapshots at a time. Since merging multiple snapshots occurs two at a time, one can infer that the pipeline effects will be retained across merging multiple snapshots if the said effects alter the worst-case behavior of the paths. Hence, the proof hold true for merging an arbitrary number of snapshots. □

3.10 Merging Register Files

To perform a merge on the register file state ("RF" from Figure 3.3) a simple technique is applied to each register:

- If the register value is *unchanged* across the snapshots, then the merged state will retain that value in the register;

- If the register value is *different*, then set the merged value to a Not-A-Number (NaN) [86]. This is to handle values that are input-dependent which will not be known until run-time. This is safe due to the conservative semantics of any operation of NaN that, by definition, results in a conservative value (NaN unless trivial arithmetic rules apply, such as multiplication with zero) and in conservative temporal requirements (worst-case number of cycles for this operation under the given operands).

Performing the above checks/modifications on every register in the register file in both snapshots allows easy construction of a new "merged" state for the register file. *Note:* a merge on register files deals with the actual register values. This is different from merging reservation stations for register files (Section 3.8.3).

The ability to extract and/or write back register file state can be realized by simple modifications of existing microarchitecture features, *i.e.*, the Precise Event-Based Sampling (PEBS) with user-selected access to selected shadow buffers [114] present in the Intel X86 architecture. The CheckerMode design makes buffers used in this and other architectural techniques uniformly available to the user.

3.11 Implementation

The *CheckerMode* infrastructure has been implemented on an enhanced *SimpleScalar* processor simulation framework [21]. It has the ability to model a variety of processor configurations (SMT, CMP, *etc.*). The previous chapter (Chapter 2) illustrated how the simulator was enhanced by adding the ability to start/stop execution at given arbitrary program counter (PC) values as well as the ability to capture timing information for the given range of PCs. It has now been further modified to include the process of capturing the state of the processor during the *issue* stage (*i.e.*, using the concept of reservation stations introduced in this chapter). It also includes the ability to capture and merge snapshots and to reset the state of the the pipeline to a given snapshot as detailed in this paper.

3.12 Conclusion

This chapter outlined a sophisticated pipeline analysis scheme that is able to estimate the worst-case behavior of out-of-order pipelines in a *safe* manner. It also showed that CheckerMode is able to correctly deal with timing anomalies and has the ability to conduct the analysis in ways that are minimally invasive with respect to the processor. More specifically, minor changes to existing micro-architectural features are suggested, that extend contemporary monitoring techniques already present in hardware. This analysis, when integrated with the CheckerMode infrastructure, utilizes interactions between hardware and software to make contemporary processors predictable and analyzable. Such processors may now be safely used in real-time systems, thus moving the state-of-the-art forward. This work will enhance the design choices that are available to designers

of embedded and real-time systems, particularly on the high-end of computational requirements. The analysis methods presented in this and the preceding chapter are the first of their kind that deal with out-of-order processing and timing anomalies.

Chapter 4

Fixed Point Loop Analysis for High-End Embedded Processors

4.1 Summary

Analysis of loops complicates the process of obtaining accurate WCET values on contemporary processors. To obtain bounds on the execution times for loops, one is forced to analyze *each* and *every* iteration. This imposes an analysis overhead linear to the number of iterations in the entire loop. Also, actual bounds on loop execution may not be statically available to perform a complete loop analysis. This chapter presents a technique that reduces the complexity of loop analysis by enumerating/executing only the first few iterations of loops through the CheckerMode architecture while analytically determining the remaining ones using a fixed point approach.

4.2 Introduction

The previous two chapters introduced the CheckerMode concept and also the process of capturing snapshots for straight-line code. The process of analyzing loops using CheckerMode is not straightforward due to the lack of information on the loop bounds at compile time. This chapter introduces techniques to reduce the complexity of the analysis for loops to ensure that analysis overhead is independent of the number of loop iterations.

Static analysis of loops has an increased complexity for a variety of reasons. To determine the worst-case execution bounds for the entire loop, it may be necessary to enumerate or symbolically execute all iterations of the loop body, which is not always a trivial task. Added complexities

arise if the loop body consists of multiple alternating paths, further increasing the complexity of bounding the WCET of paths. Also, since it may not always be possible to determine the actual execution bounds for each loop during static analysis due to input dependencies, the extent of enumeration/execution may not be discernable.

This chapter presents a technique that analyzes loop iterations until they reach a *fixed point*. This fixed point must be evaluated on multiple "dimensions," so as to speak. Two such dimensions need to be evaluated – *time* and *state* of the pipeline. Once the loop iterations reach a fixed point, it is possible to extrapolate it for the remaining iterations to estimate the execution time for the entire loop.

This chapter is organized as follows: Section 4.3 explains the analysis technique applied to loops. Section 4.4 details the experimental setup. Section 4.5 enumerates the results for experiments that only deal with the time dimension, while Section 4.6 discusses results that show the validity of analyzing pipeline state. Section 4.7 summarizes the contributions of the chapter.

4.3 Reduction of Analysis Overhead for Loops

The complexity of determining WCETs for loops is reduced by a *partial execution of loops* delineated by a fixed point in WCET such that the analysis overhead is independent of the number of loop iterations. Building on prior approaches that utilize fixed point algorithms to determine stable execution times for loop bodies [10], loop execution can be steered such that paths of a loop body are repeatedly executed until a stable value is reached. The following sections illustrate problems with the traditional fixed point timing analysis (Section 4.3.1) and how they can be overcome using the CheckerMode infrastructure (Section 4.3.2).

4.3.1 Fixed Point Timing and Out-of-order Execution

Prior approaches only studied fixed point approaches in the *time* dimension, *i.e.*, the number of cycles to execute each iteration. Hence, if the number of cycles to execute successive loop iterations reaches a stable value (or changes by a known, constant value) then it is assumed that the loop has reached a fixed point and that the execution time for the remaining iterations can be extrapolated from the information gathered thus far.

Out-of-order (OOO) execution can cause problems while trying to determine a fixed point for individual loop iterations. The main reason is that *instructions from different iterations can over-*

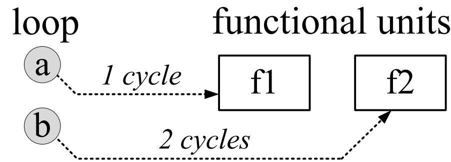

Figure 4.1: Counter example against use of only fixed point timing

lap resulting in unexpected timing differences between even neighboring iterations. For instance, while the execution time for successive iterations can monotonically decrease for the first few iterations, there is no guarantee that the number of cycles for the remaining iterations will not *increase*. It could even *oscillate*, *i.e.*, increase then decrease for successive (or groups of successive) iterations.

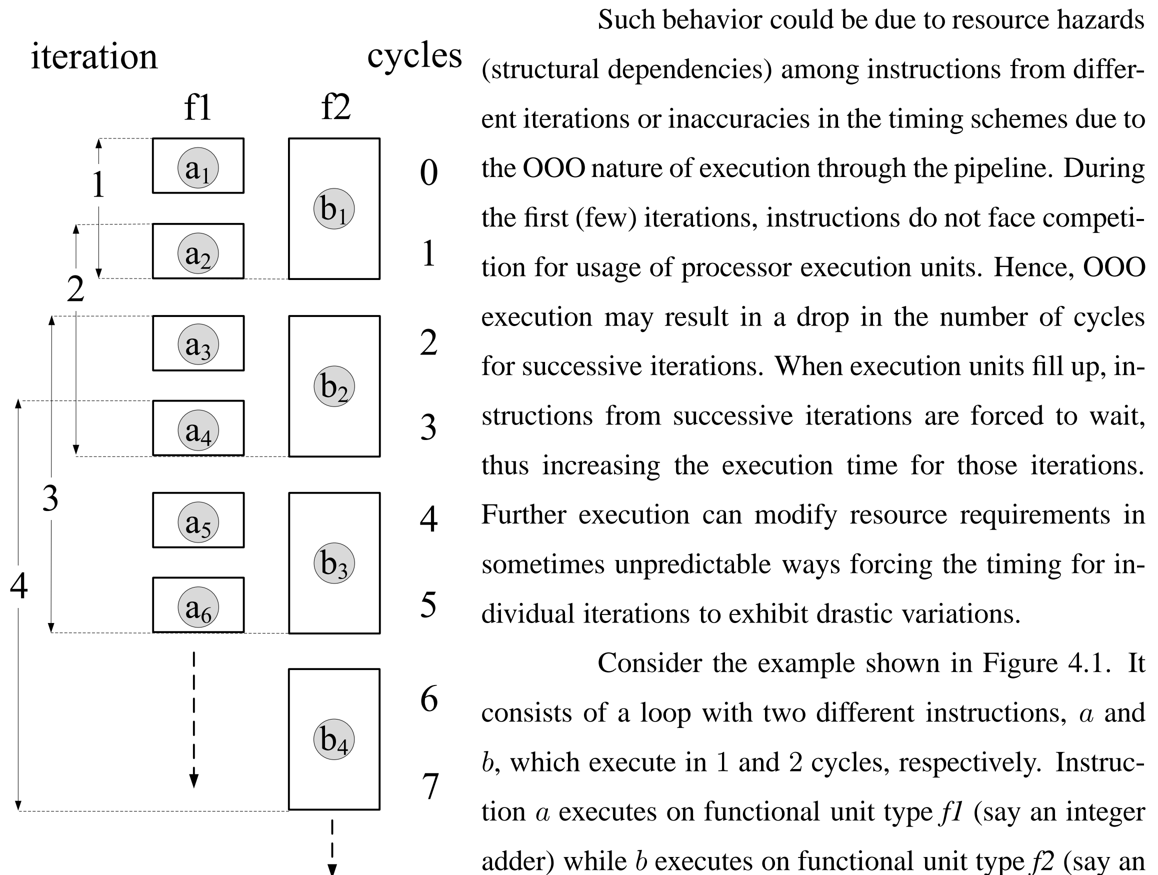

Figure 4.2: Execution of counter example through the pipeline

Such behavior could be due to resource hazards (structural dependencies) among instructions from different iterations or inaccuracies in the timing schemes due to the OOO nature of execution through the pipeline. During the first (few) iterations, instructions do not face competition for usage of processor execution units. Hence, OOO execution may result in a drop in the number of cycles for successive iterations. When execution units fill up, instructions from successive iterations are forced to wait, thus increasing the execution time for those iterations. Further execution can modify resource requirements in sometimes unpredictable ways forcing the timing for individual iterations to exhibit drastic variations.

Consider the example shown in Figure 4.1. It consists of a loop with two different instructions, a and b, which execute in 1 and 2 cycles, respectively. Instruction a executes on functional unit type *f1* (say an integer adder) while b executes on functional unit type *f2* (say an integer multiplier). Assume that the processor pipeline has just one of each type of functional units. Figure 4.2 illustrates the execution and the functional unit usage of the first few iterations of this loop. Subscripts for instructions denote which iteration that particular instruction belongs to (for *e.g.*, a_3 is instruction a from the third iteration). The instructions do not depend on each other or on previous incarnations (same instruction in previous iteration). Figure 4.2 shows that every instance of in-

struction b executes in parallel with *two* instructions of type a. This is due to the fact that instruction a takes only 1 cycle to execute, and out of order instruction issue allows an instruction (a in this case) from a future iteration to execute before instruction b completes. Hence, while a_1 and b_1 start at the same time (cycle 0), a_1 completes execution in 1 cycle, thus freeing up functional unit f1. Instruction a_2 is issued to f1 even though b_1 is not complete. Instructions b_1 and a_2 complete at the same time and vacate their respective functional units, at which time instructions a_3 and b_2 are issued.

Consider groups of instructions as successive iterations, as depicted on the left hand side of Figure 4.2. Instructions a_1 and b_1 constitute iteration 1, instructions a_2 and b_2 constitute iteration 2, *etc.* Let us make a simplifying assumption that each instruction takes the same number of cycles, t^B (representing t^{Before}), in the pipeline before reaching the issue/execute stage and also that each instruction takes the same number of cycles, t^A (representing t^{After}), to exit from the pipeline once it exits from its respective functional unit. Let c^E (c^{Enter}) represent the cycle when an instruction enters its particular functional unit (*i.e.*, its issue time) and c^e (c^{exit}) represent the time when it completed execution (*i.e.*, it released the functional unit). Hence, using the "Path-Aggregate" timing scheme described in from Section 2.4 (start timing a *path* when the first instruction from it is fetched and stop when the last instruction retires), the execution time for loop iteration i will be:

$$t_i = t^B_{a_i} + (c^e_{b_i} - c^E_{a_i}) + t^A_{b_i} \tag{4.1}$$

The middle term from Equation 4.1, $(c^e_{b_i} - c^E_{a_i})$, now denotes the *potential for variability* in execution time of each loop iteration during the execute stage. Substituting values from the example in Figure 4.2, the respective execution times for iterations 1, 2, 3 and 4 are:

$$\begin{aligned}
t_1 &= t^B_{a_1} + \mathbf{2} + t^A_{b_1} \\
t_2 &= t^B_{a_2} + \mathbf{3} + t^A_{b_2} \\
t_3 &= t^B_{a_3} + \mathbf{4} + t^A_{b_3} \\
t_4 &= t^B_{a_4} + \mathbf{5} + t^A_{b_4}
\end{aligned} \tag{4.2}$$

Hence, the number of cycles calculated using traditional techniques can actually show an *increase* for successive loop iterations (for this particular example). This is an example of a loop where it is difficult, if not impossible, to determine the fixed point for the timing of individual loop iterations.

4.3.2 Fixed point Pipeline State Analysis using Reservation Stations

To tackle the problems due to OOO execution (Section 4.3.1), the fixed point analysis technique is enhanced to find *stable values in multiple "dimensions"* (two, to be exact, for the given constraints of only pipeline analysis in this dissertation):

1. *time*: the number of cycles to execute successive iterations through the pipeline must monotonically *decrease*; and

2. *pipeline state*: the instructions in the reservation stations must repeat across groups of iterations where a "group" is defined as *one or more* iterations.

A controller records the monotonically decreasing execution times for each iteration up to the fixed point using the CheckerMode hardware. The mechanism created to capture snapshots (Chapter 3) is utilized to record the state of the reservation stations at the end of each iteration. The example in Section 4.3.1 shows that just relying on the number of cycles to reach a fixed point may not result in accurate timing values. In fact, it might not even be possible to detect a fixed point using this approach. The state of reservation stations at the end of each iteration needs to be examined across loop iterations (either with immediate neighbors, or over longer distances) to *find repeating patterns* of demands on the usage of execution units within the pipeline. *E.g.*, if the snapshots (at the end of each iteration) indicate that the *exact* same instructions are using the same functional units in successive iterations, then it can concluded that the execution of the loop through the pipeline has reached a stable state. *Note:* It might be necessary to examine multiple loop iterations (perhaps taken as groups) to find a repetitive pattern.

Hence, a search needs to be carried out on the state of the reservation stations such that after iteration i, a pattern exists between iterations $i - x$ and $i - y$ that is the same as the pattern between iterations $k - x$ and $k - y$, where $k < i$ and $x < y$. Once such a pattern is found and the execution times across those iterations are also seen to repeat, then the WCET for the remainder of loop iterations, up to the loop bound, is calculated by a closed formula based on the fixed point value. Figure 4.2 shows such a pattern repeating in loop iterations that are immediate neighbors. At the end of each iteration, *two* instructions of type a and *one* instruction of type b have executed through the functional units. This pattern repeats for all succeeding iterations. Even if the execution times do not reach a fixed point value (example in Section 4.3.1), it might be possible to obtain *correct* and *tight* fixed point values for loop iterations by examining the (stable) pipeline state. While Equation 4.2 shows that the *measured* execution times for successive loop iterations increase, it might be possible

to infer tighter and more accurate execution times for individual loop iterations by examining the state of reservation stations.

Figure 4.2 shows that 4 iterations complete in exactly 8 cycles, and that the addition of each extra iteration only increases the total time by 2 cycles. Hence, the loop has reached a fixed point both in the state of the pipeline as well as in execution time. This is not obvious by measuring the execution time but becomes evident after an examination of the state of the reservation stations. It is now possible to extrapolate for remaining iterations of this loop by using 2 cycles as the fixed point execution time for each successive iteration. *Note:* This is the advantage of using reservation stations to check for a fixed point in contrast to, *e.g.*, the reorder buffer (ROB). The ROB does not contain information about the execution time characteristics of individual instructions that flow through the pipeline.

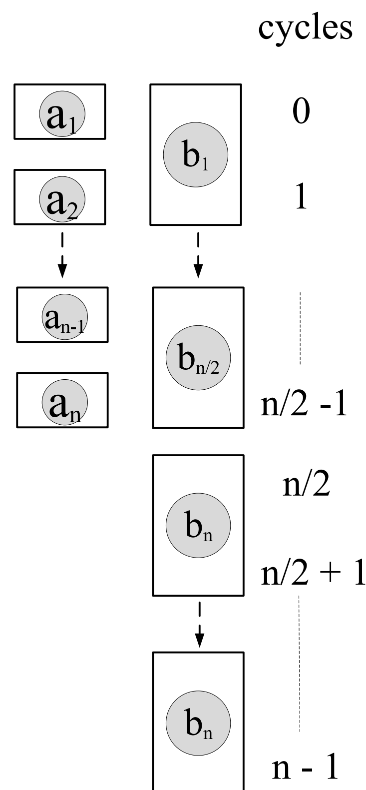

Figure 4.3: A Second Fixed Point

The loop execution pattern in Figure 4.2 shows that instructions of type a complete execution twice as fast as instructions of type b. Hence, if the entire loop executed for a total of 100 iterations, then all a instructions would complete execution within the first 100 cycles while the loop would not complete execution until cycle 200 (because of the trailing b's). Hence, halfway through the execution of the loop, the situation shown in Figure 4.3 occurs. The original fixed point with two instructions of type a and one instruction of type b ceases to exist, and a new fixed point consisting of *only* bs becomes evident. This simple example illustrates the fact that a loop can have multiple fixed points and it is necessary to detect all of them to perform a correct (and tight) analysis for the loop. In the example presented in Figure 4.3, it is possible to predict when execution patterns change and, hence, when the search for a new fixed point must be started (by examining the instruction mix of the loop). This simple loop has two instructions. Instructions of type a will complete in half the time taken by instructions of type b. Hence, a search for the *second* fixed point can be started halfway into the loop execution. While it is technically possible that a large number of fixed points can occur for more complex loop structures, in practice loops reach their fixed point relatively quickly and the number of such fixed points are small. If

the total number of loops iterations is statically known, then it is possible to predict subsequent fixed points *precisely* and then use that information to estimate the correct WCET for the entire loop. If the upper bound on loop iterations is not know, then the formulae calculating the worst-case behavior of the loop can reflect a generic estimation on the locations of these fixed point (*e.g.*, starting from cycle $n/2$ in Figure 4.3).

In the next example, if we relax the restrictive assumption that the two functional units f1 and f2 (Figure 4.1) are different, then the execution pattern changes to that shown in Figure 4.4. Since either instruction can now execute on both functional units, instruction b_2 gets issued over instruction a_3 at cycle number 2 because b_2 was fetched before a_3. Instructions a_3 and a_4 are issued in parallel with b_2, but on functional unit f2. In cycle 4, both f1 and f2 execute instructions of type b (b_3 and b_4), since they are ahead of instructions a_5 and a_6 in the issue queue. Figure 4.4 shows that the pattern set in iterations 1–4 (cycles 0 to 5) repeats starting from cycle 6. Hence, to find a fixed point, analysis must be carried out on consecutive *groups* of four iterations each. To calculate the equivalent fixed point in time, the figure shows that a group of 4 iterations complete execution in 6 cycles. This can be used to extrapolate the WCET for the remaining iterations.

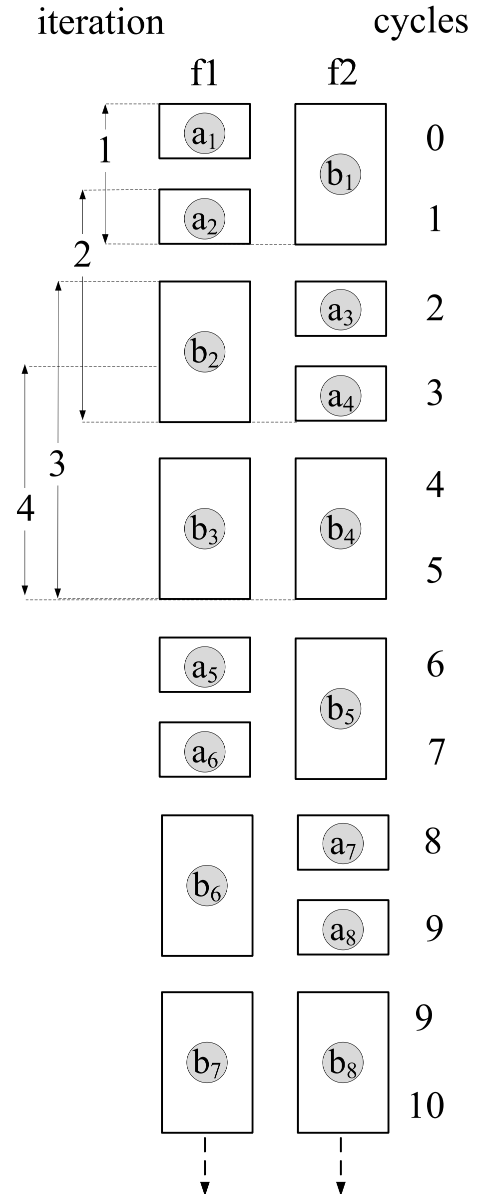

Figure 4.4: Alternative Execution Scenario for counter example

Since the work in this dissertation only deals with the analysis of the processor pipeline and related effects, it is necessary to only analyze *two* dimensions for evaluating the fixed point. In theory, similar analysis could be extended to a *multi-dimensional* fixed point analysis, with additional "dimensions" representing other processor features (*e.g.*, branch predictors, caches).

Experimental results in Section 4.5 indicate that loops reach a fixed point in the time dimension after only 3 iterations to account for pipeline effects. Another two iterations are required on average in the

presence of caches. Experiments on a simple benchmark, illustrated in Section 4.6, show that the pipeline state can reach a fixed point within the first 2 iterations. *Note:* These experiments were carried out on simple, synthetic benchmarks intended as a proof-of-concept. More complicated programs might take longer to attain a stable pipeline state.

This technique of partial executions can significantly reduce the overhead of WCET analysis. Thus, the complexity of WCET analysis is *independent of the number of loop iterations*. It does not depend on the dynamic execution time of the analyzed code.

4.4 Experimental Framework

As before, the key components of the design were implemented in an enhanced version of the SimpleScalar processor simulator [22] executing in one of three configurations: SimIO, SupIO and OOO (Chapter 2).

To illustrate how analysis of only the time dimension can yield useful results, experiments were conducted on the C-Lab benchmarks (Table 2.1). To obtain the execution times for the various paths in the benchmark, the timing schemes from Chapter 2 were used. Loops in every function of the each of the C-Lab benchmarks were analyzed. All possible paths in each loop were identified and then analyzed for one, two and three iterations. In the first iteration, paths are timed one at a time. In the second iteration, compositions of the paths in these loops were timed by considering two iterations at a time, while in the third iteration, compositions of three iterations were timed at a time.

The results of these analyses are presented in Section 4.5. *All* loops were analyzed independently (inner as well as outer), starting from the outer to inner. Worst-case execution cycles (WCECs) for inner loops were obtained and subsequently substituted in the the outer loop paths assuming an upper bound on the number of iterations for that inner loop is known.

```
int A[n] ;
main () {
    repeat (n times) {
        // Series of Arithmetic Operations
        // that involve array A
    }
}
```

Figure 4.5: Synthetic Benchmark for Analyzing Stable state of Reservation Stations

Two variants of the synthetic benchmark from Figure 4.5, “*long*” and “*short*”, were used to test the process of capturing pipeline

state (snapshots) at the end of each loop iteration. The snapshots thus captured were examined to find repeating patterns within the state of reservation stations. The two variants ("long" and "short") differ only in the number of arithmetic operations within the main loop. The "long" version has enough operations (over 30 C integer arithmetic expressions) so that each loop iteration completely fills the pipeline, thus reducing interference from instructions belonging to other iterations. The "short" version has fewer arithmetic operations (2 C integer arithmetic operations) that do not fill the pipeline, which are overlapped by instructions from neighboring iterations. The loop in each benchmark was executed for a total of $n = 10$ iterations.

4.5 Time Dimension Analysis Results

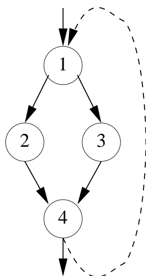

Figure 4.6: CFG

As explained in Section 4.4, compositions of loop paths were created for all loops in the benchmark. These results are explained in Sections 4.5.1 and 4.5.2. These WCECs are then reused to calculate the WCECs for loops that form longer paths in the benchmarks in Section 4.5.3. While these sections concentrate on the SRT and ADPCM C-Lab benchmarks, Section 4.5.4 provides similar results from other benchmarks in the suite.

4.5.1 Partial Analysis of Loops

Consider the CFG depicted in Figure 4.6. It shows a branch embedded within a loop. To assess the worst-case timing behavior of such a loop, consecutive executions of alternate paths in the loop must be considered. *E.g.*., in the first iteration, the L-left (BB 1,2,4) and R-right (BB 1,3,4) paths are timed; in the second iteration, concatenations of all permutations for these paths are timed (L-L/L-R/R-L/R-R); and so on for three and four iterations. This search space grows exponentially with the number of alternate paths and loop iterations thus complicating the task of worst-case timing on

Table 4.1: Path-Aggregate Cycles (3 Iterations)

Path	SimIO			SupIO			OOO		
	$+$	o	δ	$+$	o	δ	$+$	o	δ
LLL	453	443	10	291	193	98	183	123	60
LLR	580	570	10	328	230	98	216	156	60
LRL	580	570	10	328	230	98	216	156	60
LRR	707	697	10	365	267	98	249	189	60
RLL	580	570	10	328	230	98	216	156	60
RLR	707	697	10	365	267	98	249	189	60
RRL	707	697	10	365	267	98	216	189	60
RRR	834	824	10	402	304	98	282	222	60

the CheckerMode infrastructure. Hence, a bounded technique to limit the path space in depth and breadth is proposed here.

Table 4.1 depicts the results for 3 iterations of this loop around the left (L) or right (R) paths or the 3 processor models for the simple example depicted in Figure 4.6. It distinguishes path composition *without overlap* (+) from those *with overlap* (o). The former is equivalent to draining the pipeline while the latter captures continuous execution and the difference between the compositions is depicted as δ.

The table shows constant δ values for all processor models, regardless of paths executed (D-caches are disabled here), for this simple test case. More significantly, results the experiments indicate that 2–4 iterations generally suffice to reach a fixed point, after which concatenation of another iteration results in a constant increase in cycles for that particular path – this behavior does not change for the remaining execution of the loop. *E.g.*, a two-path experiment for the same benchmark (omitted here) resulted in exactly *half* of the δ values as compared to the three-path experiment, thus reinforcing the claims of reaching a fixed point.

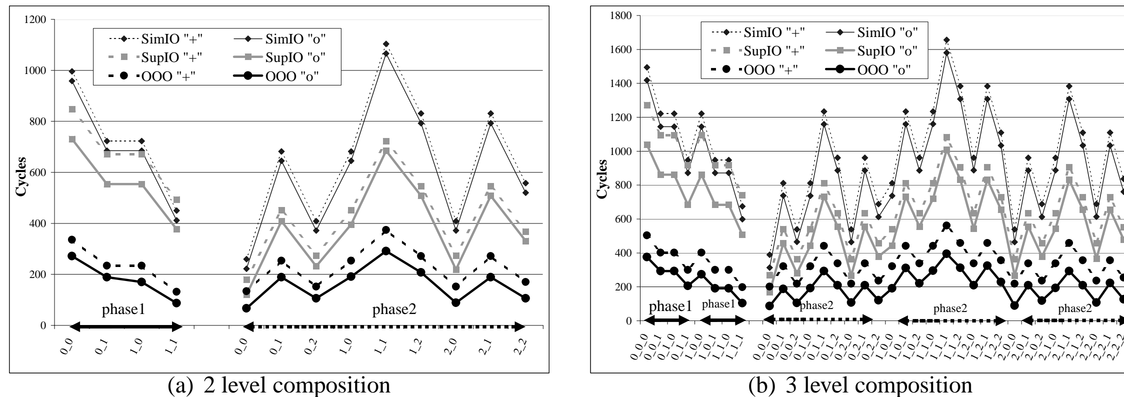

(a) 2 level composition (b) 3 level composition

Figure 4.7: Measured execution cycles for loop path compositions (SRT *bubblesort* function)

4.5.2 CLab Benchmarks: SRT benchmark

This method of composing paths from consecutive loop iterations was also carried out on the various C-Lab benchmarks. Consider the *bubblesort* function in the SRT benchmark. This function has two nested loops (loop1, loop2 – loop1 is the inner loop.) Loop 1 has two alternate paths (0/1), while loop 2 has three possible paths (0/1/2). Figure 4.7 shows the results obtained for the *bubblesort* function of the SRT benchmark for all three processor configurations as well as paths *with overlap* "o" and *without overlap* " $+$ ".

Figure 4.7(a) shows the results obtained by combinations of **two** consecutive iterations

at a time and Figure 4.7(b) shows similar results for combinations of **three** consecutive iterations at a time. *The x-axis labels in Figure 4.7 refer to path concatenations*, *i.e.*, 0_1_2 refers to the concatenated execution of paths 0, 1 and 2. They *do not* refer to loops. The two separate plots in each graph demarcate results for each loop.

Table 4.2: Path-Aggregate Cycles (2 Iterations) for the bubblesort function of SRT.

Id	Path	SimIO			SupIO			OOO		
		+	*o*	δ	+	*o*	δ	+	*o*	δ
1	0_0	996	958	38	848	731	117	336	272	64
1	0_1	723	685	38	671	554	117	234	189	45
1	1_0	723	685	38	671	554	117	234	170	64
1	1_1	450	412	38	494	377	117	132	87	45
2	0_0	260	222	38	180	120	60	134	67	67
2	0_1	682	645	37	451	409	42	254	189	65
2	0_2	409	372	37	274	232	42	152	106	46
2	1_0	682	645	37	451	396	55	254	191	63
2	1_1	1104	1066	38	722	685	37	374	291	83
2	1_2	831	793	38	545	508	37	272	208	64
2	2_0	409	372	37	274	219	55	152	89	63
2	2_1	831	793	38	545	508	37	272	189	83

At the outset, it can be seen that all path compositions follow the strict ordering of $SimIO \geq SupIO \geq OOO$. Also note that the execution of the three-level compositions exceed those of the two-level compositions by a uniform constant. This is immediately obvious while comparing the regions marked as *phases* in both graphs. For Loop 1 (phase 1) the "shape" of the graph from Figure 4.7(a) is repeated in Figure 4.7(b). The difference is that the actual execution cycles are higher (by this uniform constant) for the three-path compositions.

Hence, increasing the level of compositions increases the execution time by a constant value for each path composition. Similar results are evident for the more complicated outer loop (loop 2) with three alternate paths (0/1/2). The shape of "phase 2" repeats multiple times in the three-way composition, thus indicating that the execution cycles for the these paths are offset by a constant from corresponding two-way path compositions. Thus, any further increases in composition depth will only add a constant value to the path execution time. Hence, a fixed point has been reached for the loops in *three* iterations.

It is also interesting to note that while the actual permutation of paths are not necessarily related to each other, their relative order in the plot shows an important result – that increasing loop composition "depth" increased the cost of execution for that path by a uniform constant value, (illustrated by the shape of the graph).

It can be seen that the paths have reached a fixed point from the differences between path compositions *without overlap* and *with overlap* in Tables 4.2 and 4.3. The former (without overlap)

is akin to draining the pipe after each iteration (or a simple addition of the cycles times for each path) while the latter (with overlap) illustrates continuous execution. "Id" refers to the loop id - loop 1 is nested inside loop 2.

The δ values refer to the difference between the paths without overlap $(+)$ and paths with pipeline overlap (o). Tables 4.2 and 4.3, show that the values for δ for the three-way composition is exactly *double* that of the corresponding δ values for the two-way compositions for all three pipeline configurations. *E.g.*, the δ value for the three-way composition "0_0_0" is 76, which is twice the δ value for the "0_0" composition (38). This effect is observed for all other path compositions as well. This shows that the loop iterations have reached a fixed point.

The execution time for the remaining loop iterations can be extrapolated from information available at this fixed point. Consider the case of loop 1 in the above SRT benchmark for the OOO processor configuration. Let n be the total number of iterations (worst-case) for the loop. Assume that the loop has reached a fixed point after i iterations ($i = 3$ in this case). Also,

Table 4.3: Path-Aggregate Cycles (3 Iterations) for the bubblesort function of SRT.

Id	Path	SimIO			SupIO			OOO		
		$+$	o	δ	$+$	o	δ	$+$	o	δ
1	0_0_0	1494	1418	76	1272	1038	234	504	376	128
1	0_0_1	1221	1145	76	1095	861	234	402	293	109
1	0_1_0	1221	1145	76	1095	861	234	402	293	109
1	0_1_1	948	872	76	918	684	234	300	206	94
1	1_0_0	1221	1145	76	1095	861	234	402	274	128
1	1_0_1	948	872	76	918	684	234	300	191	109
1	1_1_0	948	872	76	918	684	234	300	191	109
1	1_1_1	675	599	76	741	507	234	198	104	94
2	0_0_0	390	314	76	270	168	102	201	87	114
2	0_0_1	812	738	74	541	457	84	321	188	133
2	0_0_2	539	465	74	364	280	84	219	105	114
2	0_1_0	812	737	75	541	444	97	321	193	128
2	0_1_1	1234	1159	75	812	733	79	441	293	148
2	0_1_2	961	886	75	635	556	79	339	210	129
2	0_2_0	539	464	75	364	267	97	219	107	112
2	0_2_1	961	886	75	635	556	79	339	210	129
2	0_2_2	688	613	75	458	379	79	237	121	116
2	1_0_0	812	737	75	541	444	97	321	191	130
2	1_0_1	1234	1159	75	812	733	79	441	311	130
2	1_0_2	961	886	75	635	556	79	339	221	118
2	1_1_0	1234	1160	74	812	720	92	441	295	146
2	1_1_1	1656	1580	76	1083	1009	74	561	395	166
2	1_1_2	1383	1307	76	906	832	74	459	312	147
2	1_2_0	961	887	74	635	543	92	339	209	130
2	1_2_1	1383	1307	76	906	832	74	459	325	134
2	1_2_2	1110	1034	76	729	655	74	357	229	128
2	2_0_0	539	464	75	364	267	97	219	89	130
2	2_0_1	961	886	75	635	556	79	339	209	130
2	2_0_2	688	613	75	458	379	79	237	119	118
2	2_1_0	961	887	74	635	543	92	339	194	145
2	2_1_1	1383	1307	76	906	832	74	459	293	166
2	2_1_2	1110	1034	76	729	655	74	357	210	147
2	2_2_0	688	614	74	458	366	92	237	107	130
2	2_2_1	1110	1034	76	729	655	74	357	223	134
2	2_2_2	837	761	76	552	478	74	255	127	128

of all the path compositions, the
"0_0_0" composition exhibits worst-case behavior. Hence, to be safe, this is the composition must be assumed to exhibit worst-case behavior and hence used for obtaining worst-case execution bound for the loop execution. Now, 3 iterations of loop 1 takes 376 cycles to execute on the OOO configuration. Since a fix-point has been reached, a constant value can be added for each remaining iteration of the loop. The constant value to be added is the difference of the δ's for the three-way and two-way compositions. Hence, for this example, the constant used is:

$$\begin{aligned} c &= \delta_3 - \delta_2 \\ c &= 128 - 64 \\ c &= \mathbf{64} \end{aligned} \tag{4.3}$$

Subsequently, a closed form for calculating the worst-case execution bounds for the loop is derived:

$$loop_wcec = fixed_point_cycles + single_path_len * (n - i) - (n - i) * c \tag{4.4}$$

From the two-level and three-level results, it can be seen that the timing values for paths without composition (plain addition of individual path times) diverges from the path times with composition by a constant (c) for each additional iteration. Hence, to obtain the total time for the loop, the time for the remaining iterations of the loop ($n - i$) along the path whose fixed point was established, must be added.

Substituting the value for c from equation 4.3, the bound the worst-case execution cycles for loop1 is calculated to be:

$$loop_1_wcec = 376 + (n - 3) * 498 - (n - 3) * 64 \tag{4.5}$$

If it is assumed that the loop executes for 100 iterations in the worst-case, then the WCEC for loop 1, according to Eq. 4.5, is 42,474 cycles. While this value might be slightly conservative, one can be assured that it is safe and the process of enumerating all possible combinations for the

Table 4.4: Loop WCEC formulae for loops in SRT benchmark

Loop Id	SimIO	SupIO	OOO
0	466+170*(n-i)-(n-i)22	260+140*(n-i)-(n-i)80	142+70*(n-i)-(n-i)34
1	1418+498*(n-i)-(n-i)38	1038+424*(n-i)-(n-i)117	376+168*(n-i)-(n-i)64
2(1)	1580+(552+1418+498* (n-i)-(n-i)38)*(n-i)-(n-i)38	1009+(361+1038+424* (n-i)-(n-i)117)*(n-i)-(n-i)37	395+(187+376+168* (n-i)-(n-i)64)*(n-i)-(n-i)83

remaining 97 iterations of the loop has been avoided. Once these values have been calculated, all parts of a path that contain the loop can be replaced with the above worst-case bound. Also, since loop 1 is an inner, nested loop, this loop_wcec can be added to the path time for those paths of the outer loop (loop 2) that contain loop 1. Thus, an accurate estimate of the WCEC for loop 2 can be obtained.

Table 4.5: Loop WCEC formulae for loops in ADPCM benchmark

Loop Id	SimIO	SupIO	OOO
0	570+212*(n-i)-(n-i)33	265+147*(n-i)-(n-i)88	138+80*(n-i)-(n-i)51
1	661+235*(n-i)-(n-i)22	378+178*(n-i)-(n-i)78	294+194*(n-i)-(n-i)144
2	1063+381*(n-i)-(n-i)40	620+314*(n-i)-(n-i)161	482+240*(n-i)-(n-i)119
3	515+197*(n-i)-(n-i)38	423+337*(n-i)-(n-i)269	401+273*(n-i)-(n-i)209
4	1063+381*(n-i)-(n-i)40	646+340*(n-i)-(n-i)187	528+286*(n-i)-(n-i)165
5	827+301*(n-i)-(n-i)38	526+296*(n-i)-(n-i)181	486+264*(n-i)-(n-i)153
6	1063+381*(n-i)-(n-i)40	620+314*(n-i)-(n-i)161	482+240*(n-i)-(n-i)119
7	92+56*(n-i)-(n-i)38	111+111*(n-i)-(n-i)111	115+115*(n-i)-(n-i)115
8	529+191*(n-i)-(n-i)22	365+179*(n-i)-(n-i)86	227+121*(n-i)-(n-i)68

The WCEC formulae for all loops in the SRT and ADPCM benchmarks were calculated. The results are depicted in Tables 4.4 and 4.5. Since loops 2 and 1 for the SRT benchmark are nested (1 with 2), the formulae for loop 2 include those for loop 1.

4.5.3 Composing longer benchmark paths using loop WCEC bounds

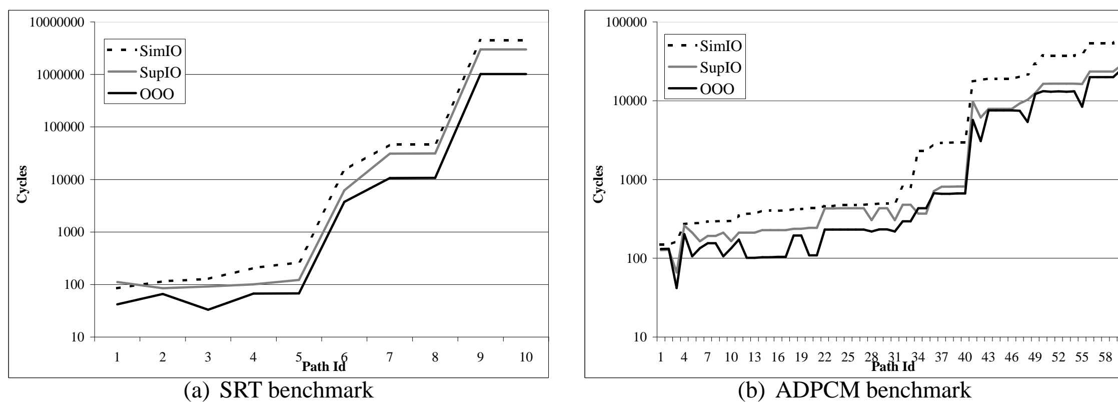

(a) SRT benchmark (b) ADPCM benchmark

Figure 4.8: Complete execution cycles for C-Lab Benchmarks – including loop WCECs

To study the effects of longer paths in the benchmark, all paths from each of the C-lab benchmarks were extracted and timed independently using the CheckerMode framework in each of the three configurations (SimIO, SupIO and OOO). The WCEC's for the loops in each function were calculated using the formulae illustrated in Tables 4.4 and 4.5. These results were included

in the timing for paths that contained these loops. It was assumed that *all* loops executed for 100 iterations each. The results for WCECs for entire paths is illustrated in Figure 4.8. The results are sorted in ascending order based on the timing results for the SimIO configuration. These graphs show that the the $SimIO \geq SupIO \geq OOO$ order is preserved except for one path in the SRT benchmark. With 14 functions and 60 paths, ADPCM is the largest benchmark in the C-lab suite. SRT is a smaller benchmarks with 10 paths. Note that the y-axis is on a logarithmic scale.

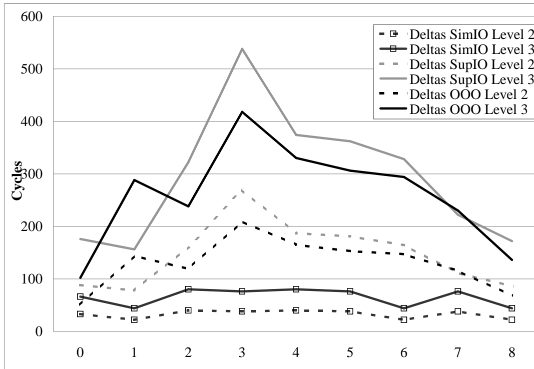

Figure 4.9: δ's for two and three level compositions for nine loops in ADPCM benchmark

Results for the ADPCM benchmark are shown in Figure 4.8(b). SimIO timings are the largest and OOO the smallest. The timing results for SimIO increase significantly around path 42. Paths 42 – 61 originate from the "encode" and "decode" functions of the ADPCM benchmark and contain a larger number of instructions and, in the case of *encode*, a large number of paths as well. While enough parallelism exists in the code for SupIO and OOO to exploit, the SimIO configuration, with its in-order behavior and single width pipeline, is unable to scale as well as the other two configurations. This also indicates that the number of dependencies between instructions in the two functions is not very high — OOO is able to scale well to handle the larger instruction load.

Table 4.6: Path-Aggregate Cycles (2 Iterations) for the FFT benchmark

Id	Path	SimIO			SupIO			OOO		
		$+$	o	δ	$+$	o	δ	$+$	o	δ
0	0_0	1684	1646	38	668	628	40	594	529	65
1	0_0	574	536	38	420	312	108	226	193	33
1	0_1	1268	1231	37	661	553	108	423	390	33
1	1_0	1268	1231	37	661	565	96	423	390	33
1	1_1	1962	1924	38	902	806	96	620	587	33
2	0_0	1684	1646	38	836	712	124	642	553	89
3	0_0	574	536	38	414	309	105	330	245	85
3	0_1	1268	1231	37	655	550	105	527	442	85
3	1_0	1268	1231	37	655	562	93	527	442	85
3	1_1	1962	1924	38	896	803	93	724	639	85

The graph for SRT (Figure 4.8(a)) shows that all three configurations scale in a similar fashion for larger paths, except for the shortest path (path 1). This path is so short that the effects described at the beginning of Section 4.5 becomes apparent. Timing is started when the first instruction of the program is fetched and stopped when the final instruction is retired. Hence, the first instruction has to wait for a while before it is dispatched. When paths become very short, the pipeline contains

a large number of instructions that do not belong to the particular path being timed, thus inflating the results for pipelines with large widths. The SimIO configuration does not suffer from this problem as the instruction is dispatched immediately after being fetched (it is a single width pipeline).

4.5.4 Other CLab Benchmark results

Figure 4.9 shows a plot of the δ values for various loops in the ADPCM benchmark. None of these loops is nested – all of them contain single paths. The figure shows that the δ values for the three-way compositions are twice of those for the two-way compositions. Hence, these loops have also reached a fixed point in just three iterations. From these results, it is possible to extrapolate for the remaining iterations to obtain the final WCECs for each loop. The other benchmarks in the C-Lab suite also exhibited similar behavior.

Table 4.7: Path-Aggregate Cycles (3 Iterations) for the FFT benchmark

Id	Path	SimIO			SupIO			OOO		
		$+$	o	δ	$+$	o	δ	$+$	o	δ
0	0_0_0	2526	2450	76	1002	922	80	891	761	130
1	0_0_0	861	785	76	630	414	216	339	273	66
1	0_0_1	1555	1481	74	871	655	216	536	470	66
1	0_1_0	1555	1480	75	871	667	204	536	470	66
1	0_1_1	2249	2174	75	1112	908	204	733	667	66
1	1_0_0	1555	1480	75	871	667	204	536	470	66
1	1_0_1	2249	2174	75	1112	908	204	733	667	66
1	1_1_0	2249	2175	74	1112	920	192	733	667	66
1	1_1_1	2943	2867	76	1353	1161	192	930	864	66
2	0_0_0	2526	2450	76	1254	1006	248	963	785	178
3	0_0_0	861	785	76	621	411	210	495	325	170
3	0_0_1	1555	1481	74	862	652	210	692	522	170
3	0_1_0	1555	1480	75	862	664	198	692	522	170
3	0_1_1	2249	2174	75	1103	905	198	889	719	170
3	1_0_0	1555	1480	75	862	664	198	692	522	170
3	1_0_1	2249	2174	75	1103	905	198	889	719	170
3	1_1_0	2249	2175	74	1103	917	186	889	719	170
3	1_1_1	2943	2867	76	1344	1158	186	1086	916	170

Tables 4.6 and 4.7 depict the two and three level compositions for the FFT benchmark. The first column depicts the loop ID while the second column shows the particular combination of paths being timed. For example, "0_1_0" represents a three-way combination of paths "0", "1" and "0". As before, the "+' ' represents path timing without overlap while the "o" represents path times with overlap. These tables indicate that the loops reach a fixed point within 2-3 iterations. For example, the δ values for the "0_0" path combination of loop 1 from Table 4.6 is exactly *half* that of the corresponding δ values for the "0_0_0" combination of the same loop (Table 4.7).

4.6 Pipeline State Analysis Results

Table 4.8: "long" Synthetic benchmark

Iter	Entry Cycle	Diff	Num. Instr.
1	7603	-	-
2	13383	5780	578
3	19163	5780	578
4	24943	5780	578
5	30723	5780	578
6	36503	5780	578
7	42283	5780	578
8	48063	5780	578
9	53843	5780	578
10	59623	5780	578

Table 4.9: "short" Synthetic benchmark

Iter	Entry Cycle	Diff	Num. Instr.
1	2213	-	-
2	2373	160	16
3	2533	160	16
4	2693	160	16
5	2853	160	16
6	3013	160	16
7	3173	160	16
8	3333	160	16
9	3493	160	16
10	3653	160	16

This section presents results obtained from analyzing pipeline state to show that reservation stations can achieve a fixed point state (Section 4.3.2). The loops in the "long" and "short" variants of the synthetic benchmark (Figure 4.5) were executed for 10 iterations each. Pipeline snapshots that include the state of the reservation stations were captured at the end of each iteration and analyzed. A concise version of the information gathered from these snapshots is presented in Tables 4.8 and 4.9. The first column in both tables represents the iteration number. The second column ("Entry Cycle") lists the cycle number when the *last* instruction in that particular iteration entered its functional unit (and, hence, the corresponding reservation station). The third column ("Diff") presents the difference between the entry cycles for consecutive iterations. For instance, the value 5780 from column 3 for iteration 2 from Table 4.8 represents the difference between the entry cycle for the last instruction in iteration 2 and the last instruction in its immediate predecessor, iteration 1. Iteration 1 does not have an entry in its difference column since there is no preceding iteration for comparison. The last column ("Num. Instr.") in both tables represents the number of instructions that made entries in their corresponding reservation stations during the execution of that particular iteration. The first entries for both benchmarks in this column are empty since there is no demarcation of the start of an iteration. The first iteration's state and timing are "polluted" by instructions that precede the loop body. Hence, it is difficult to determine the exact number of instructions that accessed functional units during that iteration.

The experiments showed that the *exact same* instructions inhabited the *same functional units* of the pipeline for each successive iteration. These tables present a summary of the informa-

tion obtained from studying the reservation station state captured after each iteration since it is not feasible to present the list of all instructions in the reservation stations (578 of them in the long version) for all iterations. An examination of the "Diff" column shows that the last instruction of each iteration enters its functional unit a constant time step after its corresponding predecessor from the previous iteration. This also reveals the fact that this benchmark has not only reached a fixed point in the pipeline state but also in the time domain. This "Diff" value can be utilized to extrapolate the WCET for the remaining iterations of the loop.

The last column shows that every iteration (except the first) has the exact same number of instructions that access functional units (and make corresponding entries in their reservation stations). In fact, a visual inspection of the snapshot state showed that the instructions (578 for "long" and 16 for "short") were *identical across iterations*. Hence, these benchmarks reached a stable pipeline state in 2 iterations. These results show that an examination of the pipeline state for loop iterations can provide a more complete fixed point analysis.

4.7 Conclusion

The work outlined in this chapter provides the means to accurately bound the worst-case execution time for a given program path using a combination of the traditional fixed point timing analysis approach and an examination of the pipeline state from each iteration. The former consists of a synergistic combination of analytical closed-formula derivations and observed actual timings of execution under the CheckerMode. The latter utilizes the snapshot mechanism of CheckerMode to capture the state of reservation stations (and, hence, the usage of functional units) after every iteration and then attempts to find repeating patterns in that state.

This chapter develops and evaluates these techniques for loop and, ultimately, whole task analysis to help derive bounds on the WCET. These techniques provide a mechanism to perform a *partial* analysis for loops. This mechanism does not require a complete enumeration or execution of all iterations in the loop. An interesting outcome of the analysis is the amount of architectural state that must be closely followed for performing an accurate analysis. The retire stage and the issue/execute stages must be captured to reflect the worst-case behavior of loop iterations in an OOO pipeline.

Chapter 5

Parametric Timing Analysis and Its Application to Dynamic Voltage Scaling

5.1 Summary

Static timing analysis derives bounds on worst-case execution times (WCETs) but requires statically known loop bounds. This chapter describes work that removes this constraint on known loop bounds through parametric analysis which expresses WCETs as functions. Tighter WCETs are dynamically discovered to exploit slack by dynamic voltage scaling (DVS) saving 60%-82% energy over DVS-oblivious techniques and showing savings close to more costly dynamic-priority DVS algorithms.

Overall, parametric analysis expands the class of real-time applications to programs with loop-invariant dynamic loop bounds while retaining tight WCET bounds.

5.2 Introduction

Static timing analysis provides bounds on the WCET but these bounds require constraints to be imposed on the tasks (timed code), the most striking of which is the requirement to statically bound the number of iterations of loops within the task. These loop bounds address the halting problem, *i.e.*, without these loop bounds, WCET bounds cannot be derived. The programmer must provide these upper bounds on loop iterations when they cannot be inferred by program analysis. Hence, these statically fixed loop bounds may present an inconvenience. They also restrict the class of programs that can be used in real-time systems. This type of timing analysis is referred to as

numeric timing analysis [49,52,53,94,132,133] since it results in a single numeric value for WCET given the upper bounds on loop iterations.

The constraint on the known maximum number of loop iterations is removed by *parametric timing analysis* (PTA) [124]. PTA permits variable length loops. Loops may be bounded by n iterations as long as n is known prior to loop entry during execution. Such a relaxation widens the scope of analyzable programs considerably and facilitates code reuse for embedded/real-time applications.

This chapter *(a)* derives parametric expressions to bound WCET values of dynamically bounded loops as polynomial functions. The variables affecting execution time, such as a loop bound n, constitute the formal parameters of such functions, while the actual value of n at execution time is used to evaluate such a function. This chapter further *(b)* describes the application of static timing analysis techniques to dynamic scheduling problems and *(c)* assesses the benefits of PTA for dynamic voltage scaling (DVS). This work contributes a novel technique that allows PTA to interact with a dynamic scheduler while discovering actual loop bounds, during execution, prior to loop entry. At loop entry, a tighter bound on WCET can be calculated on-the-fly, which may then trigger scheduling decisions synchronous with the execution of the task. The benefits of PTA resulting from this dynamically discovered slack are analyzed. This slack could be utilized in two ways – *(a)* execution of additional tasks as a result of admissions scheduling, and *(b)* power management.

Recently, numerous approaches have been presented that utilize DVS for both, general-purpose systems [43, 46, 98, 129] and for real-time systems [11, 11, 45, 65, 69, 78, 100, 107, 111, 112, 137]. Core voltages of contemporary processors can be reduced while lowering execution frequencies. At these lower execution rates, power is significantly reduced, as power is proportional to the frequency and to the square of the voltage: $P \propto V^2 \times f$.

In the past, real-time scheduling algorithms have shown how static and dynamic slack may be exploited in inter-task DVS approaches [11,45,63,65,68,69,78,100,107,112,137–140] as well as intra-task DVS algorithms [2,11,90,111]. Early task completion and techniques to assess the progress of execution based on past executions of a task lead to dynamic slack discovery.

This chapter illustrates the use of a novel approach towards dynamic slack discovery. Slack, in this method, can be *safely predicted for future execution* by exploiting early knowledge of parametric loop bounds. This allows the remainder of execution of a task to be bound tightly. The potential for dynamic power conservation via *ParaScale*, a novel intra-task DVS algorithm, is assessed. ParaScale allows tasks to be *slowed down* as and when more slack becomes available. This is in sharp contrast to past real-time DVS schemes, where tasks are sped up in later stages as

they approach their deadline [45, 63, 68, 138–140].

This chapter also describes a novel enhancement to the static DVS scheme which, incorporated with the intra-task slack determination scheme results in significant energy savings. The energy savings approach those obtained by one of the most aggressive dynamic DVS algorithms [100].

The approach is evaluated by implementing PTA in a gcc environment with a MIPS-like instruction set. Execution is simulated on a customized SimpleScalar [21] framework that supports multi-tasking. The effects of instruction cache misses are bounded in the experiments, but preclude the effects of data cache misses. The framework has been modified to support customized schedulers with and without DVS policies and an enhanced Wattch power model [20], which aids in assessing power consumption. A more accurate leakage power model [64] was also implemented to estimate the amount of leakage and static power consumed by the processor. This framework is used to study the benefits of PTA in the context of ParaScale as a means to exploit DVS.

Results show that ParaScale, applied on a modified version of a static DVS algorithm, provides significant savings by utilizing the parametric approach to timing analysis. These savings are observed for generated dynamic slack and potential reduction in overall energy. In fact, the amount of energy saved is very close to that obtained by the lookahead EDF-DVS scheme [100] – a popular, aggressive *dynamic* DVS algorithm. Thus, ParaScale makes it possible for static inter-task DVS algorithms to be used on embedded systems. This helps avoid more cumbersome (and difficult to implement) DVS schemes while still achieving similar energy savings. The approach presented here utilizes online intra-task DVS to exploit parametric execution times resulting in much lower power consumptions, *i.e.*, even without any scheduler-assisted DVS savings. Hence, even in the absence of dynamic priority scheduling, significant power savings may be achieved, *e.g.*, in the case of cyclic executives or fixed-priority policies such as rate-monotonic schedulers [76]. Overall, parametric timing analysis expands the class of applications for real-time systems to include programs with dynamic loop bounds that are loop invariant while retaining tight WCET bounds and uncovering additional slack in the schedule.

This chapter is structured as follows. Sections 5.3 and 5.4 provide information on numeric and parametric timing analysis respectively. Section 5.5 explains derivation of the parametric formulae and their integration into the code of tasks. This section also shows the steps involved in obtaining accurate WCET analysis for the new, enhanced code. Section 5.6 discusses the context in which parametric timing results are used. Section 5.7 introduces the simulation framework. Section 5.8 elaborates on the experiments and results. Section 5.9 summarizes the work.

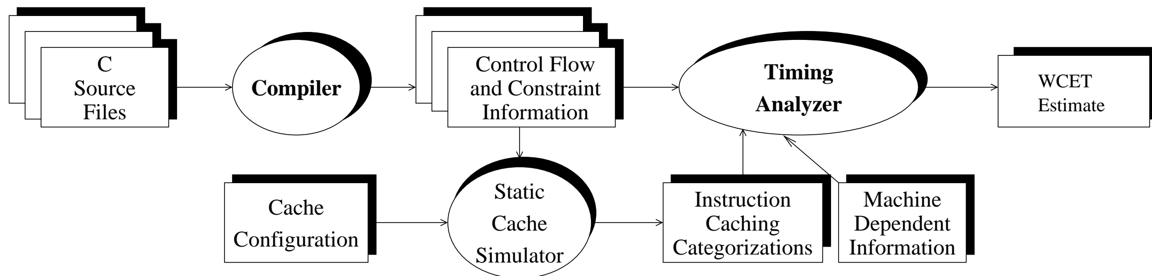

Figure 5.1: Static Timing Analysis Framework

5.3 Numeric Timing Analysis

The work described in this chapter builds on a static timing analysis tool developed in previous work [51, 89, 94, 133]. The framework models the traversal of all possible execution paths in the code. Execution timing is determined independent of program traces or input data to program variables. The behavior of architectural components is captured as execution paths are traversed. Paths are composed to form functions, loops, etc. until finally the entire application is covered. Hence, a bound on the WCET and the worst-case execution cycles (WCECs) is obtained

Table 5.1: Instruction Categories for WCET

Cache Category	Definition
always miss	Instruction may not be in cache when referenced.
always hit	Instruction will be in cache when referenced.
first miss	Instruction may not be in cache on 1st reference for each loop execution, but is in cache on subsequent references.
first hit	Instruction is in cache on 1st reference for each loop execution, but may not be in cache on subsequent references.

The organization of this timing analysis framework is presented in Figure 5.1. An optimizing compiler is modified to produce control-flow and branch constraint information, as a side-effect of the compilation process. Control-flow graphs and instruction and data references are obtained from assembly code. One of the prerequisites of traditional static timing analysis is that an upper bound on the number of loop iterations be provided to the system.

The control-flow information is used by a static instruction cache simulator to construct a control-flow graph of the program and caching categorizations for each instruction [94]. This control-flow graph consists of the call graph and the control flow for each function. The control-flow graph of the program is analyzed, and a caching categorization for each instruction and data reference in the program is produced using a data-flow equation framework. Each loop

level containing the instruction and data references is analyzed to obtain separate categorizations. These categorizations for instruction references are described in Table 5.1. Notice that references are conservatively categorized as *always-misses* if static cache analysis cannot safely infer hits on one or more references of a program line.

The control-flow, the constraint information, the architecture-specific information and caching categorizations are used by the timing analyzer to derive WCET bounds. Effects of data hazards (load-dependent instruction stalls if a use immediately follows a load instruction), structural hazards (instruction dependencies due to constraints on functional units), and cache misses (obtained from the caching categorizations) are considered by a pipeline simulator for each execution path through a function or loop. *Static branch prediction* can be accommodated into the WCET analysis by adding the misprediction penalty to the non-predicted path.

```
cycles = iter = 0;
do {
    iter = iter + 1;
    wcpath = find the longest path;
    cycles = cycles + wcpath→cycles;
} while (caching behavior of wcpath changes
    && iter < max_iter);
cycles += (wcpath→cycles * (max_iter - iter));
```

Figure 5.2: Numeric Loop Analysis Algorithm

Path analysis is then performed to select the longest execution path, and once timing results for alternate paths are available, a fixed point algorithm quickly converges to safely bound the time for all iterations of a loop. Figure 5.2 illustrates an abstraction of the fix-point algorithm used to perform loop analysis. The algorithm repeatedly selects the longest path through the loop until a *fixed point* is reached (i.e., the caching behavior does not change and the cycles for the worst-case path remains constant for subsequent loop iterations). WCETs for inner loops are predicted before those for outer loops; an inner loop is treated as a single node for outer loop calculations, and the control flow is partitioned if the number of paths within a loop exceeds a specified limit [6]. The correctness of this fixed point algorithm has been studied in detail [10].

By composing the WCET bounds for adjacent paths, the WCET of loops, functions and the entire task is then derived by the timing analyzer by the traversal of a *timing tree*, which is processed in a bottom up manner. WCETs for outer loop nest/caller functions are not evaluated until the times for inner loop nests/callees are calculated.

5.4 Parametric Timing Analysis

```
call IntraTaskScheduler(eval_loop_k(n));
for (i = 0; i<n ; i++ ) // max n = 1000
        loop body ;
// Parametric Evaluation Function
int eval_loop_k(int loop_bound) {
        return (102 * loop_bound);
}
```

Figure 5.3: Use of Parametric Timing Analysis

In the static timing analysis method presented in Section 5.3, upper bounds on loop iterations must be known. They can be provided by the user or may be inferred by analysis of the code. This severely restricts the class of applications that can be analyzed by the timing analyzer. This class of timing analyzers is often referred to as *numeric timing analyzers* since they provide a single, numeric cycle value provided that upper loop bounds are known. *Parametric timing analysis* (PTA) [124], in contrast, makes it possible to support timing predictions when the number of iterations for a loop is not known until run-time.

Consider the example in Figure 5.3. The for loop denotes application code traditionally subject to numerical timing analysis for an annotated upper loop bound of 1000 iterations. PTA requires that the value of n be known prior to loop entry. The bold-face code denotes additional code generated by PTA.

```
cycles = iter = 0;
do {
    iter = iter + 1;
    wcpath = find the longest path;
    cycles = cycles + wcpath→cycles;
} while (caching behavior of wcpath changes);

base_cycles = cycles - (wcpath→cycles * iter);
```

Figure 5.4: Parametric Loop Analysis Algorithm

The concept behind PTA is to calculate a *formula* (or closed form) for the WCET of a loop, such that the formula depends on *n*, the number of iterations of the loop. The calculation of this formula, ($102 * n$ in Figure 5.3), needs to be relatively inexpensive since it will be used at run-time to make scheduling decisions. These decisions may entail selection/admission of additional tasks or modulation of the processor frequency/voltage to conserve power. Hence, instead of passing a numeric value representing the execution cycles for loops or functions up the timing tree, a symbolic formula is provided if the number of iterations of a loop is not known.

The algorithm in Figure 5.4 is an abstraction of the revised loop analysis algorithm for PTA. This algorithm iterates to a fixed point, *i.e.*, until the caching behavior does not change. The number of base cycles obtained from this algorithm is then saved. The $base_cycles$ denote the extra cycles cumulatively inflicted by initial loop iterations before the cycles of the worst-case path reach

a fixed point ($wcpath \rightarrow cycles$). The base cycles are subsequently used to calculate the number of cycles in a loop as follows:

$$\mathbf{WCET_{loop} = wcpath \rightarrow cycles * n + base_cycles} \tag{5.1}$$

The correctness of this approach follows from the correctness of numeric timing analysis [51]. When instruction caches are present in the system, the approach assumes monotonically decreasing WCETs as the cache behavior of different paths through the loop is considered. This integrates well with past techniques on bounding the worst-case behavior of instruction and data caches [94, 133].[1]

Equation 5.1 illustrates that the WCET of the loop depends on the base cycles and the WCET path time (both constants) as well as on the number of loop iterations, which will only be known at run-time for variable-length loops. The potential for significant savings from such parametric analysis over the numeric approach are illustrated and discussed later in Figure 5.7. The algorithm in Figure 5.4 is an enhancement of the algorithm presented in Figure 5.2. Since the cycles for the worst-case path for the algorithm in Figure 5.2 has been shown to be monotonically decreasing, the *worst-case path cycles for the algorithm in Figure 5.4 also monotonically decreases*.

If the actual number of iterations (say: 100) exceeds the number of iterations required to reach the fixed point for calculating the base cycles (say: 5), then the parametric result closely approximates that calculated by the numeric timing analyzer. If, on the other hand, the actual number of iterations (say: 3) is lower than the fixed point (say: 5), then there could be an overestimation due to considering cycles on top of the WCET path cost (for iterations 4 and 5). The formulae could be modified to deal with the special case that has fewer iterations, *e.g.*, by early termination of the algorithm if actual bounds are lower than the fixed point (future work).

The general constraints on loops that can be analyzed by the parametric timing analyzer are:

1. Loops must be *structured*. A structured loop is a loop with a single entry point (*a.k.a* reducible loop) [5, 121].

2. The compiler must be able to generate a *symbolic expression* to represent the number of loop iterations.

[1] Other cache modeling techniques or consideration of timing anomalies due to caches [13] may require exhaustive enumeration of all paths and cache effects within the loop or an entirely different algorithm.

$$
\begin{aligned}
//\ induction_variable \;&:\; strictly\ monotonically\ increasing/decreasing\ value;\\
//loop_invariant_variable \;&:\; loop\ invariant\ relative\ to\ all\ nested\ loops\ up\ to\\
// \;&\; outermost\ parametric\ loop\\
\\
\mathbf{induction_operation_value} \;&:\; < \mathbf{constant} > || < \mathbf{loop_invariant_variable} >\\
initialization \;&:\; induction_variable = < induction_operation_value >;\\
loop \;&:\; < for, while, do > < termination_condition >\\
&\; \#\mathbf{pragma\ max}(\mathbf{100})\\
&\; < body >\\
body \;&:\; < statement >;\\
&\; < induction_variable > < op >\\
&\; < induction_operation_value >;\\
op \;&:\; + = || - =\\
condition \;&:\; < induction_variable >< comparison_op >\\
&\; < induction_operation_value >
\end{aligned}
$$

Figure 5.5: Syntactic and Semantic specifications for constraints on analyzable loops.

3. Rectangular loop nests can be handled, as long as the induction variables of these loops are independent of one other.

4. The value of the *actual* loop bound must be known *prior to entry into the loop*

Syntactic and semantic specifications that suffice to meet these constraints are presented in Figure 5.5. The pragma value is the pessimistic worst-case bound for the number of loop iterations. Figure 5.5 is only informative. Actual analysis is performed on the intermediate code representation. Hence, the analysis is able to handle transformations due to compiler optimizations, *e.g.*, loop unrolling.

The timing analyzer processes inner loops before outer loops, and nested inner loops are represented as single blocks when processing a path in the outer loop. Loops are represented with

symbolic formulae (rather than a constant number of cycles) when the number of iterations is not statically known. The WCET for the outer loop is simply the symbolic sum of the cycles associated with a formula representing the inner loop as well as the cycles associated with the rest of the path.

The analysis becomes more complicated when paths in a loop contain nested loops with parametric WCET calculations of their own. Consider the example depicted in Figure 5.6, which contains two loops, where an inner loop (block 4) is nested in the outer loop (blocks 2, 3, 4, 5). Assume that the inner loop is also parametric with a symbolic number of iterations. The loop analysis algorithm requires that the timing analysis finds the longest path in the outer loop. This obviously depends on the number of iterations of the inner loop. The minimum number of iterations for a loop is one, assuming that the number of loop iterations is the number of times that the loop header (loop entry block) is executed. If the WCET for path A (2→3→5) is less than the WCET for path B (2→4→5), for a single iteration, then path B is chosen, else a *max()* function must be used to represent the parametric WCET of the outer loop. Equation 5.2 illustrates this idea of calculating the maximum of the two paths. Note though, that the WCET of these paths is obtained after the caching behavior reaches a steady state, and the base cycles are the extra cycles before either of these paths reach that steady state. The first value passed to the *max()* function in this example would be numeric, while the second value would be symbolic.

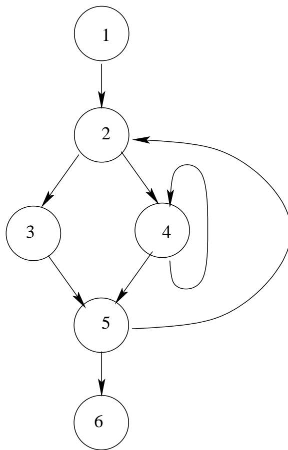

Figure 5.6: Example of an outer loop with multiple paths

$$WCET_{loop} = max(WCET_{path_A_time}, WCET_{path_B_time}) * n + base_cycles \tag{5.2}$$

In a manner similar to numeric timing analysis, certain restrictions still apply. Indirect calls and unstructured loops (loops with more than one entry point) cannot be handled. Recursive functions can, in theory, be handled if the recursion depth is known statically or if the depth can be inferred dynamically prior to the first function call (*via parametric analysis*). Upper bounds on the loop iterations, parametric or not, still need not be known but the bounds can be pessimistic as the actual bounds are now discovered during runtime. In addition, the timing analysis framework has to be enhanced to automatically generate symbolic expressions reflecting the parametric overhead of loops, which will be evaluated at runtime.

Table 5.2 shows the results of predicting execution time using the two types of tech-

niques. Pipeline and instruction cache performance were analyzed for these programs. *Formula* is

Table 5.2: Examples of Parametric Timing Analysis

Program	Formula	Iters	Observed Cyc.	Numeric Analysis		Param. Analysis	
				Est. Cyc.	Ratio	Est. Cyc.	Ratio
Matcnt	$160n^2 + 267n + 857$	100	1,622,034	1,627,533	1.003	1,627,557	1.003
Matmul	$33n^3 + 310n^2 + 530n + 851$	100	33,725,782	36,153,837	1.072	36,153,851	1.072
Stats	$1049n + 1959$	100	106,340	106,859	1.005	106,859	1.005

the formula returned by the parametric timing analyzer and represents the parametrized predicted execution time of the program. In order to evaluate the accuracy of the parametric timing analysis approach, each loop in these test programs iterates the same number of times. Thus, n Iters represents the number of loop iterations for each loop in the program and n also represents that value in the formulae. The power of n represents the loop nesting level and the constant factor represents the cycles spent at that level. Note that most of the programs had multiple loops at each nesting level. For example, $160n^2$ indicates that 160 cycles is the sum of the cycles that would occur in a single iteration of all the loops at nesting level 2 in the program. If the number of iterations of two different loops in a loop nest differ, then the formula would reflect this as a multiplication of these factors. For instance, if the matrix in Matcnt had m rows and n columns, where $m \neq n$, then the formula would be:

$$(160n + 267)m + 857$$

Parametric timing analysis supports any rectangular loop nest (with independent bounds known prior to loop entry), and is able to obtain bounds for each loop in an inner-most-out fashion using the algorithm in Figure 5.4. An extension could handle triangular loops with bounds dependent on outer iterators as well [50]. The *Observed Cycles* were obtained by using an integrated pipeline and instruction cache simulator, and represents the cycles of execution given worst-case input data. The *Numeric Analysis* represents the results using the previous version of the timing analyzer, where the number of iterations of each loop is bounded by a number known to the timing analyzer. *Parametric Analysis* represents cycles calculated at run-time when the number of iterations is known and, in this case, equal to the static bound. *Estimated Cycles* and *Ratio* represent the predicted number of cycles by the timing analyzer and its ratio to the Observed Cycles. The estimated parametric cycles were obtained by evaluating the number of iterations with the formula returned by the parametric timing analyzer. These results indicate that the parametric timing analyzer is almost as accurate as the numeric analyzer.

PTA enhances this code with a call to the *intra-task scheduler* and provides a dynamically

calculated, tighter bound on the WCET of the loop. The tighter WCET bound is calculated by an *evaluation function* generated by the PTA framework. It performs the bounds calculation based on the dynamically discovered loop bound n. The scheduler has access to the WCET bound of the loop derived from the annotated, static loop bound by static timing analysis. It can now anticipate dynamic slack as the difference between the static and the parametric WCET bounds provided by the evaluation function. Without parametric timing analysis, the value of n would have been assumed to be the maximum value ()100 in this case).

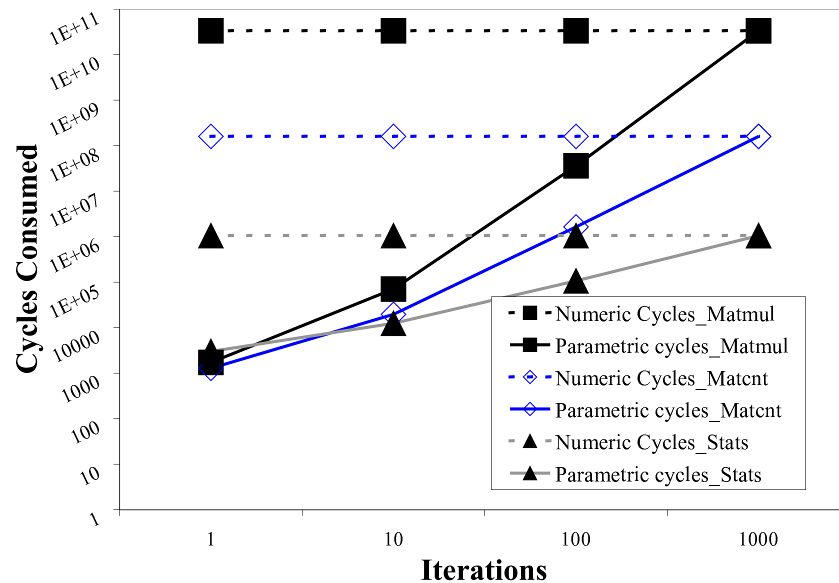

Figure 5.7: WCET Bounds as a Function of the Number of Iterations

Figure 5.7 shows the effect of changing the number of iterations on loop bounds for parametric and numerical WCET analysis. Parametric analysis is able to *adapt bounds to the number of loop iterations*, thereby more tightly bounding the actual number of required cycles for a task (Table 5.2). Hence, it can save a significant number of cycles compared to numerical analysis (which must always assume the worst case – *i.e.* 1000 iterations in Figure 5.7). This effect becomes more pronounced as the number of actual iterations becomes much smaller than the static bound. In such situations, parametric timing analysis is able to provide significantly tighter bounds.

5.5 Creation and Timing Analysis of Functions that evaluate Parametric Expressions

In the previous section, the methodology for deriving WCET bounds from parametric formulae was introduced. In this section, problems in embedding such formulae in application code are discussed. An *iterative reevaluation of WCETs* is provided as a solution.

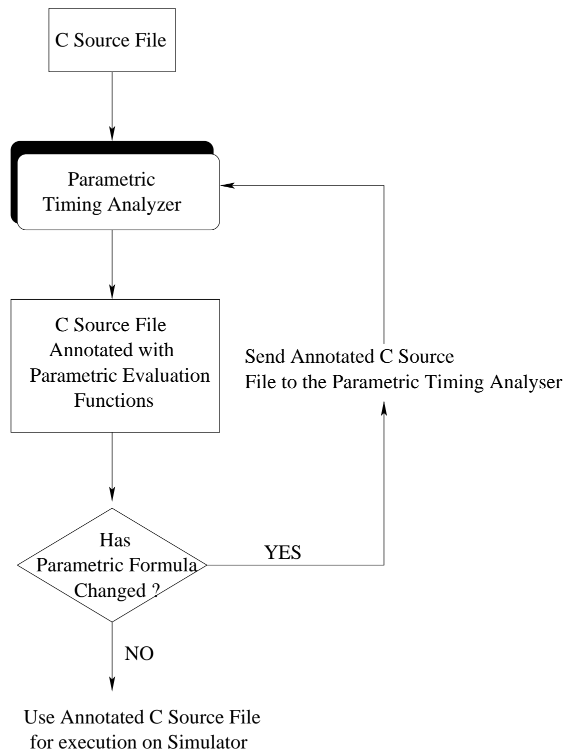

Figure 5.8: Flow of Parametric Timing Analysis

The challenge to embedding evaluation functions for parametric formulae is as follows. When the code within a task is changed to include parametric WCET calculations, previous timing estimates and the caching behavior of the task might be affected. One may either inline the code of the formula or invoke a function that evaluates the symbolic formula. Since both approaches affect caching, another pass of cache analysis has to be performed on the modified code. An arbitrary design decision was made to pursue the latter approach. Using this modular approach, the cache analysis can reach a fixed point in fewer iterations as changes are constrained to functional boundaries rather than embedded within a function (affecting the caching of any instructions below if the inlined code changes in size). The cost of calling an evaluation function is minimal compared to the benefit, and a subsequent call to the scheduler is required in any case to benefit from the *actual* lower bounds.

Once a task has been enhanced with these parametric functions and their calls prior to loop entries, the timing analyzer must be reinvoked to analyze the newly enhanced code. This allows the timing analyzer to capture the WCET of generated functions and their invocations in the context of a task. Notice that any re-invocation of the timing analyzer potentially changes the parametric formulae and their corresponding functions such that it is necessary to iterate through the timing analysis process. This is illustrated in Figure 5.8 where the process of generating formulae is presented. The iterative process converges to a *fixed point* when parametric formulae reach stable

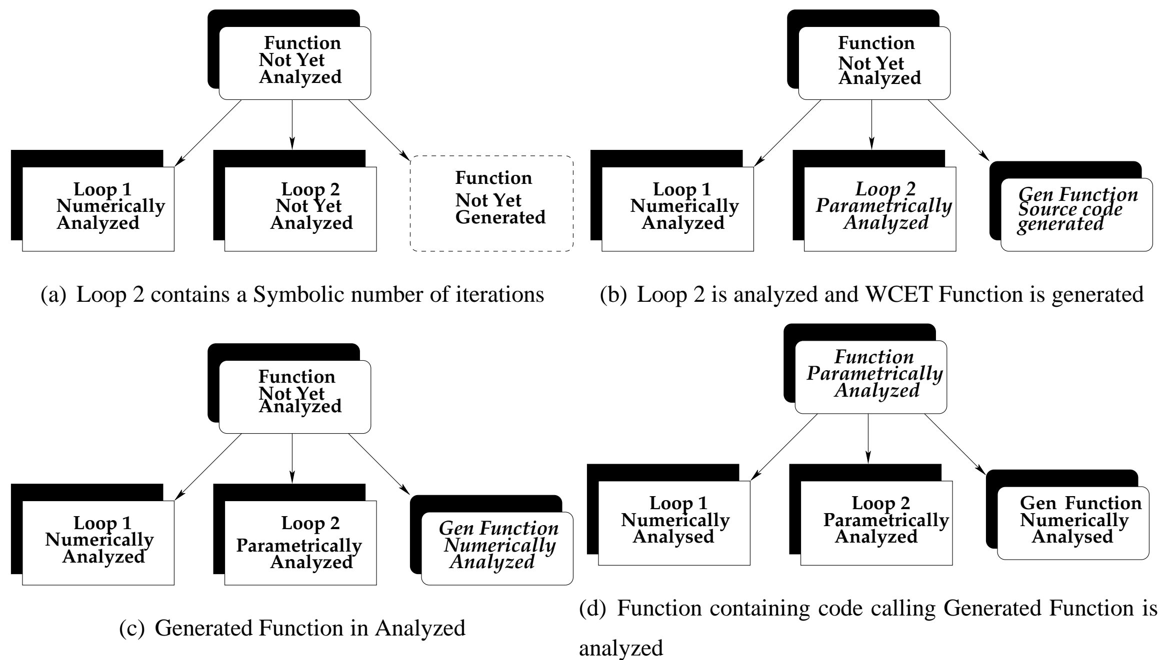

(a) Loop 2 contains a Symbolic number of iterations

(b) Loop 2 is analyzed and WCET Function is generated

(c) Generated Function in Analyzed

(d) Function containing code calling Generated Function is analyzed

Figure 5.9: Example of using Parametric Timing Predictions

states. Typically, the parametric timing analysis and calculation of the parametric formulae take *less than a second* to complete. Since this is an offline process, it does not add to the overhead of the execution of the parametrized system.

An example is presented in Figure 5.9, where timing analysis is accomplished in stages, as parametric formulae are generated and evaluated later. In the example shown, a function is generated by the timing analyzer to calculate the WCET for loop 2, whose number of iterations is only known at run-time. The following sequence of operations takes place:

1. A call to a function is inserted that returns the WCET for a specified loop or function based on a parameter indicating the number of loop iterations that is available at run time. The instructions that are associated with the call and the ones that use the return value after the call are generated during the initial compilation. For instance, in Figure 5.9(a) a function calls the yet-to-be generated function to obtain the WCET of loop 2, which contains the symbolic number of iterations.

2. The timing analyzer generates the source code for the called function in a separate file when processing the specified loop or function whose time needs to be calculated at run time. For instance, Figure 5.9(c) shows that after loop 2 has been parametrically analyzed, the code for the *evaluation function* has been generated. Note that the timing analysis tree representing

the loops and functions in the program is processed in a *bottom-up* fashion. The code in the function invoking the generated function is not evaluated until after the generated function is produced. The static cache simulator can initially assume that a call to an unknown function invalidates the entire cache. Figure 5.3 shows an example of the source code for such a generated function.

3. The generated function is compiled and placed at the end of the executable. The formula representing the symbolic WCET need not be simplified by the timing analyzer. Most optimizing compilers perform constant folding, strength reduction, and other optimizations that will automatically simplify the symbolic WCET produced by the timing analyzer. By placing the generated function after the rest of the program, instruction addresses of the program remain unaffected. While the caching behavior may have changed, loops are unaffected since the timing tree is processed in a bottom-up order.

4. The timing analyzer is invoked again to complete the analysis of the program, which now includes calculating the WCET of the generated function and the code invoking this function. For instance, Figure 5.9(c) shows that the generated function has been numerically analyzed and Figure 5.9(d) shows that the original function has been parametrically analyzed, which now includes the numeric WCET required for executing the new function.

In short, this approach allows for timing analysis to proceed in stages. Parametric formulae are produced when needed and source code functions representing these formulae are produced, which are also subsequently compiled, inserted into the task code and analyzed. This process continues until a formula is obtained for the entire program or task.

5.6 Using Parametric Expressions

In this section, potential benefits of parametric formulae and their evaluation functions are discussed. A more accurate knowledge of the remaining execution time provides a scheduler with information about additional slack in the schedule. This slack can be utilized in multiple ways:

- A dynamic admission scheduler can accept additional real-time tasks due to parametric bounds of the WCET of a task, which become tighter as execution progresses.

- Dynamic slack can also be used for *dynamic voltage (and frequency) scaling (DVS) in order to reduce power*.

In the remainder of this chapter, the latter case will be detailed.

Recall that parametric timing analysis involves the integration of symbolic WCET formulae as functions and their respective evaluation calls into a task's code. Apart from these inserted function calls, calls to transfer control to the DVS component of an optional dynamic scheduler are also inserted *before* entering parametric loops, as shown in Figure 5.3. The parametric expressions are evaluated at run-time (using evaluation functions similar to the one in the figure) as knowledge of actual loops bounds becomes available. The newly calculated tighter bound on the execution time for the parametric loop is passed along to the scheduler. The scheduler is able to determine newly found dynamic slack by comparing worst-case execution cycles (WCECs) for that particular loop with the parametrically bounded execution time. The WCECs for each loop and the task as a whole are provided to the scheduler by the static timing analysis toolset. Static loop bounds for each loop are provided by hand. Automatic detection of bounds is subject to future work.

Dynamic slack originating from the evaluation of parametric expressions at run-time is discovered and can be exploited by the scheduler for admission scheduling or DVS (see above). This work is unique in that it exploits early knowledge of parametric loop bounds, thus allowing the possibility to tightly bound the overall execution of the *remainder* of the task. To this effect, an intra-task DVS algorithm has been developed, to lower processor frequency and voltage. Another unique aspect of this approach is that every successive parametric loop that is encountered during the execution of the task potentially provides more slack and, hence, allows the system to further scale down the processor frequency. This is in sharp contrast to past real-time schemes where DVS-regulated tasks are sped up as execution progresses, mainly due to approaching deadlines.

5.7 Framework

An overview of the experimental framework is depicted in Figure 5.10. The instruction information fed to the timing analyzer is obtained from the P-compiler, which preprocesses gcc-generated PISA assembly. The C source files are also fed simultaneously to both the static and the parametric timing analyzers. Safe (but, due to the parametric nature of loops, not necessarily tight) upper bounds for loops are provided as inputs to the static timing analyzer (STA). The worst-case execution times/cycles, for tasks as well as loops, provided by the STA are provided as input to a scheduler. The C source files are also provided to the PTA. The PTA produces source files annotated with parametric evaluation functions as well as calls to transfer control to the scheduler *before* entry into a parametric loop. These annotated source files form the task set for execution by the scheduler.

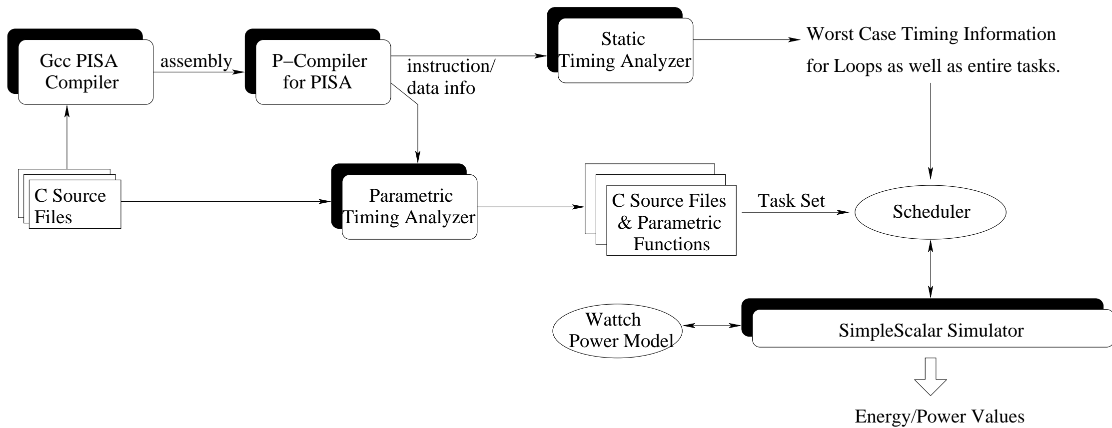

Figure 5.10: Experimental Framework

To simplify the presentation, Figure 5.10 omits the loop that iterates over parametric functions till they reach a fixed point (as discussed in Figure 5.8). This would create a feedback between the PTA output and the C source files that provide the input to the toolset. For the sake of this discussion, the set of timing analysis tools is combined into one component in Figure 5.10, *i.e.*, the internal structure of a static cache simulator and the timing analyzer depicted in Figure 5.1 are omitted.

An *EDF scheduler* has been implemented, that creates an initial execution schedule based on the pessimistic WCET values provided by the STA. This scheduler is also capable of lowering the operating frequency (and, hence, the voltage) of the processor by way of its interaction with two DVS schemes:

1. an *inter-task* DVS algorithm, which scales down the frequency based on the execution of whole tasks (using a *static* and a *dynamic* DVS algorithm)

2. *ParaScale*, an *intra-task* DVS scheme that, on top of the scaled frequency from *(1)*, which provides further opportunities to reduce the frequency based on dynamic slack gains due to PTA

The static DVS scheme is similar to the static EDF policy by Pillai *et al.* [100]. However, it differs in that the processor frequency and voltage are reduced to their respective minimum during idle periods. Two dynamic DVS schemes have been implemented. The first one, named "*greedy DVS*", is a modification of the static DVS scheme and aggressively reduces the frequency below the statically determined value until the next scheduler invocation. The slack accrued from early

completions of jobs is used to determine lower frequencies for execution. The second dynamic DVS algorithm is the "lookahead" EDF-DVS policy by the same authors – it is a very aggressive dynamic DVS algorithm and lowers the frequency and voltage to very low levels.

Throughout this chapter, the name "*ParaScale*" refers to the intra-task DVS technique that uses the parametric loop information to accurately gauge the number of remaining cycles and lower the voltage/frequency. "*ParaScale-G*" and "*ParaScale-L*", to refer to the ParaScale implementations of the greedy and lookahead inter-task DVS algorithms, respectively. ParaScale always starts a task at the frequency value specified by the inter-task DVS algorithm. It then dynamically reduces the frequency and voltage according to slack gains from the knowledge on the recalculated bounds on execution times for parametric loops. The effect of scaling is purely limited to intra-task scheduling, *i.e.*, the frequency can only be scaled down as much as the completion due to the non-parametric WCET allows. Hence, each call to the scheduler due to entering a parametric loop potentially results in slack gains and lower frequency/voltage levels.

Table 5.3: WCECs for inter-task and intra-task schedulers for various DVS algorithms.

Scheduler Type	DVS Algorithm		
	no dvs	static dvs	lookahead dvs
Inter-task	6874	7751	8627
Intra-task	1625	2502	3378

Numeric timing analysis was performed on the two schedulers in the system. The worst-case execution cycles for the schedulers (Table 5.3) were then included in the utilization calculations. The WCEC for the inter-task DVS algorithm was used as a preemption overhead for all lower priority tasks. The worst-case behavior was assumed while dealing with preemptions, *i.e.*, the upper bound on the number of preemptions of a job j is given by the number of higher priority jobs released before job j's deadline.

The execution time for the intra-task DVS algorithm (ParaScale) was added *once* to the WCEC of each task in the system. The intra-task scheduler is called exactly *once* for each invocation of a task – prior to entry into the outermost parametric loop.

The simulation environment (used in a prior study [7]) is a customized version of the SimpleScalar processor simulator that executes so-called (MIPS-like) PISA instructions [21]. PISA assembly, generated by gcc, also forms the input to the timing analyzers. The framework supports multitasking and the use of schedulers that operate with or without DVS policies. This enhanced SimpleScalar simulator is configured to model a static, in-order pipeline, with universal, unpipelined function units. The simulator has a $64k$ instruction cache and *no data cache*. A static instruction cache simulator accurately models all accesses and produces categorizations, such as

those illustrated in Table 5.1. The data cache module has not been implemented yet, as the priority was to accurately gauge the benefits and energy savings of using parametric timing analysis. For the time being, a constant memory access latency for each data reference is assumed and leave static data cache analysis for future work. Also, pipeline-related and cache-related preemption delays (CRPD) [67, 104, 108, 115, 116] are currently not modeled but, given accurate and safe CRPD bounds, could easily be integrated.

The Wattch model [20], along with the following enhancements, also forms part of the framework – it closely interacts with the simulator to assess the amount of power consumed. The original Wattch model provides power estimates assuming perfect clock gating for the units of the processor. An enhancement to the Wattch model provides more realistic results in that apart from perfect clock gating for the processor units, a certain amount of fixed leakage is also consumed by units of the processor that are not in use. Closer examination of the leakage model of Wattch revealed that this estimation of static power may resemble but does not accurately model the leakage in practice. Static power is modeled by assuming that unused processor components leak approximately 10% of the dynamic power of the processor. This is inaccurate since static power is proportional to supply voltage while dynamic power is proportional to the *square* of the voltage. The effect of using the Wattch model is discussed in the following section. To reduce the inaccuracies of the Wattch model in determining the amount of leakage/static power consumed, a more accurate leakage model [64] was implemented. The implementation is configurable so that it can be used to not only study current trends for silicon technology (in terms of leakage), but also able to extrapolate on future trends (where leakage may dominate the total energy consumption of processors).

The minimum and maximum processor frequencies under DVS are 100MHz and 1GHz, respectively. Voltage/frequency pairs are loosely derived from the XScale architecture by extrapolating 37 pairs (five reported pairs between 1.8V/1GHz and 0.76V/150MHz) starting from 0.7V/100MHz in 0.03V/25MHz increments. Idle overhead is equivalent to execution at 100MHz, regardless of the scheduling scheme.

Table 5.4: Task Sets of C-Lab Benchmarks and WCETs (at 1 GHz)

C Benchmark	Function	WCET	
		Cycles	Time [ms]
adpcm	Adaptive Differential Pulse Code Modulation	121,386,894	121.39
cnt	Sum and count of positive and negative numbers in an array	6,728,956	6.73
lms	An LMS adaptive signal enhancement	1,098,612	10.9
mm	Matrix Multiplication	67,198,069	67.2

5.8 Experiments and Results

Table 5.5: Parameters Varied in Experiments

Parameter	Range of Values
Utilization	20%, 50%, 80%
Ratio WCET/PET	1x, 2x, 5x, 10x, 15x, 20x
Leakage Ratio	0.1, 1.0
DVS algorithms	Base Parametric Static DVS Greedy DVS ParaScale-G Lookahead ParaScale-L

Several task sets using a mixture of floating-point and integer benchmarks were created from the C-Lab benchmark suite [25]. The actual tasks used are shown in Table 5.4.

For each task, the main control loop was parametrized. Initially loops at all nesting levels were parametrized, but diminishing returns were observed as the levels of nesting increased. In fact, the large number of calls to the parametric scheduler due to nesting had adverse effects on the power consumption relative to the base case. Hence, parametric calls are limited to *outer loops only*.

Table 5.6: Periods for Task Sets

Utilization	Period = Deadline [ms]			
	adpcm	cnt	lms	mm
20%	1200	240	600	1200
50%	1200	75	60	600
80%	1200	50	40	240

Table 5.6 depicts the period (equal to deadline) of each task. All task sets have the same hyperperiod of 1200 *ms*. All experiments executed for exactly one hyperperiod. This facilitates a direct comparison of energy values across all variations of factors mentioned in Table 5.5. The parameters for the experiments are depicted in Table 5.5. The utilization, the ratio of worst-case to parametric execution times (PETs), and DVS support as follows are varied as explained below.

Base: Executes tasks at maximum processor frequency and up to n, the actual number of loop iterations for parametric loops (not necessarily the maximum number of statically bounded iterations). The frequency is changed to the minimum available frequency during idle periods.

Parametric: Same as Base except that calls to the parametric scheduler are issued prior to parametric loops without taking any scheduling action. This assesses the overhead for scheduling of the parametric approach over the base case.

Static DVS: Lowers the execution frequency to the lowest valid frequency based on system utilization. For example, at 80% utilization, the frequency chosen would be 80% of the maximum frequency. Idle periods, due to early task completion, are handled at the minimum frequency.

Greedy DVS: This scheme is similar to static DVS in that it starts with the statically fixed frequency but then aggressively lowers the frequency for the *current time period* based on accrued slack from previous task invocations. Every time a job completes early, the slack gained is passed on to the job which follows immediately. Let job i be the job that completes early and generates slack and let job j be the job which follows (consumer). The greedy DVS algorithm calculates the frequency of execution, α', for j as follows:

$$\alpha' = \left[\frac{\alpha * C_j}{\alpha * C_j + slack_i}\right] \alpha \tag{5.3}$$

where α is the frequency determined by the static DVS scheme. Notice that *(a)* this slack is "lost" or rather reset to zero when the next scheduling decision takes place and *(b)* Equation 5.3 ensures that the new frequency scales down job j so that it attempts to completely utilize the slack from the previous job, but it does not stretch beyond the time originally budgeted for its execution based on the higher, statically determined, frequency. From (a) and (b) above, it can be seen that the new DVS scheme will never miss a deadline if the original static DVS scheme never misses a deadline since greedy DVS accomplishes at least the same amount of work as before. Hence, it never utilizes processor time which lies beyond the original completion time of task j. The processor switches to the lowest possible frequency/voltage during idle time.

ParaScale-G: Combines the greedy and intra-task DVS schemes so that jobs start their execution at the lowest valid frequency based on system utilization. Before a parametric loop is entered the frequency is scaled down further according to the difference between the WCET bound of the loop and the parametric bound of the loop calculated dynamically. ParaScale-G also exploits savings due to already completed execution relative to the WCET for frequency scaling. (These savings are small compared to the savings of parametric loops since parametric loops generally occur early in the code). It also utilizes job slack accrued from previous task invocations to further reduce the frequency. As in the case of the Static and Greedy DVS schemes, the processor switches to the lowest possible frequency/voltage during idle time.

Lookahead: Implements an enhanced version [139] of Pillai's [100] *lookahead* EDF-DVS algorithm – a very aggressive dynamic DVS algorithm.

ParaScale-L: Combines the lookahead and intra-task DVS which utilizes parametric loop information. It is similar in operation to ParaScale-G. While ParaScale-G uses static values for initial frequencies, ParaScale-L uses frequencies calculated by the aggressive, dynamic EDF-DVS

algorithm (lookahead).

Notice that all scheduling cases result in the *same amount of work* being executed during the hyperperiod (or any integer multiple thereof) due to the periodic nature of the real-time workload. Hence, to assess the benefits in terms of power awareness, the energy consumed over such a fixed period of time can be measured and compares between scheduling modes.

The scheduler overhead for the greedy DVS scheme differs from those of the static DVS scheme by only a few cycles, as the only additional overhead is the calculation to determine α' (Equation 5.3). This calculation is performed only once per scheduler invocation because the new frequency only needs to be calculated for the next scheduled task instance. Three types of energy measurements are carried out during the course of the experiments:

PCG: Energy used with *perfect* clock gating (PCG) – only processor units that are used during execution contribute to the energy measurements. This isolates the effect of the parametric approach on *dynamic power*.

PCGL: Energy consumed by *leakage only*, based on prior methods [64]. This attempts to capture the amount of energy exclusively used due to leakage.

PCGL-W: Energy used with perfect clock gating for the processor units including *leakage*. Leakage power is modeled by Wattch as 10% of dynamic power, which is not completely correct, as discussed before.

The ratio of worst-case to actual (parametric) execution times is varied to study the effect of variations in execution times and make the experimental results more realistic. More often than not, the worst-case analysis of systems results in overestimations of WCET. ParaScale can take advantage of this to obtain additional energy savings.

As part of the setup for the experiments PCGL leakage model's operating parameters were initialized with the ratio of leakage to dynamic power for one particular experimental point. The ratio of dynamic and leakage energies for the WCET overestimation of $1x$ and utilization of 50% was chosen for this purpose. This ratio was used to set up appropriate operating parameters (number of transistors, body bias voltage, *etc.*), after which the experiments were allowed to execute freely to completion. This provides a unique opportunity to study the effects of leakage for *(a)* current processor technologies, where the ratio of leakage to dynamic are close to $1 : 10$ and *(b)* future trends where the leakage may increase significantly as the above ratio approaches $1 : 1$. The "leakage ratios" mentioned in table 5.5 refer to these two settings.

5.8.1 Overall Analysis

Figure 5.11 depicts the dynamic energy consumption for two sets of experiments – Figure 5.11(a) shows the dynamic energy values for the case where the WCET overestimation is assumed to be *twice* that of the PET, while Figure 5.11(b) shows the results for the instance where the WCET overestimation is assumed to be *ten times* that of the PET. Both graphs depict results for different utilization factors for each of the DVS schemes. These graphs show that the energy consumption by the ParaScale implementations outperform (*i.e.* use *less* energy) their corresponding non-ParaScale implementations. Note that the greedy DVS scheme is able to achieve some savings relative to the static DVS scheme. These savings are fairly small, as the slack from the early completion of a job is passed on to the next scheduled job, if at all. ParaScale-G, on the other hand, is able to achieve *significant* savings over both the aggressive greedy algorithm and the static DVS algorithm. This shows that most of the savings of ParaScale-G is due to the early discovery of dynamic slack by the intra-task ParaScale algorithm.

ParaScale-L also shows *much* lower energy consumptions than the static DVS, greedy DVS, and the base case, always consuming the least amount of energy for all utilizations among the three DVS schemes. Note that *higher relative savings are obtained for the higher utilization tasksets*.

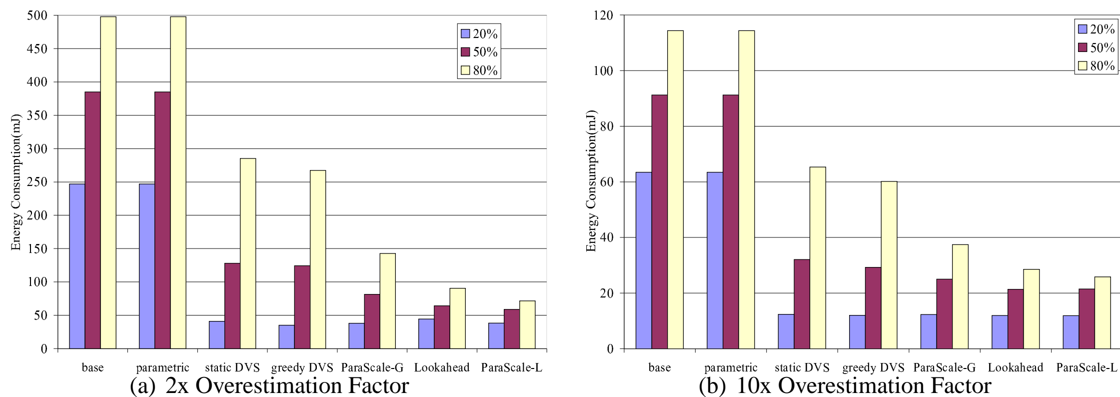

(a) 2x Overestimation Factor (b) 10x Overestimation Factor

Figure 5.11: Energy consumption for PCG Wattch Model – Dynamic Energy consumption

Also, ParaScale-L outperforms the lookahead DVS algorithm, albeit by a small margin. The reason for the difference being small is that lookahead is a very aggressive dynamic scheme, which tries to lower the frequency and voltage as much as possible and often executes at the lowest frequencies. ParaScale-L is able to outperform the lookahead algorithm due to the early discovery of future slack for parametric loops, which basic lookahead is unable to exploit fully.

One very interesting result is the relatively small difference between the ParaScale-G and the lookahead energy consumption results (for dynamic energy consumption). Thus, ParaScale-G, an intra-task DVS scheme that enhances a *static* inter-task DVS scheme, results in energy savings that are close to those of the most aggressive *dynamic* DVS schemes, albeit at lower scheduling overhead of the static scheme.

5.8.2 Leakage/Static Power

The results presented in Figure 5.11 are for energy values assuming perfect clock gating (PCG) within the processor, *i.e.*, they reflect the dynamic power consumption of the processor. These results isolate the *actual* gains due to the parametric approach. However, dynamic power is not the only source of power consumption on contemporary processors, which also have to account for an increasing amount of *leakage/static power* for inactive processor units.

Figures 5.12 and 5.13, present the energy consumed due to leakage. Figure 5.12 presents energy consumption with perfect clock gating and a constant leakage for function units that are not being utilized, as gathered by the Wattch power model. In reality, Wattch estimates the leakage to be 10% of the dynamic energy consumption at maximum frequency. This is not entirely accurate. Even with this simplistic model, ParaScale implementations outperform all other DVS algorithms, as far as leakage is concerned. Notice that the absolute energy levels are very similar for $2x$ and $10x$ for the corresponding schemes. This is due to the dominating leakage in these experiments.

Figure 5.13 depicts leakage results for a more realistic and accurate leakage model similar to prior work [64]. As mentioned earlier, two sets of experiments were performed, with two ratios of leakage to dynamic energy consumptions – 0.1 and 1.0. While the former models current processor

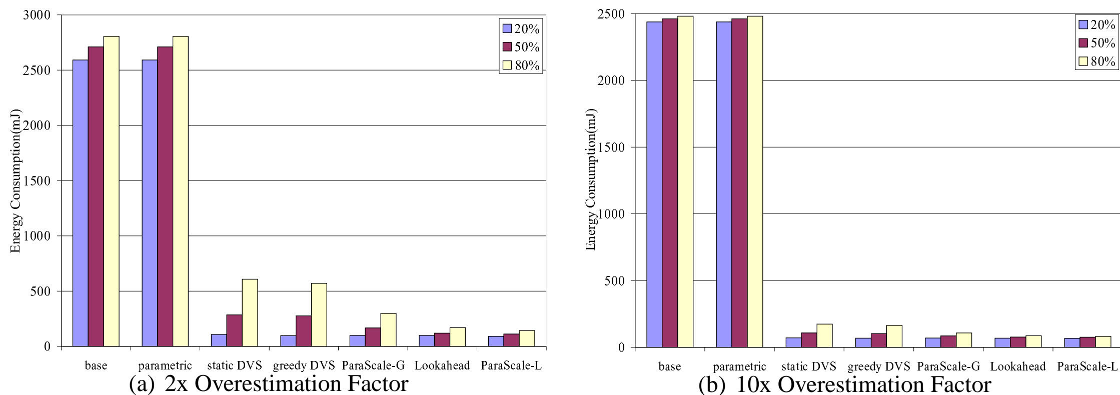

(a) 2x Overestimation Factor (b) 10x Overestimation Factor

Figure 5.12: PCGL-W – Leakage Consumption from the Wattch Model

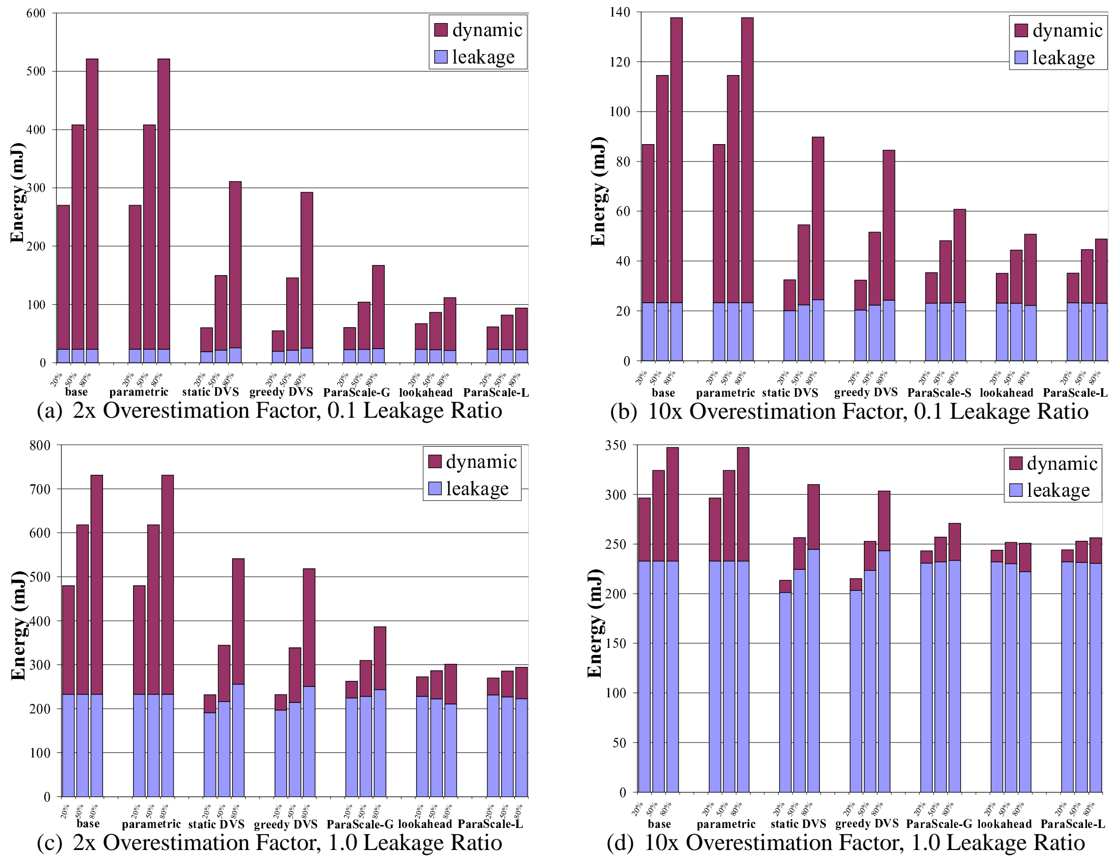

(a) 2x Overestimation Factor, 0.1 Leakage Ratio

(b) 10x Overestimation Factor, 0.1 Leakage Ratio

(c) 2x Overestimation Factor, 1.0 Leakage Ratio

(d) 10x Overestimation Factor, 1.0 Leakage Ratio

Figure 5.13: PCGL – Leakage Consumption from the Wattch Model

and silicon technologies, the latter extrapolates future trends for leakage. The top portions of the graphs in Figure 5.13 indicate the dynamic energy consumed while the lower portions indicate leakage. Figures 5.13(a) and 5.13(b) show the results for a leakage ratio of 0.1 for the $2x$ and $10x$ WCET overestimations respectively, and Figures 5.13(c) and 5.13(d) show similar results for a leakage ratio of 1.0.

These graphs show that even when the leakage ratio is small, the leakage power consumed might be a significant part of the total energy consumption of the processor. In fact, as Figure 5.13(b) shows, with a higher amount of slack in the system, the leakage could become dominant eventually accounting for more than half of the total energy consumption of the processor. Of course, Figures 5.13(c) and 5.13(d) show that even when the amount of slack in the system is low (2x WCET overestimation case), leakage might dominate energy consumption for future processors.

The ParaScale algorithms either outperform or are very close to their respective DVS algorithms (greedy DVS and lookahead) in all cases. The energy consumption of ParaScale-G often

results in energy consumption similar to that of the dynamic lookahead DVS algorithm. This holds true for leakage as well as the total energy consumption (dynamic+leakage). Also, the combination of lookahead and the inter-task ParaScale (ParaScale-L) outperforms all other implementations.

The graphs in Figure 5.13 indicate identical static energy consumptions for all utilizations for the base and parametric experiments. The DVS algorithms, on the other hand, leak different amounts of static power for each of the utilizations. This effect is due to the fact that leakage depends on the actual voltage in the system. The static DVS algorithm consumes more leakage with increasing systems utilizations since it executes at higher, statically determined frequencies (and, hence, voltages) for higher utilizations. The greedy scheme performs *slightly* better as it is able to lower the frequency of execution due to slack passing between consecutive jobs. The lookahead and all ParaScale algorithms are able to aggressively lower their frequencies and voltage. Thus, they have a different leakage pattern compared to the constant values seen for the non-DVS cases or the increasing pattern for static DVS.

5.8.3 WCET/PET Ratio, Utilization Changes and Other Trends

Consider the effects of changing the WCET overestimation factor and utilization on energy consumption. The ParaScale-G algorithm is used as a case study and compare it to static DVS and the base cases as depicted in Figures 5.11.

These graphs show slightly smaller relative energy savings for higher WCET factors ($10x$) compared to lower ones ($2x$). This is due to the fact that more slack is available in the system for the static algorithm to reduce frequency and voltage. Irrespective of the overestimation factor, ParaScale-L performs best for all utilizations, as discussed further in this section. The absolute energy level of $2x$ overestimation is about 3.5 times that of the $10x$ case without considering leakage for the highest utilization.

Furthermore, the ParaScale technique performs better for higher utilizations, as seen for experiments with 80% utilization in Figure 5.11(a). As the ParaScale technique is able to take advantage of intra-task scheduling based on knowledge about past as well as future execution for a task, it is able to lower the frequency more aggressively than other DVS algorithms. This is more noticeable for higher utilization tasksets because less static slack is available to static algorithms for frequency scaling.

Figure 5.14 shows the trends in energy consumption across WCET/PET ratios ranging from $1x$ (no overestimation) to $20x$ (large overestimation). Energy values for both DVS algorithms,

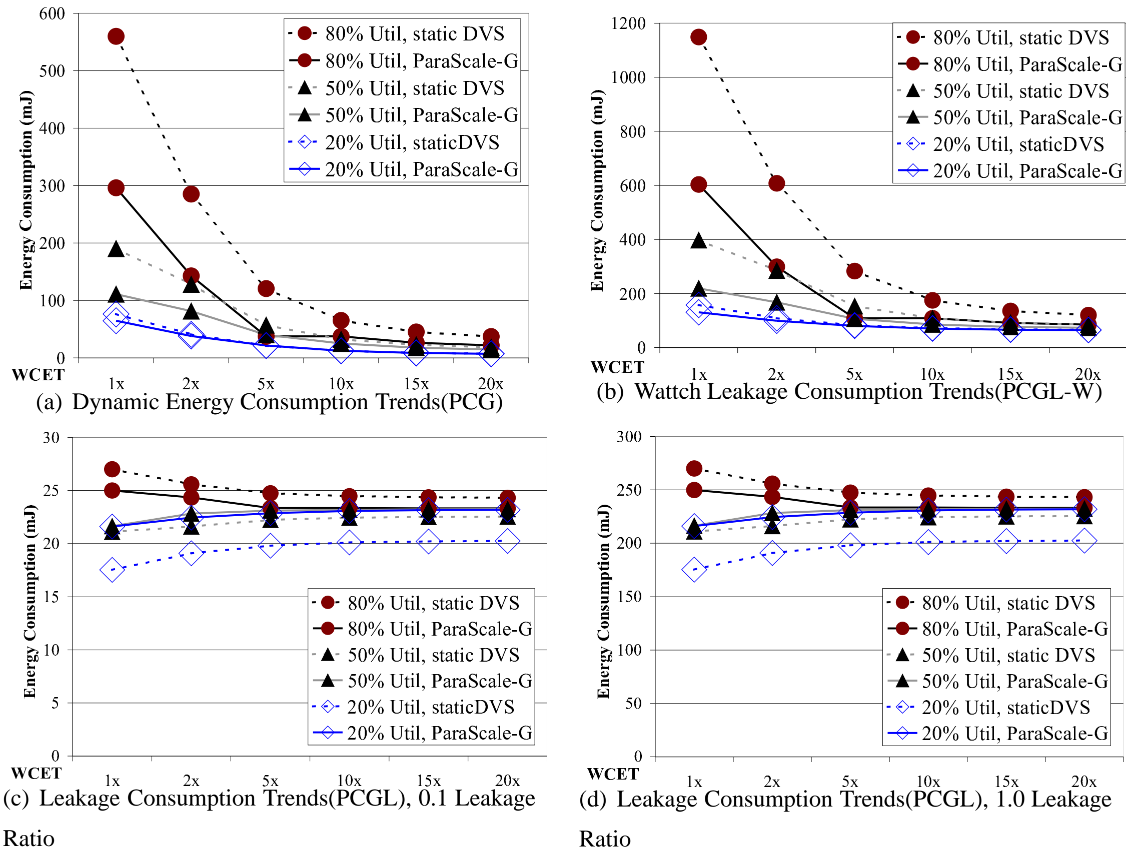

(a) Dynamic Energy Consumption Trends(PCG)

(b) Wattch Leakage Consumption Trends(PCGL-W)

(c) Leakage Consumption Trends(PCGL), 0.1 Leakage Ratio

(d) Leakage Consumption Trends(PCGL), 1.0 Leakage Ratio

Figure 5.14: Energy Consumption Trends for increasing WCET Factors for ParaScale-G

static DVS and ParaScale-G, are presented. Figure 5.14(a) shows that energy consumption drops as the over-estimation factor is increased, since less work has to be done during the same time frame. It also illustrates that the ParaScale-G algorithm is able to obtain more *dynamic* energy savings relative to the static DVS algorithm.

Similar trends exist in the results for PCGL-W (Figure 5.14(b)), except that the leakage, which permeates all experiments, results in lower relative savings compared to the PCG measurements. Contrasting Figure 5.14(a) to Figure 5.14(b) shows that the overall energy consumption is higher in the latter. This is due to additional static power that is modeled by Wattch as 10% of dynamic power.

The graphs for leakage (PCGL) (Figures 5.14(c) and 5.14(d)) depict a more accurate modeling of leakage prevalent in the system. As the WCET overestimation factor is increased from $1x$ to $20x$ the leakage consumption trends appear similar, across the board, for both – ParaScale-G as well as static DVS . More and more the time is spent in idling (executing at the lowest frequency and operating voltage) and less in execution. The leakage energy increases slightly from $2x$ to $5x$,

but from there on remains nearly constant until $20x$.

5.8.4 Comparison of ParaScale-G with Static DVS and Lookahead

This section presents a comparison of ParaScale with greedy DVS and lookahead since the latter are two very effective DVS algorithms. Both algorithms have been implemented as standalone versions as well as hybrids integrated with ParaScale.

ParaScale-G was compared to static DVS based on results provided in Figure 5.14. The energy consumption for ParaScale-G is significantly lower than that of static DVS across all experiments in Figure 5.14(a). This is because ParaScale-G can lower frequencies more aggressively as compared to static DVS algorithms. Static DVS can only lower frequencies to statically determined values. From Figure 5.14 it can be inferred that the relative savings drop in lower utilization systems and in systems with a high overestimation value. Due to the amount of static slack prevalent in such systems, the static DVS scheme is able to lower the frequency/voltage to a higher degree. For higher utilizations and for systems where the PETs match WCETs more closely, ParaScale-G is able to show the largest gain. This underlines one advantage of the ParaScale technique, *viz.* its ability to *predict dynamic slack* just before loops. This is particularly pronounced for higher utilization experiments resulting in lower energy consumption.

Consider the leakage results from Figure 5.14(b) which show that the differences between the energy values for static DVS and ParaScale are much larger, especially for the lower utilization and higher WCET ratios. There exist two reasons for this result. *(1)* Static power depends on the voltage. When running at higher frequencies/voltages, as necessitated by higher utilizations, both static and dynamic power increases. *(2)* Static power is estimated to be 10% of the dynamic power by Wattch. Hence, higher utilizations with higher voltage and power values result in larger static power as well. This is compounded by the inaccurate modeling of leakage by the Wattch model. Dynamic power is proportional to the square of the supply voltage, whereas static power is directly proportional to the supply voltage. By assuming that static power accounts for 10% of power, Wattch makes the simplifying assumption that static power also scales quadratically with supply voltage.

Results from the more accurate leakage model are presented in Figures 5.14(c) and 5.14(d). These graphs show that for the highest utilization (80%) ParaScale-G is able to lower the frequency and voltage enough so that the leakage energy dissipation is lower than that for static DVS. For the 50% and 20% utilizations, ParaScale-G shows a slightly worse performance. The leakage model

used [64] biases the per-cycle energy calculation with the inverse of the frequency (f^{-1}), which is the delay per cycle. Hence, aggressively lowering the frequency to the lowest possible levels may actually be *counter-productive as far as leakage is concerned.* The static DVS scheme lowers the frequency of execution to a lowest possible value of 200 MHz (for the 20% utilization experiments) while the ParaScale schedulers often hit the lowest frequency value (100 MHz). It is possible that the quadratic savings in energy due to a lower voltage are overcome by the increased delay per cycle at the lowest frequencies. Hence, if the number of execution cycles is large enough, ParaScale experiments "leak" more energy than the static DVS scheme. Figure 5.13, though, shows that the *total* energy savings for the system is still lower for the ParaScale experiments compared to their equivalent non-ParaScale implementations, and ParaScale-L still consumes the least amount of energy.

Figure 5.15 depicts ParaScale-G, the inter-task DVS enhancement to the static DVS algorithm. It shows an energy signature that comes close to that of lookahead, one of the best dynamic

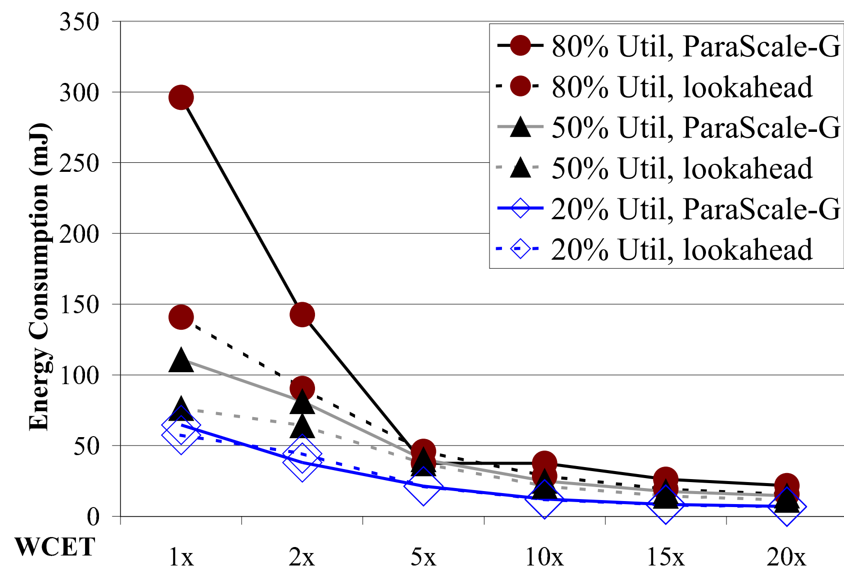

Figure 5.15: Comparison of Dynamic Energy Consumption for ParaScale-G and Lookahead

DVS algorithms. At times, ParaScale-G equals the performance of lookahead. This is particularly true for lower WCET factors where lookahead has less static and dynamic slack to play with. Here, ParaScale-G's performance is just as good, because it detects future slack on entry into parametric loops. This implies that ParaScale can achieve energy savings similar to those obtained by lookahead with a potentially lower algorithmic and implementation complexity. In fact, ParaScale-G is an $O(1)$ algorithm evaluating the parameters for only the *current* task whereas lookahead, an $O(n)$

algorithm traversing through all tasks in the system. This becomes more relevant as the number of tasks in the system is increased.

5.8.5 Overheads

The overheads imposed by the scheduler (especially the parametric scheduler, due to multiple calls made to it during task execution) and the frequency/voltage switching overheads are side-effects of the ParaScale technique. These scheduler overheads impose additional execution time on the system. The scheduler overheads were modeled using the timing analysis framework and are enumerated in Table 5.3. When compared to the execution cycles for the tasks (Table 5.4) in the system, the scheduler overheads are almost negligible. For example, the largest number of cycles used during a scheduler invocation is for the inter-task lookahead scheduler (8627 cycles). This value is less than 0.8% of the WCEC for the smallest task in the system, *viz.* LMS. Hence, the scheduler overheads have no significant impact on the execution of the tasks or the amount of energy savings.

Frequency Switch Overheads

To study the overheads imposed by the switching of frequencies and voltages, we imposed the overhead for a synchronous switch observed on an IBM PowerPC 405LP [139]. The actual value used was $162\mu s$ for the overhead.Data was collected on the number of frequency/voltage transitions for each experiment. The exact value of switching overhead varies depending on the actual difference between the voltages and whether it is being increased or decreased. This pessimistic, worst-case value was used to measure the worst possible switching overhead for the system. The highest overhead is incurred for the $20x$ overestimation case with utilization of 80% for ParaScale-G. The cumulative value for the overhead in this case was $42ms$. To put this in perspective, assume that the entire simulation had executed at the maximum frequency of 1 GHz. (thus completing in the shortest possible duration). The hyperperiod for each experiment was 1.2 seconds. All experiments were designed to execute for *one hyperperiod*s. Since the tasksets execute at lower frequencies than the maximum, they will take longer to complete but still finish within their deadlines. Also, the frequency switch overhead is typically lower than $162\mu s$ (depending on the exact difference between the voltage/frequency levels). Hence, it is safe to assume that the frequency switch overheads would be *much* less than the worst-case value of $42ms$. Typically, the overheads would be close to, or even less than, 1% of the total execution time of all tasks.

The energy consumption for the time period when the switching is taking place ($162\mu s$)

was also measured, for all three energy schemes – PCG, PCGL and PCGL-W. The respective values were 0.493 mJ, 0.007 mJ and 0.732 mJ, respectively, at 1 GHz. Considering the energy signature of the entire task set and the experiments, it is possible to conclude that the energy overheads for frequency switching will be negligible.

5.9 Conclusion

This chapter details:

1. the development of a novel technique of parametric timing analysis that obtains a formula to express WCET bounds, which is subsequently integrated into the code of tasks
2. the derivation of techniques to exploit parametric formulae *via* online scheduling and power-aware scheduling.

Parametric formulae are integrated into the timing analysis process without sacrificing the tightness of WCET bounds. A fixed point approach to embed parametric formulae into application code is derived, which bounds the WCET of not only the application code but also the embedded parametric functions and their calls once integrated into the application. Prior to entering parametric loops, the actual loop bounds are discovered and then used to provide WCET bounds for the remainder of execution of the tasks that are tighter than their static counterpart.

The benefit from parametric analysis is quantified in terms of power savings for sole intra-task DVS as well as *ParaScale-G*, the combined intra-task and greedy inter-task DVS. Processor frequency and voltage are scaled down as loop bounds of parametric loops are discovered. Power savings ranging between 66% to 80% compared to DVS-oblivious techniques are observed, depending on system utilization and the amount of overestimation for loop bounds. These energy savings are comparable to other DVS algorithms based on dynamic priority scheduling. Yet, the intra-task scheme (*ParaScale*) incurs a lower time complexity and can be implemented as an extension to *static priority scheduling* or cyclic executives. Conventional timing analysis methods will be unable to achieve these benefits due to the lack of knowledge about remaining execution times of tasks in conventional static timing analysis. This illustrates the potential impact of PTA on the filed of timing analysis and real-time systems practitioners.

Overall, parametric timing analysis expands the class of applications for real-time systems to programs with dynamic loop bounds that are loop invariant while retaining tight WCET bounds and uncovering additional slack in the schedule.

Chapter 6

Temporal Analysis for Adapting Concurrent Applications to Embedded Systems [1]

6.1 Summary

Embedded services and applications that interact with the real world often, over time, need to run on different hardware (low-cost microcontrollers to powerful multicore processors). It is difficult to write one program that would work reliably on such a wide range of devices. This is especially true when the application must be temporally predictable and robust, which is usually the case since the physical world works in real-time.

This chapter introduces a representation of the temporal behavior of distributed real-time applications as colored graphs that capture the timing of temporally continuous sections of execution and dependencies between them, thereby creating a partial order. A method of extracting the graph from existing applications is introduced through a combination of analysis techniques. Once the graph has been created, a number of graph transformations are carried out to extract "meaning" from the graph. The knowledge thus gained can be utilized for scheduling and for adjusting the level of parallelism suitable to the specific hardware, for identifying hot spots, false parallelism, or even candidates for additional concurrency.

The importance of these contributions is evident when such graphs can be sequentialized

[1]This is collaborative work with Johannes Helander that the author conducted during an internship at Microsoft Research in Summer 2007.

and can then be used as input for offline, online, or even distributed real-time scheduling. Results from analysis of a complete TCP/IP stack and smaller test applications are presented to show that the use of different analysis models result in a reduction of the complexity of the graphs. An important outcome is that increasing the expression of concurrency can reduce the level of parallelism required, thus saving memory on deeply embedded platforms while keeping the program parallelizable whenever complete serializability is not required. Applications that were previously considered to be too complex for characterization of their worst-case behavior are now analyzable due to the combination of analysis techniques presented here.

6.2 Introduction

Previous chapters introduced analysis techniques to deal with hardware complexity (Chapters 2, 3, 4) and *some* complexities in software (Chapter 5). While the latter was able to improve analysis techniques for some types of embedded software, it still dealt with relatively simple, straight-line, *single-threaded* code. It did not deal with situations where embedded systems need to be distributed in nature with *multiple threads* of execution. This chapter aims to analyze such complex pieces of software. We are increasingly depending on such systems in our everyday lives in health care, robotics, infrastructure, entertainment and even clothing. Such applications and other cyber-physical systems run on different embedded hardware platforms ranging from 8-bit microcontrollers to sophisticated multicores. Since we depend on these devices, they must be robust and as they interact with the real world, they must work in real time. Hence, their temporal behavior must be robust and predictable. Unfortunately, it is quite difficult to write one program that would work reliably on such a wide range of devices. This is particularly difficult if timing depends not only on the application, but also on hardware details and other applications on the device. This makes application development slow and expensive.

6.2.1 Awareness of Hardware Capabilities

It is important to pay attention to the hardware capabilities of a given target platform, such as the number of processors and amount of available memory. In a low-cost microcontroller the scarcest resource is often memory, and in particular physical RAM. Early experience with service-oriented cyber-physical systems [55] shows that one of biggest RAM users tend to be thread stacks. *Note:* this represents actual, *physical memory* since such embedded systems do not have memory

management units or virtual memory. They also require that each thread be allocated the largest possible, worst-case memory for stack space. This is true even for non real-time systems, because running out of stack space can be catastrophic as the thread will crash and potentially take down the entire system. Hence, solutions aim at reducing the number of threads. This implies that the amount *of parallelism needs to be reduced – i.e.*, the application needs to be executed sequentially.

In contrast, on a high-end multicore processor the bottleneck is not memory but the amount of parallelism available in the application. It often makes sense to execute the same service application on both ends of the embedded spectrum with only the throughput and the number of services being varied. Thus, the applications need to be tuned in such a way as to address the bottlenecks on each platform – the application needs to be *sequentialized for the low-end platform* and *parallelized for the high-end platform*. To this end, the *future*, a delayed function call (originally proposed for handling synchronization in MultiLisp [47] and later used in other languages), is used as a way of expressing *light-weight potential parallelism*.

6.2.2 Model-based Development

Having a model that would enable

1. analysis of the program's temporal behavior and

2. provide the ability to match it to a given hardware

would be most helpful. Helander *et al.* [57] showed how new programs could be written together using such a model. The model can be represented and manipulated as a graph, as discussed in this chapter, or serialized to XML as shown by the authors of that paper. The serialized version of the model is called "*partiture*", an expression analogous to a short score in music where the conductor can see what instruments should play at a given time without regard to the details of how they do it.

In practice though, most pre-existing applications do not follow model-based development practices, but it is still desirable to adapt them to new platforms. This even applies to large software projects in general where few, if any, engineers understand how a program actually behaves due to large development teams and changes over product revisions. Helping engineers understand and modify complex software would be useful. This chapter proposes an automated process whereby existing applications can be transferred to use *partitures* and *futures* [57] to make model-based scaling possible while maintaining correct program execution. This would reduce the tedious and

error prone methods for transforming applications by hand when they need to be deployed on new platforms.

A tool that *extracts temporal models from existing applications* is introduced in this chapter. The knowledge gained can help designers of such systems in:

1. optimization of programs for *different platforms*,
2. distributed orchestration,
3. adaptation and *scheduling* [57, 102], and
4. execution on modeling engines [62] to check for *correctness*.

6.2.3 Limitations of Analysis Techniques

Knowledge of the temporal behavior of an application is hidden inside the application logic where it is extremely difficult to analyze and model for any given hardware. While static and dynamic timing analyses are used to obtain the worst-case execution times (WCETs) for real-time applications, they may not able to provide a complete picture of a program. This is particularly true in the case of larger, more complex programs. Programs that contain function pointers are typically out of the reach of static analyzers. Dynamic analyzers are unable to gauge the true nature of the program and have shown to be unsafe [126] – *i.e.*, they may underestimate the WCET of the program, which could lead to dangerous effects. If the application uses *concurrency constructs* such as signals, locks or mutexes, then *neither* of these techniques can fully analyze the application.

6.2.4 Contributions

This chapter presents the use of a combination of a variety of techniques to form the complete picture of the structure and execution characteristics of a *distributed embedded application*. The collected information is used to create *timing graphs*. The timing graph and the *partiture* are two representations of the same information. The nodes in the timing graph could represent simple code sections (*e.g.* basic blocks) or complex structures (*e,g,* groups of functions), all combined into *temporal phases*. The edges in the graph represent transitions between the phases, both between phases within the same thread as well as interactions between threads. A *bar* corresponds to a node in the graph. Triggers and sequences between the bars correspond to the graph edges. This means that the graph can simply be converted to a partiture and then be used for purposes such

as inputs for offline, online, or distributed real-time scheduling or potentially even converted to a model program [57].

Finally, results are presented from a prototype analyzer that was used on a complete *TCP/IP stack* in addition to smaller test applications. Perhaps the most interesting and surprising result is that *increasing the expression of concurrency can reduce the level of parallelism required* and save memory on deeply embedded platforms. Hence, the main contributions of this chapter are:

1. To extend the scope of static (and dynamic) timing analysis to more complex applications by combining it with other techniques, in particular run-time traces and type inference. Applications that were previously considered to be “un-analyzable” due to their inherent complexity are now analyzed using the graph capture and transformation techniques – their worst-case behavior can now be characterized correctly.

2. To define a colored graph representation of a program’s temporal behavior, including invariants and transformations. The graph corresponds to a *partiture*, a programmatic expression. Transitively, it also corresponds to a model program that can be executed on a modeling tool.

3. To derive information from the topology of graphs, thus allowing an engineer to optimize an application such as to make it more scalable and amenable to being transformed into the application model presented here (partitures, futures, *etc.*). Some such knowledge that can be gleaned – the minimum number of threads required for an application to correctly execute, graph sections with potential false parallelism, and dependencies that prevent parallelization.

4. To observe that adding concurrency can save memory and present methods to an engineer to pinpoint areas where concurrency can be increased.

5. To allow an engineer to learn something about the application behavior and augment the automatically generated model with manually provided domain knowledge. Due to the incremental nature of the analysis, even an incompletely understood application can be explored. This is a critical step forward as embedded designers now have more choices in the type of applications that they can develop, especially for time-constrained systems.

6. To demonstrate that creating the timing graph and performing subsequent transformations is feasible by means of presenting an implementation that was applied to actual embedded software – the TCP/IP stack of an embedded operating system.

One important feature of the techniques presented in this chapter is that they are *independent of the programming language* used.

The use of the combination of analysis techniques presented in this chapter enables the process of extracting temporal behavior from existing applications. This ultimately leads to the development of distributed embedded applications on varied platforms. Such analysis is the first of its kind.

The rest of this chapter is organized as follows: The use of *futures* in embedded software is discussed in Section 6.3. The colored graph representing a program's temporal behavior is introduced in Section 6.4, together with invariants that define a valid graph. The algorithm for creating temporal graphs is introduced in Section 6.5. Transformations that can be used to simplify and/or reveal interesting topological properties of the graph are defined in Section 6.6. Section 6.7 explains insights obtained from the graph transformations. Section 6.8 details the experimental framework and methods to collect the raw data required for graph generation. Section 6.9 presents the results followed by the conclusion being presented in Section 6.10.

6.3 Saving Memory through Sequential Execution

In low-end microcontrollers a multi-threaded application uses one stack for each thread. Since microcontrollers do not usually have a memory management unit, each thread stack must be allocated from physical memory. The maximum size of the stack is limited by the available memory The minimum is the largest stack the thread may ever need. Once a thread has been created it cannot give up its stack, whether running or blocked, since there are live stack frames occupying part of the stack. This is the case even before the thread has run for the first time as an initial stack frame must be created by the runtime. The stacks cannot be moved as frames in it contain pointers to data in other stack frames and cannot be compacted as executing code may need to push additional frames. As a final option, copying, compressing, and decompressing stacks at each context switch to the side and sharing the actual stack between threads would be complex and inefficient. Clearly, threads are problematic on low-end embedded systems.

The most common alternative is an event loop. Instead of creating a thread to handle a sensor reading, for instance, an event is posted. A loop in the program then picks up an event and examines it. The disadvantages to this are – *(1)* all applications turn into state machines with complex interactions. Thus, the code becomes hard to understand. *(2)* The development process becomes error prone with skyrocketing maintenance costs.

One approach is to transform an application written with threads to use the so-called split-phase operation [4] where the temporal phases of a thread are split into separate functions. However, no automated transformation from existing programs has been available because significant engineering effort is required for carrying out such a transformation. The approach has been codified in the NesC programming language [40]. Unfortunately the split-phase mode is essentially the same as an event-driven model, including the need to communicate state from one phase to another in global variables or objects pointed to by global variables.

One attempt at combining the features of thread-based programming and event handling is protothreads [32] where stacks are unwound at blocking points. While this appears to work only in the C programming language, the implementation relies on non-standard features in a specific compiler (which it uses in a clever way). More importantly, protothreads do not save local variables during blocks, making the appearance of thread programming at best an appearance and at worst an endless source of difficult bugs.

6.3.1 Futures

Futures [37] were originally proposed in the Lisp community as a way of deferring evaluation and increasing performance [39]. They were used as a primary construct for concurrency and synchronization in MultiLisp [47]. Futures have also been implemented in mid-level languages, such as Java [31] or C#. Futures have been natively implemented in C on a microcontroller in earlier work [57]. When C programs are written in an object-oriented fashion, it is easy to turn any method call into a future with few modifications to the program. Threads can also be converted to futures. Creating a future is similar to calling a method or function, yet the call is executed asynchronously. Parameters are delivered like regular function calls. If a split-phase program was rewritten in terms of futures, its phases could send values to the following phase in normal function parameters, including *this* pointers in object-oriented programs, thus obviating the use of global variables, an engineering practice commonly advocated in the last few decades. Compared to protothreads, the normal language rules are in effect and asynchrony is explicit and controlled.

Instead of being implied or encoded in the program, such as in traditional threads programming, timing parameters and any required concurrent execution is expressed in a partiture where each future is associated with one or more bars. The advantage of futures over threads is that futures can be inserted anywhere (there is *no predetermined parallelism, only concurrency*), stack allocation can be deferred until the future is ready to run, and the cost of creating a creating a future

is low. Control loops can be moved into the partiture leaving just the worker function in the future. Thus, a typical construct where a thread waits for an event, then processes it and then waits again can, with little effort, be changed to give up its stack during the wait. This is why futures exhibit all the advantages of split-phase operation when used generously. However, it is not always necessary to convert all blocking points to futures so as to make it possible to run the entire software on exactly *one* stack. Often, an embedded device only has room for a small number of stacks. Section 6.7 shows how to discover the number of stacks required and how to reduce the number one step at a time.

The real strength of futures is, however, in parallelizing the program. On a multicore processor futures can be executed in parallel. The parallelism is only limited by the dependencies between futures, which are conveyed to the scheduler by the partiture. The future, combined with *partitures* [57] and the "temporal timing analyzer" presented in this chapter allows for an aided and incremental program transformation that has all the positive features of split-phase operations while being more flexible and structured. This allows programs to execute in parallel when parallelism is available on the hardware and sequentially otherwise. The future is an explicit expression of concurrency. Adding concurrency, thus, not only adds *potential* parallelism but also reduces the *required* parallelism resulting in memory savings.

False parallelism between two (or more) threads refers to the situation where in reality the constituent threads can actually only execute *sequentially*. Using threads with *false parallelism* between them leads to a requirement for multiple stacks. This is not really necessary but is merely an artifact of the programming model. With futures, such dependencies can be broken or made explicit when *real* parallelism exists.

6.4 The Timing Graph

At the core of the analysis is the *timing graph*, which is a graph that enumerates the timing and execution characteristics of a program (including concurrent programs).

6.4.1 Representation of the Timing Graph

To reason about and distinguish between the various constructs in the timing graph in a precise manner, colors (and corresponding shapes) were allocated to the nodes as well as for each type of edge. The five colors used are depicted in Figure 6.1.

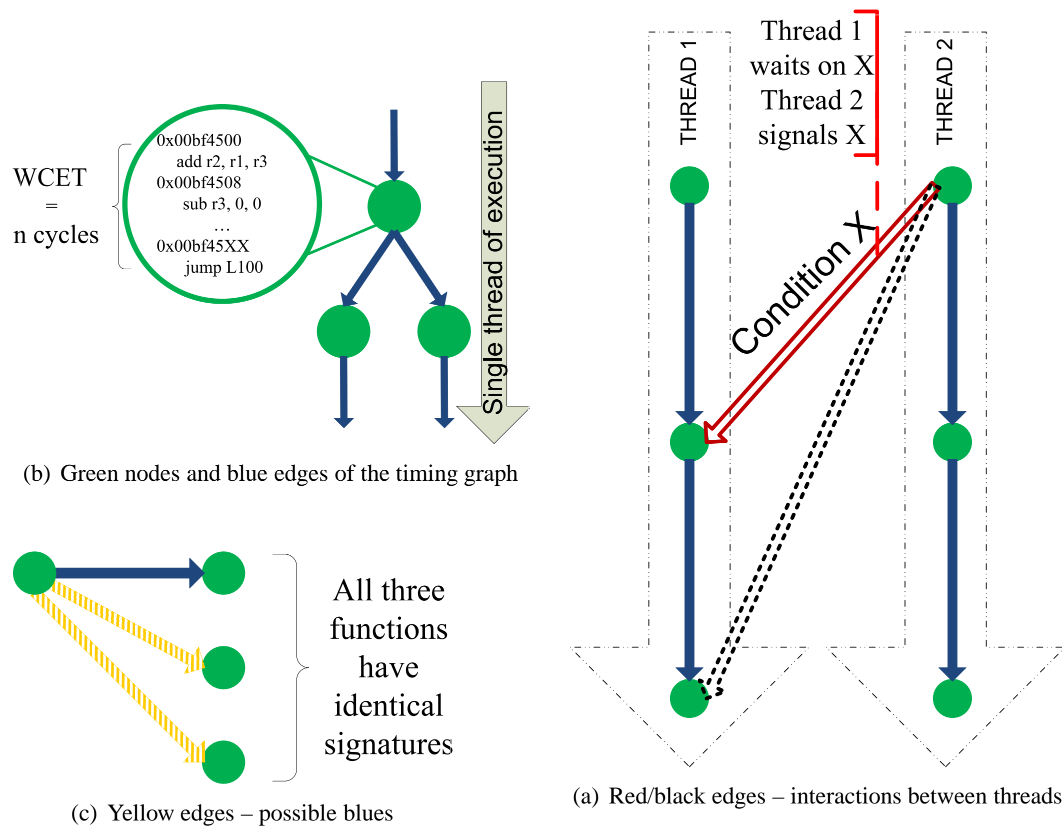

(b) Green nodes and blue edges of the timing graph

(c) Yellow edges – possible blues

(a) Red/black edges – interactions between threads

Figure 6.1: Edges and Nodes in the Timing graph

Code that runs within a single thread without external interactions is represented by *green (circular)* nodes (Figure 6.1(b)). These nodes represent straight line code, possibly entire functions or call graphs between temporal program phases. A temporal phase is delimited by potential sleeping, waiting, signaling, message passing, or other points of interaction with other threads (or futures). Green (circular) nodes correspond to *bars* in the *partiture*. Static timing analysis is performed to obtain the WCET of this block of code. Transitions between green nodes *within the same thread of execution* is represented using *blue (solid)* arrows. Figure 6.1(c) shows *yellow (dotted)* edges, which are "possible" blue edges representing transitions that could potentially occur, but it is not possible to determine if they occur.

Applications consisting of multiple threads that communicate via various concurrency constructs are illustrated in Figure 6.1(a). Blue edges are restricted to their own threads. Calls to communication constructs are depicted as *red (hollow)* edges, where an incoming edge represents a *wait* and an outgoing edge a *wakeup/signal* on a shared synchronization object. Further analysis reveals other possible synchronization objects that could be called/waited upon leading to more edges

in the graph. These edges are colored *black (dotted hollow)* and represent "possible" reds. The black edges represent the signaling of an unknown object if the wait and the signal are the same object.

condition_wait(x) = wait for condition 'x' to be signalled	
condition_signal(y) = signal condition 'y'.	
	Wake up the next thread waiting on this condition.

Figure 6.2: Synchronization constructs

If it turns out that the wait and signal are for different synchronization objects then the edge is eliminated. For analysis presented here and for the sake of simplicity, it is assumed that all concurrency constructs reduce to one of those defined in Figure 6.2. All other basic synchronization constructs face situations where one process waits while the other signals can be expressed in a manner similar to the condition waits/signals used here.

6.4.2 Graph Invariants

The timing graph has certain invariants that must *never* be violated, neither during the creation process nor while performing one of the transformations:

1. the final schedule that is created will retain all dependencies among the various threads; and
2. a transformation must not, inadvertently, change the semantics of the program.

This second invariant is important, *i.e.*, if a transformation will result in the creation of a deadlock, then that transformation is *not* carried out. For a timing graph, a "deadlock" is defined as a directed cycle formed by one of the following:

- red edges only;
- red edges with one or more black edges; or
- one or more blue edges with one or more red and/or black edges.

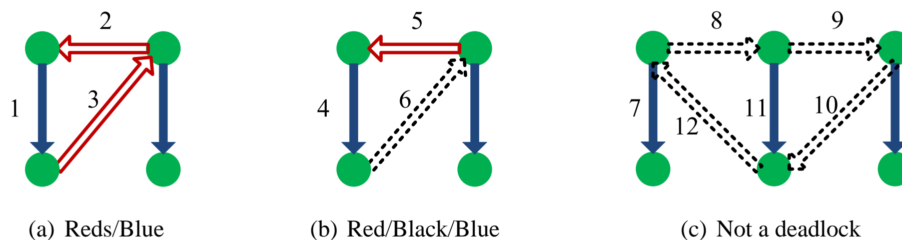

(a) Reds/Blue (b) Red/Black/Blue (c) Not a deadlock

Figure 6.3: Deadlocks in Timing Graphs

In Figure 6.3(a), edges “1”, “”2 and “3” form a cycle, while in Figure 6.3(b), edges “4”, “5” and “6” form a cycle. Hence, these two graphs have deadlocks. Deadlocks formed by black edges *only* (Figure 6.3(c)) are acceptable because black edges represent alternate schedules. A deadlock consisting of only black edges cannot exist in the same graph/schedule since it is assumed the program is valid unless proven otherwise. This means that in an actual schedule it is not known, ahead of time, which condition variables will be used, but it can guarantee that it will be only those that do not form a deadlock. Hence, the analysis can proceed in the presence of “false deadlocks” formed by black edges based on the premise that the program is and will remain valid.

For real-time programs, timing issues will also be a factor. A full real-time schedulability analysis will take these additional factors into account and perform constraint solving. However, the invariants mentioned above will still be true, and the graph transformations presented in this chapter are just as valid for real-time schedulability. In such cases, the graph is evaluated with the above topological invariants in the first pass. Schedulability analysis can then be performed in the second pass with an extended set of invariants, but the details are beyond the scope of the work presented here.

6.5 Information Sources and Graph Creation

This section enumerates the process of creating timing graphs. It shows how the information is gathered from a variety of sources and then put together to create the actual graph. Section 6.5.1 enumerates the various sources of information while Section 6.5.2 describes the composition of the graph.

```
void func1( int i ) ;

int func2( int i, double d ) ;
int func3( int i, double d ) ;

double func4( char c1, char c2, int i ) ;

void foo(){
        void (*fptr)( int, double ) ;
        func1( 10 ) ; // static call
        fptr = func2 ;
        (*fptr)( 10, 5.0 ) ; // dynamic call
}
```

Figure 6.4: Sample code to illustrate creation of the Timing Graph

6.5.1 Information Gathering Techniques

Information gathered from a variety of sources is used to create the timing graph. They are a mixture of static and dynamic data as well as higher level information. *Four* such techniques, combined together, are used to ob-

tain the complete picture of the control flow and dependence information within the application. The sample application in Figure 6.4 is used to the explain each step while Figure 6.5 shows the final results obtained after applying these techniques. The information sources are:

1. *Static Analysis*: The control flow graph (CFG) of the application is created and analyzed at compile time to obtain the static function call graph of the application. Static analysis shows that function “foo” calls “func1” (Figure 6.4), represented by the horizontal blue arrow between the two nodes (Figure 6.5).

2. *Dynamic Tracing*: The program is executed with sample inputs and the function calls are traced during execution. This step finds *some* of the dynamic calls that were made in the program, represented by calling “func2” using the function pointer “fptr” (Figure 6.4). This gives a better picture of the control flow in the program and results in the addition of the vertical blue arrow in Figure 6.5.

3. *Type Information*: Once step (2) is complete, type (signature) information of all other functions in the application is compared pairwise to see which ones have the *potential* to be called. If the signature of a (dynamically) called function matches that of another uncalled function, then there is a possibility that the latter may be called at the *same call site*. Functions “func2” and “func3” (Figure 6.4) have identical signatures. Since “func2” was called, there is a possibility that the same function pointer could have called “func3” as represented by the yellow arrow (Figure 6.5). Type information can also be used to reduce the universe of possibilities for dynamic function calls. For instance, between the static analysis and dynamic tracing phases, there was a possibility that any one of the functions in the program (func1, func2, func3, func4, or even foo) could have potentially been called using the function pointer. Once dynamic analysis tells us that “func2” was called, “foo”, “func1” and “func4” can immediately be eliminated from the list of possibilities because their types are different from that of “func2”. The true value of type information comes when trying to gather information about concurrency constructs. If, during runtime tracing, information is obtained that a particular concurrency call was made, then the possibilities of other concurrency constructs that the call site can then invoke are limited by the use of type information of the first callee.

4. *Incremental development* with inputs from the domain expert/programmer: Outgoing edges can be further pruned by inputs based on domain knowledge. For instance, “func3” was determined to be a potential callee because its type matches that of “func2”. A domain expert

might be able to point out that based on the application design there is *never* a possibility that both "func2" and "func3" are called during the same execution instance of the application. This could be the case in a typical network stack where "tcp_send" and "udp_send" probably have the same function signatures but can never be called from the same call site. Hence an incremental development process that combines inputs from the automated techniques and the programmer can improve the understanding of the application.

Further known techniques, such as abstract execution, flow analysis, *etc.*, as well as techniques that will be developed in the future, can be used to gather more information and make the graph more complete. The analysis can remain the same and take advantage of a graph that has more information. This will reduce the time for the analysis and provide more accurate results.

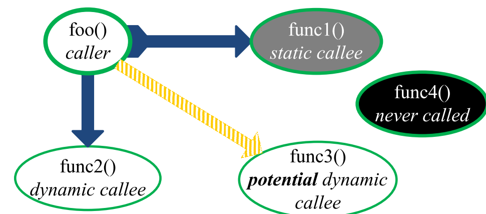

Figure 6.5: Timing graph created by application of various information gathering techniques

6.5.2 Graph Creation

The timing graph is actually created in stages. The green nodes in the graph which represent straight-line execution within the same thread could be basic blocks in the CFG or even single (or groups of) functions (at a higher level). Traditional static timing analysis is performed to obtain the worst-case execution time (WCET) for this block of code. Edges obtained from static analysis as well as those obtained from the dynamic traces form the blue arrows, which are added next. Yellow edges are gleaned from type information and are then added to the graph. Red edges are a result of dynamic tracing where calls to concurrency constructs are also traced. Further type analysis reveals other possible conditions that could be called/waited upon, based on the type signature of the previous callee, leading to black edges being inserted into the graph.

Before the analysis is started, the number of "possible" edges in the function call graph is large, *i.e.*, any function can call any other function or signal/wait on any condition variable. With static analysis, some of the yellow edges are turned into blue edges while some of the black edges are turned into reds. Also, since static analysis fixes one outgoing edge per call site, it also eliminates other yellow/red edges from the same call site, thus reducing the universe of possibilities. Further analysis (runtime tracing) turns more of the yellows into blues and blacks into reds. However, this step does not reduce any edges, as there is no guarantee that each call site has only one outgoing edge. In fact, as seen in the case of function pointers, each call site could call many potential callees.

Type information, on the other hand, can prune some edges. It restricts possible outgoing edges based on the type signature to blue and red edges that have been discovered during runtime analysis. Hence, some yellow and black edges are removed from the graph. Finally, domain knowledge can prune the graph further by removing impossible yellow and black edges from the graph. This multi-colored, pruned graph is used for the analysis that follows in the next section.

6.6 Timing Graph Transformations

This section presents certain fixed graph transformations aimed at reducing the complexity of these timing graphs. The transformations will also help the programmer find interesting topological and programmatic properties. As explained in Section 6.2, embedded systems have severe resource constraints. Executing parallel code could lead to a high number of context switches and a large number of threads, which ultimately leads to a high demand for stack space. Hence, reducing the program to obtain the *least* number of threads required for correct execution of the program aids in reducing stack pressure. This also helps determine the limits of serializability of the program. The transformation described in the remaining part of this section aids in achieving both of these goals. The larger goals for performing these transformations are:

1. To find the *minimum* number of threads required for the application to function correctly;
2. To aid in understanding the program behavior/structure and help system designers to optimize it. [2]; and
3. To provide the ability to *automatically* generate partitures and, from them, the schedules of execution on a particular system.

The timing graph and subsequent transformations could also be used, in the future, to achieve the following goals:

- To aid in visualizing the program so that system designers could gain an understanding of the true nature of the program;
- To aid in increasing the parallelism of the program by finding spots that are synchronization bottlenecks, *i.e.*, a concentration of edges in close vicinity;

[2] Specifically, this could find candidate spots for additional concurrency in the program, which makes the program more scalable. It is also possible to find false parallelism in the program, wherein multiple threads must execute in a serial fashion for forward progress of the application

- To provide inputs for real-time schedulability analyzers and constraint solvers; and
- To aid in model-based testing of the application.

6.6.1 Assumptions

The transformations presented here rest on the following assumptions (or rather the preconditions):

- A *strict partial order* is always maintained for the graph.
- The graph cannot have any deadlocks or race conditions (*i.e.*, no unguarded resources). This condition implies that the program must be *correct*. Of course, benign races (such as bounded atomic adds) are fine.

If the timing graph represents a real-time application, then certain additional constraints apply:

- Loop bounds must either be statically known or at least known prior to loop entry.
- No code can be dynamically loaded, *i.e.*, all modules in the application must be statically known. This rule can be relaxed to state that all applications that could possibly be loaded must be known. The system could then be treated as if everything had been preloaded. Of course, this would introduce some pessimism into the analysis.
- The program must use a *finite* set of condition variables.

Note: The analyzer does not check for the correctness of programs but will axiomatically assume the validity of programs and try to apply transformations.

6.6.2 Graph Pruning and Reduction

This section examines techniques used to reduce and simplify the graph. First, *graph pruning* techniques are presented. They help in reducing "maybe" edges, either by transforming them to actual, known edges (blue or red) or getting rid of them entirely. Section 6.4 already introduced some methods for performing this pruning, *e.g.*, dynamic traces prune some yellow edges to blues, *etc.* Other techniques used are:

1. Black edges that result in "potential" deadlocks (with red or blue edges) are removed. The program is assumed valid unless proven otherwise.

2. In case of alternate yellow edges, pick the *worst* one of all. Hence, pick the yellow edge with the largest WCET of all.

3. If alternate paths exist and each one waits on different condition variables (or none), then the longest path must wait on a *union* of those condition variables. Hence, execution waits on all of the condition variables to be signaled.

4. If, in the face of alternate paths, the application signals different condition variables (or none) on each one of the alternate paths, then execution must wait for an *intersection* of those condition variables to be signalled.

Remarks: Techniques *(3)* and *(4)* aim at preserving the worst-case behavior and strict partial ordering, respectively. The former ensures that all resources must be acquired before execution proceeds while the latter guarantees that all branches are valid and does not result in deadlocks.

Graph reduction operations are broadly classified into two groups:

1. *point-of-view* simplifications and

2. simplifications that *restrict the partial order*.

Of course, the transformations must not violate the invariants for the graph (Section 6.4.2). *Note*: The examples in the figures indicate artificially created graphs to illustrate the transformation being performed. While these graphs are not extracted from actual code, it is entirely feasible that such situations could occur in real programs.

Point-of-View Simplification

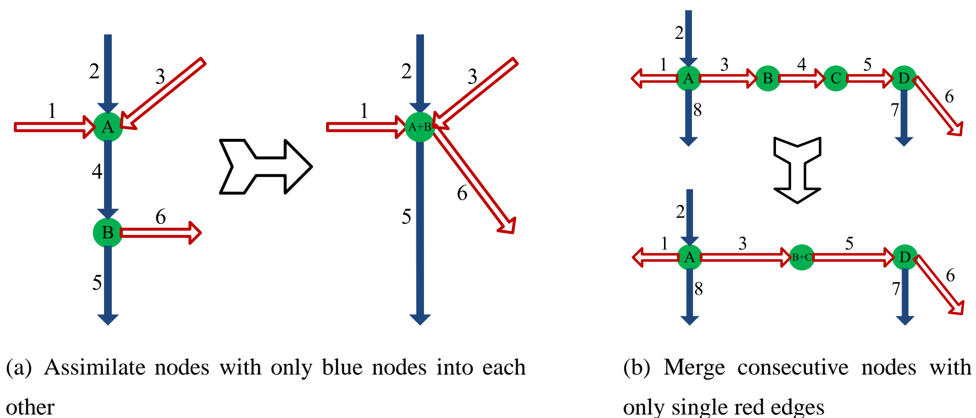

(a) Assimilate nodes with only blue nodes into each other

(b) Merge consecutive nodes with only single red edges

Figure 6.6: Two Point-of-View Simplifications

The following point-of-view transformations are illustrated in Figures 6.6 and 6.7:

1. Consecutive nodes connected by a blue edge are merged where either the blue node's source has no outgoing red edges or its destination has no incoming edges or both. This is a simple concatenation of sequential code.

2. Two consecutive nodes that have single incoming and outgoing red edges can be fused into a single node. Nodes "B" and "C" in Figure 6.6 were combined into node "B+C". This transformation corresponds to inlining the code from one thread into the other thread.

3. Remove a direct red edge if a longer, indirect path consisting entirely of red edges exists between the source and destination nodes as shown in Figure 6.7.

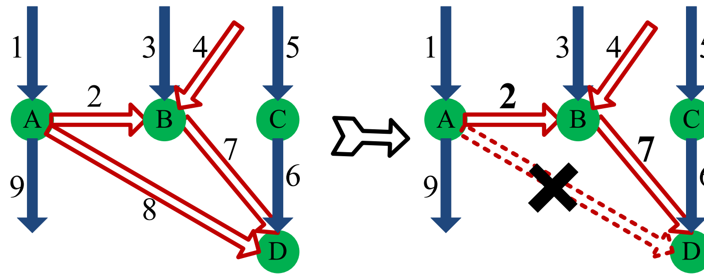

Figure 6.7: Remove direct red edges

Remarks: Application of one or more of these simplifications does not result in a reduction of the nodes or edges in a graph – they are just dropped from the visualization. Hence, while they may exist in the graph, for all practical purposes they may be ignored. Transformation *(a)* is shown in Figure 6.6(a), where node "A" has only one outgoing edge, which is blue, and node"B" has only one incoming edge ("4"), which is also blue. Hence, they are merged into a single node ("A+B"). This transformation is equivalent to merging consecutive basic blocks (or function inlining) where no other dependencies exist for the caller or the callee. The WCETs of "A" and "B" can now be combined to form the WCET of the new block as follows:

$$WCET_{A+B} = WCET_A + WCET_B - pipeline_interactions$$

where "pipeline_interactions" refer to the reduction in execution time due to the concatenation of the trailing edge of A and the leading edge of B [51]. Note: edge "4" is missing from the new graph because it is actually included within the new node, "A+B".

The *pipeline_interactions* term in the above formula refers to the worst-case *execution* time for the flow of instructions through the pipeline. By performing the concatenation of nodes "A"

and “B” the WCET of the combined node does not change – only the visualization and treatment in the graph becomes more convenient.

Figure 6.6(b) shows that the WCET of the combined node is the sum of the two nodes, with pipeline effects considered (as in transformation (a)). This transformation is possible because the real dependence between “A” and “D” is not changed by merging the intermediate dependence (edge “4”).

Edge “8” between “A” and “D” (Figure 6.7) can be removed as an alternate path (A→B→D composed of edges “2” and “7”) exists. This follows from the intrinsic transitive nature of a partial order. Of course, in a real-time system, this may be interpreted as retaining the sequence of edges that exhibit worst-case behavior – two or more dependencies are worse than one, direct dependency.

Restricting the Partial Order

These transformations aim to restrict the partial ordering for the graph. They actually change the edges in the graph – either by moving their source or their destination nodes, and sometimes both (though this will be done one at a time). The graph transformations that restrict the partial order and, hence, result in a reduction of the graph are:

1. Move all outgoing red edges of a node to its successor. A “successor” is defined as a node which is the destination of a blue outgoing edge from the current node. This transformation is depicted in Figure 6.8.

2. Move all incoming red edges of a node to its predecessor. A “predecessor” is defined as a node which is the source of a blue incoming edge. This particular transformation is depicted in Figure 6.9.

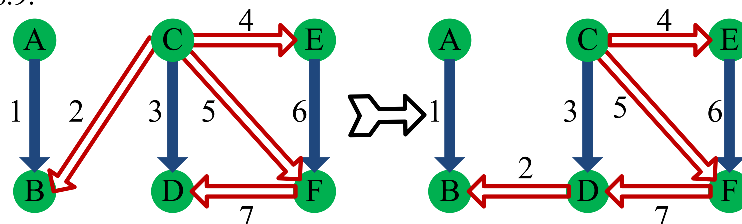

Figure 6.8: Move outgoing red edges to successor

Remarks: These transformations are applied to every possible node, and their edges are transformed except in cases where they violate the graph invariants. Figure 6.8 shows transformation *(1)*, where nodes “B”, “D” and “F” are successors to nodes “A”, “C” and “E” respectively. The figure shows that outgoing edge “2” (from node “C”) is transformed to *originate at* node D. Hence, the outgoing

nodes for “C” are moved to C’s successor “D”. Note: Edge “5” is not transformed because doing so would have created a deadlock with edge “7”. Similarly, transforming edge “4” would have resulted in a deadlock as well (4 $\rightarrow$ 6 $\rightarrow$ 7).

In Figure 6.9, nodes “A”, “C” and “E” are predecessors to nodes “B”, “D” and “F”, respectively. After transformation *(2)*, incoming edge “2” now points *to* node “C”. Edge “5” was not transformed because it would have created a deadlock with edge “4”, thus violating an invariant. Similarly, transforming edge “7” would have resulted in a deadlock as well (4 $\rightarrow$ 6 $\rightarrow$ 7).

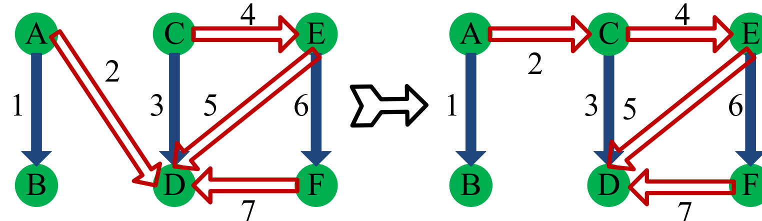

Figure 6.9: Move incoming red edges to predecessor

The above graph transformations are *valid*. They are analogous to known deadlock avoidance techniques. Transformation (1) is the same as releasing all locks held by a process at the same time, *i.e.*, at the end of the execution of the *outermost* critical section. Hence, all condition signals are moved to the successor (node). The second transformation is the same as delaying execution of the critical section until *all* locks requested by a process have been acquired, *i.e.*, move all condition waits to the predecessor (node). These transformations can be performed recursively, thus ensuring that the critical section execution starts only after all locks have been acquired and will release all locks at the same time, *i.e.*, at the end of the execution of the critical section. These two transformations could be further restricted with more invariants in hard real-time systems, such as the deadline, startup time, period, phase, *etc*. *Note*: A combination of transformations (1) and (2) achieves the same effect as the priority ceiling protocol (PCP) [42] assuming all resources had the same ceiling value.

6.7 Outcome of Timing Graph Transformations

When iteratively applying the graph transformations (Section 6.6), one of the following situations occurs:

1. The graph is *entirely serializable*. In this case the entire program can be executed using a single thread.

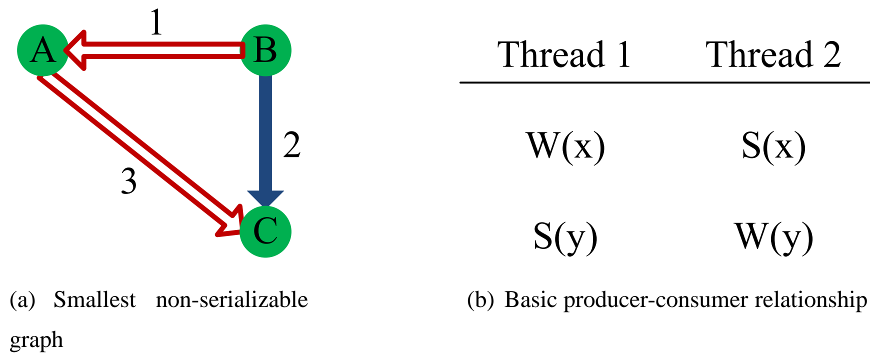

(a) Smallest non-serializable graph

(b) Basic producer-consumer relationship

Figure 6.10: Outcome of graph transformations

2. The graph is *non-serializable* where, at the simplest level, it resembles the graph shown in 6.10(a).

The latter case is a graphical representation of a producer-consumer relationship (Figure 6.10(b)) where "x" and "y" are condition variables. "W" signifies a condition wait while "S" represents a condition signal. Hence, Figure 6.10 represents the case where one thread (Thread 1, the producer) waits for another thread (Thread 2, the consumer) to send a request which it then responds to. Note that the consumer is not able to make forward progress as it must wait for results from the producer to be sent back. Hence, it can be deduced that this simple program can make progress only if the producer and consumer execute on *two separate threads*.

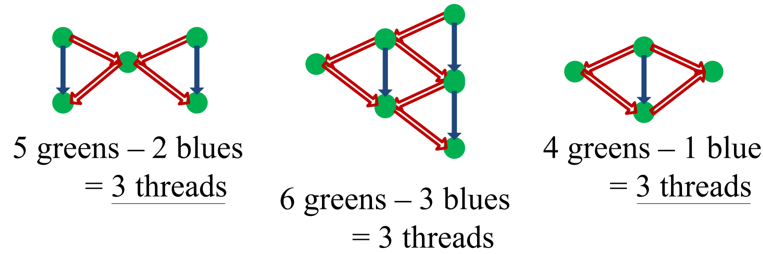

Figure 6.11: Multiple producer-consumers

The graph in Figure 6.10(a) is the basic building block for larger, complicated, non-serializable graphs. Each of the green nodes could themselves be more intricate nodes that are constructed using the same basic building block (selected examples in Figure 6.11). It is possible to calculate the minimum number of threads required for the application from the reduced graph using the following equation:

$$N_t = N_g - N_b \tag{6.1}$$

where N_t is the minimum number of threads, N_g is the number of green nodes and N_b is the number of blue edges in the graph. The reasoning for this equation is simple. Each green node

indicates a separate point of execution and possibly a separate thread. Each blue arrow ties one green node to another, thus indicating that both must execute in the same thread. Hence, each blue edge removes one green node from the contention for a separate thread. Thus, the remaining green nodes represent the minimum concurrency requirements of the application. Once the effects of the blue edges have been thus accounted for, only interactions between threads (red arrows) remain, and since all possible reductions on the graph have been carried out, the existence of a red arrow indicates interactions across threads.

The simple example shown in Figure 6.10(a) has three green nodes and one blue edge. Hence, it requires two threads to execute. Similarly, it is possible to calculate the minimum number of threads for larger, more complex graphs, such as the ones shown in Figure 6.11.

6.7.1 Futures and Program Modifications

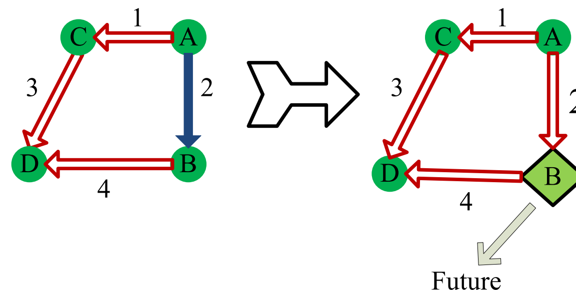

Figure 6.12: Converting Blue edges to Red – creating futures

The final graph obtained after performing all reductions can be further reduced by simplifying the actual program using one of the following two methods:

1. Remove all red edges (*i.e.*, the interactions among threads). This is difficult to do because removing red edges results in modifying the inherent, expected behavior of the program and could easily make it incorrect. However, reducing red edges, when done with care, may make the program *more* parallelizable.

2. Convert blue edges to red edges. This is possible by using the *futures* [57] mechanism. If all the targets of blue edges (green nodes) are converted into futures, then consequently blue edges turn into red edges, and since futures are expected to execute at some point after they are invoked, the correctness of the program is maintained. Figure 6.12 shows that when edge "2" is changed from blue to red, node "B" is converted into a future.

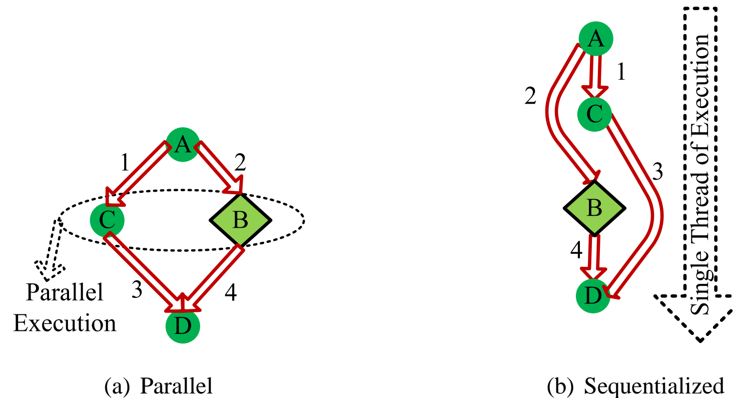

(a) Parallel

(b) Sequentialized

Figure 6.13: Options for the Future

Turning nodes into futures *increases* the expressed concurrency of the program. If multiple processors are available then the futures can often execute in *parallel* (Figure 6.13(a)) to the extent allowed by the dependency graph (which would be expressed as a *partiture*). It also increases the flexibility available to the scheduler in deciding when to execute the code in the future. Another important result is that because these nodes are now futures, they can execute independently of each other and only a loose order has to be maintained. Hence, they can even be executed *sequentially* on a single processor as long as the callees execute at some time in the future *after* the callers. One such sequentialization is seen in Figure 6.13(b). The order of nodes "B" and "C" can be switched around to form another sequential schedule.

This shows an interesting and surprising result: *increasing the concurrency of the program, also increases its serializability*! This result may seem counter-intuitive, but has great potential. It shows that by using the graph transformations outlined in this chapter followed by the "futurization" of some nodes, the scheduler is given the flexibility to either parallelize the program for larger systems or sequentialize it for execution on small, constrained, embedded systems. The choice of which nodes must be "futurized" can either be done automatically (where all targets of blue edges transformed into red edges are converted into futures), or is left up to the designer/programmer where only selected nodes need be converted. The latter method can help fine-tune an application based on the exact requirements for the particular hardware system and application domain.

6.7.2 False Parallelism and Hot Spots

One of the goals of this work is to provide a "visualization" of the reduced graph for the programmers to analyze, which could be achieved by feeding the graph structure from the "tem-

poral timing analyzer" into the GLEE visualization tool [95]. This will help the programmer in weeding out *false parallelism* and problem spots in the program (*hot spots*). Hot spots are parts of the program where a large number of interactions could be concentrated (thus degrading the overall program performance). Hot spots are identified by finding nodes that have an unusually large number of interactions centered around it (either incoming condition waits or outgoing condition signals, or perhaps both). The quantification of an "unusually large number" is decided by designers of the systems based on the demands of the target application. Sometimes two could be large, and sometimes nodes can handle 20 interactions. While both of these problems are identified by visual inspection of the graph structure, it is not particularly difficult to automate the process.

Each of the basic producer-consumer blocks (Figure 6.10) is an indicator of *false parallelism* in the program. While it requires multiple threads (at least two) for forward progress, the execution actually happens in sequential order – *i.e.*, B $\rightarrow$ A $\rightarrow$ C. No other order will work, and none of these nodes can execute in parallel with one another without intervention by the system designer. *Note*: Futures can *still* express concurrency without breaking existing relationships. Futures do not obliterate concurrency. In fact, they make the relationships explicit while moving the control logic out (into partitures).

6.8 Experimental Framework

The simulation environment used for the experiments and analysis is the Giano [38] simulator configured for the eMips CPU model running the lightweight MMLite [56] operating system. Apart from the synthetic benchmark presented in Figure 6.4, the main benchmark used for analysis was the *network stack* from the MMLite operating system. The network stack was compiled down to a single loadable module. The original MMLite network stack was an extension of the BSD implementation of the networking protocol. A unique tool, named "*temporal timing analyzer*" (TTA), was created. It aids in the creation of timing graphs. Other tools used in the information gathering process are the MIPS compiler for Giano and the nm command line tool. The various steps used in the creation of the graph are as follows:

1. A disassembly of the object code of the network stack is obtained using the MIPS compiler.

2. The list of functions in the network module is obtained using the nm tool.

3. Both of the above are provided as inputs to TTA, which, at first, creates a static control-flow graph of the entire program. It is able to express information at the basic block level or even

at a higher function level. The TTA is also able to determine the static dependencies among the various basic blocks/functions in the program, *i.e.*, it generates the green nodes and some of the blue nodes of the timing graph. It is also able to provide an estimate of the yellow and black edges in the graph.

4. A dynamic trace of the network stack running on Giano is obtained. The inputs are various web service calls that trigger different functionality in the network. While this does not guarantee complete dynamic coverage of the network stack, it is able to obtain a number of dynamic dependencies (function pointers) and is also able to match many condition variables to their wait/signal sites. These traces and the information gleaned from them are fed into the TTA, which is able to form a more complete picture of the timing graph. From the dynamic traces it is possible to restrict some yellow edges to blue edges while completely removing some other yellow edges (as explained in Section 6.5). From information on the wait/signals on condition variables, the TTA is also able to change some of the red edges to black edges and eliminate other impossible black edges. In fact, if it is possible to determine the entire range of possible inputs for a function/application, then tracing will be able to provide a complete picture of the dynamic behavior of the application.

5. Type analysis is performed and the information is then fed into TTA. This adds more information to the timing graph.

6. Information from other sources, such as domain knowledge, abstract execution *etc.* (Section 6.5) can also be plugged in to obtain a more comprehensive graph.

Any static timing analysis framework [86, 136] can be plugged in to the TTA to obtain the WCETs for the green nodes after step *(b)*. Step (e) was performed by hand and did not implement (f). The purpose of the experimental framework is to show that creation of the timing graph using information collected from various sources is entirely feasible, which it did, as indicated in the results section (Section 6.9). In fact, the design of TTA is such that it can be provided with information about the graph from any of the above mentioned (or even other sources), which will then be plugged into the graph to obtain a better understanding of the timing and runtime behavior of the application. The most interesting part about the analysis (graph reductions and subsequent observations) is that it can be performed on an incomplete graph as well as a graph which has all of its characteristics mapped. While the former will yield approximate results, the latter can yield precise results. These insights (on the state of the concurrency, sequentialization and resource constraints

of the application) can greatly assist programmers and system designers.

6.9 Results

Section 6.9.1 enumerates the results obtained by performing the transformations and analyses on the timing graph. Section 6.9.2 lists results obtained from the temporal timing analyzer showing that the process of creating the timing graph is a feasible one.

6.9.1 Graph Results

The following insights were obtained by performing the various analyses and transformations on the timing graph:

- The most important and perhaps most surprising result is that *increasing the concurrency* of the timing graph, using certain program modifications, resulted in *increased serializability*. This provides the scheduler with a lot of flexibility in creating the final schedule and tailoring it to the particular hardware system in use.
- Various graph transformations finally lead to three types of graphs – those that can be completely serialized, those that resulted in deadlocks and those that are constructed of basic producer-consumer relationships. The last result shows that it is possible to calculate the minimum resource requirements (threads and corresponding execution stacks) for correct forward progress in the program. This results in memory usage reduction in embedded systems.
- The analysis is able to direct the programmer's attention towards false parallelism and hot spots in the program.
- The final graph is the worst-case schedule possible for the program.
- The graph reduction shows that it is possible to minimize the number of context switches in the application.
- Inter-thread communication/dependencies are reduced.
- The transformations result in the smallest partiture.
- The graph helps programmers visualize and understand the application. This will tell them if their original design was correctly translated into code and perhaps even show them if there were any deficiencies in the original design.

6.9.2 Temporal Timing Analyzer Results

Results from the temporal timing analyzer are tabulated in Table 6.1. **Note**: These results are not intended to show the runtime performance of the analysis tool but rather the benefits of applying the combination of analysis techniques on the timing graph.

Table 6.1: Graph edges based on static/dynamic information

Call Type	Possible	Actual	Call Sites	Remaining
Toy (S)	5*5 = 25	1	1	0
Toy (D)	25	1	1	2
Network (S)	169,744	2386	412	0
Network (D)	169,744	76	76	31,312

The first column represents the type of information being analyzed, where “S” represents the static call information and “D” represents the dynamic call information. The second column lists the number of possible (yellow) edges. The third column represents the actual calls that were made (blue edges), while the fourth column lists the number of call sites for each type of call (static or dynamic). The last column lists the remaining yellow edges after each type of analysis.

Experiments were first conducted on the synthetic benchmark (Figure 6.4) to show that the ideas are feasible. This simple example shows that static analysis alone will not be able to capture the true nature of the program as it will not be able to deal with calls through function pointers (func2). The benchmark has 5 functions and at the outset, it is possible that any function could call any other function (including itself) leading to $5 * 5 = 25$ edges. Once static analysis has been used, information that func1 is called is captured, which leads to the creation of a blue edge. Dynamic analysis results provide the information that another call (func2) was made. This adds a second blue edge, but there is a possibility that this dynamic call site could be used to call any other function as well. Type information informs that only func3 has the same signature as func2 and has the *potential* to be called while func4 has an entirely different type signature and will never be called. Assuming that none of the other functions made any calls, the number of edges was reduced from a possible 25 to 3 actual edges.

The next benchmark to be analyzed was the network stack for MMLite (lower half of table 6.1). This module contains 412 functions which are broken down into a total of $4,886$ basic blocks. With such a large number of functions, the number of yellow edges considering only static calls for all of these functions is $412^2 = 169,744$ as every function can potentially call every other function. Static analysis of the interactions among the functions is able to gauge that only $2,386$

functions were called statically by all 412 functions. This converts $2,386$ of the yellow edges to blue edges and also eliminates all of the remaining $169,744 - 2,386 = 167,358$ ones.

Similar results are presented for dynamic calls. The remaining yellow edges were calculated as follows: Each one of the 76 call sites can potentially call any one of the 412 functions leading to $76 * 412 = 31,312$ possible yellow edges. Type analysis now calculates that only functions that match the signature of these 76 callees can ever be called from these dynamic call sites, which leads to a further reduction in the number of possible edges. Domain knowledge can further reduce this number as some of these "potential" callees (with function signature matches) cannot be called during the same execution instance. Hence, the number of edges drop further.

Hence, the initial estimates of $339,488$ potential edges (static + dynamic) have been reduced to a more manageable one that is in the tens of thousands, if not less – an order of a magnitude (or more) difference. Hence, analysis of complex programs using the TTA framework and graph transformation techniques is feasible. It is able to handle large programs, which, to date, have been excluded from such analyses due to their inherent complexity. *Note*: These are not claims of reducing the *time complexity* of these programs. Such programs were considered to be inherently un-analyzable due to the programmatic constructs they contain (*e.g.*, function pointers). In the past, analysis of such programs would not have been possible by any one of static analysis, dynamic analysis, type information, domain knowledge alone. In this work, it was achieved as a result of combining all these methods.

6.10 Conclusion

This chapter presented a combination of analysis tools and methods to glean information from programs and then combined them into a graph. The graph represents a model of the temporal behavior of a program. This chapter defines the graph coloring, invariants, and a set of valid transformations that are used to extract information out of the graph. One insight gained was that increasing the concurrency of the application can lead to increased serializability. The graph could be output as a partiture that is usable as a manifesto of the program behavior as well as in scalable and distributed scheduling. This chapter also extended the reach of static timing analysis to applications that were, due to their complexity, not previously analyzable for determination of worst-case behavior. This was done by combining static analysis with dynamic analysis based on traces and with other techniques, such as type inference. The practicality of the graph generation and analysis methods were demonstrated with an implementation that was used to create a graph of

an entire TCP/IP stack. The topological properties that the graph transformations reveal are useful in understanding and optimizing an application for variable levels of parallelism. The methodology presented here forms a solid base for further work in schedulability analysis.

Chapter 7

Related Work

This dissertation aims to present analysis techniques for modern embedded systems along three broad areas as presented in Chapters 2 – 6. This chapter on related work is also split along these lines but first, Sections 7.1 – 7.4 present an overview of the field of timing analysis.

Section 7.5 presents research related to the CheckerMode concept that deals with attempts to analyze contemporary architectures. Section 7.6 presents literature that deals with reducing constraints on the development of embedded software and the use of such techniques in reducing power consumption. Section 7.7 presents other attempts to analyze distributed embedded and real-time systems.

7.1 WCET Requirements

Knowledge of worst-case execution times (WCETs) is necessary for most hard real-time systems. The WCET must be known or safely bound *a priori* so that the feasibility of scheduling task sets in the system may be determined based on a scheduling policy (*e.g.*, rate-monotone or earliest-deadline-first scheduling [76]). The WCET values obtained by the process of *timing analysis* are required to be

1. **Safe**: They should *never* underestimate the actual WCET of the task. Failure to do so could result in catastrophic failures to the system putting human beings, their environment, or both in danger.

2. **Tight**: The overestimations in the WCET calculation should be minimized as much as possible. This is aimed at reducing a wastage of resources because the scheduling policy, in

general, must account for the worst-case execution time for *every* task in the system, potentially resulting in infeasible task sets whose deadlines cannot be guaranteed (even though those task sets never exceed their deadlines in practice).

Methods to obtain upper bounds on execution time range from *static* analysis (safe but not always tight) to *dynamic* (but unsafe [126]) observations. Recently, *hybrid* methods have been proposed as a way to obtain accurate WCETs for complex architectures.

7.2 Static Timing Analysis

The process of static timing analysis can be broadly described as containing the following steps or phases:

1. **Program analysis**: This phase break down the program into its constituent parts. These parts, depending on the analysis, could be basic blocks, paths, functions, *etc.* The information could be represented in a variety of ways, for *e.g.*, control flow graphs (CFG), tables, mathematical expressions, *etc.*

2. **Low-level/architectural analysis**: In this step, the timing for some or all of the above "parts" is obtained on an architectural (pipeline/processor) model(s).

3. **Calculation/combination**: This final phase combines the low-level results in an orderly fashion to obtain the WCET for larger constructs – functions, libraries, tasks, *etc.* This can be done explicitly by matching execution times to actual paths and then propagating the results to calculate WCETs for the larger constructs. A timing tree is constructed such that each loop (or function) corresponds to a node in the tree. The tree is processed in a bottom-up manner (the WCET for an inner loop is calculated before that of an outer loop nest). The root of the tree corresponds to the WCET for the entire task or module. This phase could also be performed in an "implicit" manner using Integer Linear Programming (ILP) techniques.

Past work mainly focuses on *static* timing analysis techniques [14, 15, 26, 27, 34, 36, 49, 52, 53, 59, 73, 74, 82, 84, 89, 94, 97, 103, 119, 126, 133]. Methods of analysis range from unoptimized programs on simple CISC processors over optimized programs on pipelined RISC processors and uncached architectures to instruction and data caches. Harmon *et al.* [49] use time consuming reverse-engineering methods that require error-prone data acquisition methods with, *e.g.* an oscilloscope, to obtain WCET values.

The static timing analysis framework that originated from Florida State University [52, 53, 70, 84, 89, 94, 132, 133] relies on accurate knowledge of: *(a)* the pipeline model/behavior; *(b)* the execution times for each individual instruction through the pipeline; and *(c) exact* static knowledge of the order of instruction scheduling within the pipeline. While (b) can be obtained by studying the processor manuals, (a) and (c) are harder to model/understand, especially in the face of processor features that introduce non-determinism, such as out-of-order processing.

Bernat and Burns proposed algebraic [14] expressions to represent the WCET of programs. Bernat *at el.* [15] used probabilistic approaches to express execution bounds down to the granularity of basic blocks that could be composed to form larger program segments. Yet, the combiner functions are not without problems, and timing of basic blocks requires architectural knowledge similar to static timing analysis tools.

Implicit path enumeration techniques (IPET) [72, 136] apply path constraints to an execution graph by expressing them as inequalities. They calculate the execution times and number of times each statement (or "part") of the program executes using CPU models and run-time information. This information is then fed into integer linear program (ILP) solvers to find the worst-case number of executions for each program part. IPET techniques allow infeasible paths to be eliminated, handling of loops (simple and complex) and recursion, but suffer from some serious drawbacks. These techniques still require some CPU models and run-time information (execution times and number of executions for most program "parts.") There is also a price to pay in time complexity because the ILP solvers used to solve these constraints, in general, are *NP-hard*.

Li *et al.* [71] present an integer linear programming (ILP) technique to handle cache misses, speculative execution and branch prediction in WCET analysis. They consider various combinations of cache hits/misses and branch predictions/mispredictions. Only one outstanding branch and one outstanding cache miss is considered at a time. This may not be an accurate representation of a modern microprocessor where more than one branch might be outstanding. The ILP formulation occurs alongside the creation of a Cache-Conflict Graph(CCG). Also, excessive time will be required to formulate and solve the ILP equations. Although this paper works toward analyzing some of the difficult-to-analyze features of modern microprocessors (*viz.* caches and speculative branches), it does not cover microprocessors with dynamic scheduling and out-of-order execution, which can actually be captured using CheckerMode.

7.3 Dynamic and Stochastic Timing Analysis

Dynamic timing analysis methods [14, 15, 19, 119, 125, 127] are based on trace-driven, experimental or stochastic methods. Also, evolutionary testing techniques [101, 125, 127, 128] are being used to automatically calculate WCETs for embedded software. They all suffer from the same drawback that they *cannot* guarantee the safety of the WCET values produced [126]. Architectural complexities, difficulties in determining worst-case input sets and the exponential complexity of performing exhaustive testing over all possible inputs are also reasons why dynamic timing analysis methods are infeasible in general. *Note*: These techniques may be used to obtain WCET values for *soft* real-time systems where missing a deadline is not necessarily a catastrophic event.

Some early work has suggested probabilistic analysis [15,33,60,122] for handling WCET variations due to software factors (such as data dependency and history dependency). However, these prior approaches for statistical WCET analysis did not model hardware execution time variations caused by process variations and cannot guarantee the safety of the WCET values obtained.

7.4 Timing Anomalies

While Graham [44] was the first to introduce the concept of *timing anomalies*, Lundqvist *et al.* [80, 81] presented their significance in WCET estimation:

> "Consider the execution of a sequence of instructions containing two different cases where the latency of instructions is modified. In the first case, the latency is increased by *i* clock cycles. In the second case, the latency is decreased by *d* clock cycles. Let C be the future change in execution time resulting from the increase or decrease of the latency. Then, *a timing anomaly is a situation where, in the first case, $C > i$ or $C < 0$, or in the second case, $C < d$ or $C > 0$.*"

Hence, timing anomalies represent counter-intuitive effects on timing when trying to analyze instruction flow through the processor. Lundqvist *et al.* introduced the following three types of anomalies:

- Cache hits can be worse than cache misses in WCET analysis. This effect shows up in out-of-order (OOO) instruction scheduling, which executes instructions (or groups of instructions) in a greedy manner. Instructions missing (instead of hitting) in cache could force certain groups of instructions to exhibit different ordering during execution thus resulting in *reduced* execution times. A detailed example is presented by Lundqvist *et al.* ([80] Figure 2).

- Cache miss penalties can be higher than expected. Static WCET analysis usually looks for the longest sequence of execution through a program. This may not always be true as cache misses on supposedly shorter paths could result in them being longer during execution, thus invalidating the timing for the "longest" path ([80] Figure 3).

- Unbounded effects on the WCET may exist. Usually, changes in the execution times of paths can be bounded statically while computing WCETs for them. Lundqvist *et al.* showed that *domino* effects could cause the effects to the WCET to be unbounded (*e.g.*the delay in WCET is proportional to the number of iterations), thus making it difficult to estimate the correct WCET without danger of underestimation ([80] Figure 4).

The concept of timing anomalies was extended and generalized by others [13, 34, 106, 109, 118, 130]. It was shown that timing anomalies are not necessarily restricted to OOO processors, cache replacement policies can affect the existence or effects of timing anomalies, unequal overlapping resources can lead to timing anomalies, *etc.* The concept of timing anomalies was also formalized and classified to fit into one of the following three types [106]:

- **Scheduling Anomalies**. Most timing anomalies fall into this category and often occur due to the *greedy* nature of schedulers.

- **Speculative Timing Anomalies**: These occur at a higher, task level where task sets are influenced by previous decisions of the scheduler.

- **Cache Timing Anomalies**: These are caused by unexpected cache behavior, such as the non-local worst-case cache hit results in a different future cache state than the local worst-case cache miss.

All of these effects make the process of timing analysis difficult. Any analysis technique must be able to correctly handle timing anomalies that could potentially occur in the processor. There are two broad methods to deal with timing anomalies while performing worst-case analysis:

1. **Identify** timing anomalies and points where they may occur. The effects of the anomalies can then be accounted for in the worst-case schedule of instructions. This is extremely hard to do because it would involve an *exhaustive* search of *all potential effects* of scheduling each permutation of instructions. As the relevant literature shows, the effects of the anomaly could occur at locations quite distant from the source of the anomaly, further complicating the analysis.

2. **Preserve** the effect of the anomaly in the analysis. Ensure that the effects of the anomalies, if any, are propagated through the analysis so they do not "disappear" when performing the WCET estimation. This avoids the laborious process of trying to detect the anomalies and their effects while ensuring that the WCETs obtained are safe and tight.

CheckerMode utilizes the latter method to correctly deal with timing anomalies. This is illustrated in Chapter 3.

7.5 CheckerMode Related Work (Hybrid Techniques)

Recently, hybrid timing analysis methods [15, 48, 134] as well as hardware-related methods [8, 81] have been proposed. Yet, none of these approaches capture advanced hardware features transparently while providing tight bounds. While static timing analysis methods or abstract interpretation methods [117, 119] can provide reasonably tight bounds for branches that can be statically analyzed, they are not able to provide tight bounds for execution along speculatively predicted branch directions at runtime or out-of-order instruction-issue pipelines. The complexity and overhead of modeling the behavior of even moderately complex pipelines [54] and interactions of instructions within them is high for any of these methods. Whitham [134] presents a combination of hardware and software techniques to capture WCETs accurately for complex processors that avoids problems with timing anomalies. Instruction scheduling is carried out by the compiler and relies on custom microcode executing in the processor. It might be difficult to convince processor vendors to undergo such radical changes in their design because it leads to an expensive verification process. They may also be unwilling to provide such internal details due to intellectual property considerations. Also, as detailed in the introduction, each new processor design requires that the model be manually adapted and cannot reflect fabrication-level timing variability within a processor batch. CheckerMode, in contrast, automatically adapts with changing processor details, including timing variations due to fabrication. CheckerMode fills this gap and contributes to high confidence in embedded systems design for time-critical missions.

CheckerMode is closely related to two prior approaches. First, Bernat *et al.* [15] used probabilistic approaches to express execution bounds down to the granularity of basic blocks, which could then be composed to form larger program segments. Second, the VISA framework [8] suggested architectural enhancements to gauge the progress of execution by sub-task partitioning and exploiting intra-task slack with DVS techniques. CheckerMode combines the benefits of these two

prior approaches without their shortcomings. While performing analysis on paths, cycles are measured in a special execution mode of the processor that supports checkpoint/restart and unknown value execution semantics to reflect proper architectural state and path coverage. While Bernat struggled with considerable timing perturbation from instrumentation, CheckerMode is much less intrusive. Instead of a VISA-like *virtual processor* around a complex core, CheckerMode is promoted as a realistic feature building on existing internal processor buffers widely used for speculation / precise event handling. Hence, this method is able to provide more precise results compared to Bernat's work. In contrast to VISA, CheckerMode is able to support hybrid timing analysis on the actual processor core.

Lundqvist et al. [81] use symbolic execution with a tight integration of path analysis and timing analysis to obtain accurate WCET estimates. They use the concept of an *"unknown"* value to account for register values and addresses that cannot be statically determined, just as CheckerMode does. However, their work did not utilize a fixed point approach but rather required each iteration of a loop to be symbolically executed. Furthermore, they did not propose any architectural modifications and focused on static timing analysis over the entire program within an architectural simulator using in-order execution without dynamic branch prediction etc. The term "timing anomaly", *i.e.*, an anomaly in the execution of code in dynamically scheduled processors, stems from their work (see discussion in Section 7.4).

CheckerMode contends that the instruction window may be large enough that even if instructions get blocked due to anomalies, other instructions, that are ready may execute, thus reducing the overall execution time of the program. Thus, by taking a larger context (path) into account, one can provably compensate for localized anomalies at a larger scale within CheckerMode.

Petters [99] measures the execution times of parts of the program on actual microprocessors to obtain an accurate WCET estimate. He uses measurement techniques using hardware/software probes and interrupts to obtain the execution times. Software instrumentation and debug routines are also employed for this purpose. The main drawback of these techniques is that they change either the behavior or the timing of the programs being analyzed. *E.g.*, instrumentation changes the software behavior of the program and may require manual intervention, interrupts modify the timing characteristics of the program, while hardware probes may not obtain accurate timing results. The CheckerMode approach does not suffer from any of these drawbacks and will produce tight WCET results.

Schneider [109] illustrates the combination of WCET analysis and schedulability (response-time) analysis for applications and real-time operating systems. He also performs WCET analysis

for superscalar, out-of-order processors while mentioning *"late-order"* effects for pipelines. These are basically the "timing anomalies" discussed earlier, yet he considers handling multiple tasks in the system. The work being presented here does not consider multiple tasks in the system and concentrates on obtaining the WCETs for the complete execution of a single task. This WCET value can be used to perform multiple-task scheduling as well. The CheckerMode system can be extended to include the capability to obtain WCETs for a multiple-task real-time system.

The CheckerMode approach combines the best features of static and dynamic analysis required for obtaining WCET bounds for modern processors. Chapter 2 introduced the *hybrid* timing analysis technique that obtains actual execution times for short paths on the actual hardware and then combines these intermediate worst-case bounds, offline, using a static tool.

7.6 ParaScale Related Work

This section is focused on timing analysis work related to parametric timing analysis and dynamic voltage scaling (DVS).

Chapman *et al.* [26] used path expressions to combine a source-oriented parametric approach of WCET analysis with timing annotations, verifying the latter with the former. Bernat and Burns proposed algebraic expressions to represent the WCET of programs [14]. Bernat *at el.* used probabilistic approaches to express execution bounds down to the granularity of basic blocks that could be composed to form larger program segments [15]. Yet, the combiner functions are not without problems, and timing of basic blocks requires architectural knowledge similar to static timing analysis tools.

Parametric timing analysis by Vivancos *et al.* [124] first introduced techniques to handle variable loop bounds as an extension to static timing analysis. That work focuses on the use of static analysis methods to derive parametric formulae to bound variable-length loops. The ParaScale work presented here, in contrast, assesses the benefits of this work, particularly in the realm of power-awareness.

The effects of DVS on WCET have been studied in the FAST framework [110] where, parametrization was used to model the effect of memory latencies on pipeline stalls as processor frequency is varied. Due to DVS and constant memory access times, a lower processor frequency results in fewer cycles to access memory, which is reflected in WCET bounds in their FAST framework. This work is orthogonal to the method of PTA. In the timing analyzer presented in Chapter 5, these effects are not currently modeled. This does not affect the correctness of the approach since

WCET bounds are safe without such modeling, but they may not be tight, as shown in the FAST framework. Hence, the benefits of parametric DVS may even be better than what is reported here.

The VISA framework suggested architectural enhancements to gauge progress of execution by sub-task partitioning and exploits intra-task slack with DVS techniques [7, 8]. Their technique did not exploit parametric loops. ParaScale, in contrast, takes advantage of dynamically discovered loop bounds and does not require any modifications at the micro-architecture level.

Lisper [75] used polyhedral flow analysis to specify the iteration space of loop nests and express them as parametric integer programming problems to subsequently derive a parametric WCET formula suitable for timing analysis using IPET (Implicit Path Enumeration Technique). Recent work by Byhlin *et al.* [24] underlines the importance of using parametric expressions to support WCET analysis in the presence of different modes of execution. They parametrize their WCET predictions for automotive software based on certain parameters, such as frame size. Their work focuses on studying the relationship between parameters unique to modes of execution and their effect on the WCET. Other work by Gheorghita *et al.* [41] also promotes a parametric approach but at the level of basic blocks to distinguish different worst-case paths. The ideas, in this chapter, of using parametric expressions, predating any of this work, accurately bound the WCET values for *loops*. This extends the applicability of static analysis to a new class of programs. These accurate predictions at run-time are utilized for benefits such as power savings and admission of additional tasks.

The most closely related work in terms of intra-task DVS is the idea of power management points (PMPs) [1–3] where, path-dependent power management hints (PMHs) were used to aggregate knowledge about “saved” execution time compared to the worst-case execution that would have been imposed along different paths. This work differs in that it exploits knowledge about *past* execution while ParaScale discovers loop bounds that then provides tighter bounds on past and *future* execution within the same task. Their work is also evaluated with SimpleScalar, albeit with a more simplistic power model ($E = CV^2$) while ParaScale assess power at the micro-architecture level using enhancements of Wattch [20] as well as a more accurate leakage model [64]. Again, ParaScale results could potentially be improved by benefiting from knowledge about past execution, which may lead to additional power savings. This is subject to future work.

An intra-tasks DVS algorithm that “discovers” the amount of execution left in the system and appropriately modifies the frequency and voltage of the system is presented in [111]. Their work depends on inserting various instrumentation points at compile time into various paths in the code. Evaluation of these instrumentation points at runtime provides information about the paths taken

during execution and the *possible* amount of execution time left along that path similar to PMPs. They insert instrumentation points in *every basic block* to determine the exact execution path, which would incur a significant overhead during runtime. This may also affect the caching and, hence, timing behavior of the task code. ParaScale differs significantly in that it only assess the amount of execution time remaining *once* (prior to entry into a parametric loop), thus incurring an overhead only once. Hence, it is able to accurately gauge the *amount of execution remaining with a single overhead per loop and per task instance*. It also estimates the new caching and timing behavior of the code after the call to the intra-task scheduler by invoking the timing analysis framework on the modified code until the parametric WCET formulae stabilize. Another technique presented in their paper is that of ”L-type voltage scaling edges”. They utilize the idea that loops are often executed for a smaller number of iterations than the worst-case scenario. During run-time, they discover the actual number of loop iterations at loop exit and then gauge the number of cycles saved. In contrast, parametric timing analysis determines loop savings *prior* to loop entry and exploits savings early, *e.g.*, using DVS, such as in ParaScale. This difference is a significant advantage for the parametric approach, particularly for tasks where a single loop nest accounts for most of the execution time.

7.7 Temporal Timing Analysis Related Work

The work presented in chapter 6 is unique in that it is able to transform large applications into a graph representation on which transformations are applied to gather the “meaning” of the program with the aim of making distributed embedded systems more scalable, primarily by creating models of the program based on the ideas of *partitures* and *futures*.

Helander *et al.* [57] introduced the concepts of partitures and futures as building blocks for model-based design of distributed embedded systems. While they focus on techniques to build applications, using these techniques, from the ground up, the work in Chapter 6 aims to understand and possibly transform *existing* multi-threaded embedded systems with temporal constraints into that model. Along the way, it aims at providing useful information and hints to designers of such systems to improve the quality and scalability of the application.

Andersson [9] studied the temporal behavior of embedded programs and also used dynamic traces to add more information to his analysis. This work differs from that presented in Chapter 6 in that he creates a model of the application and uses model checking and regression analysis coupled with dynamic traces to reason about the temporal characteristics of the program. It stops with analyzing the impact of the behavior of the temporal characteristics of the program

and does not provide any further insights (like Section 6.7). The work in Chapter 6 also deals with concurrent programs as part of the analysis.

The level of parallelism required by an application has been explored by Motus *et al.* [91, 92]. They focus on model-driven development where an engineer writes a timing model (Q model) including educated guesses for minimum and maximum times of processes in periodic applications such as those found in telephone switches. The model is based on processes and channels. While the work in the previous chapter facilitates writing the model by hand, it may also be used to analyze existing programs and does not require the processes to be periodic.

Henzinger *et al.* [58] introduced the idea of compiler-driven feasibility checking of scheduling code. In their approach, the compiler creates an executable that represents the schedule, which is then attached to the end of the task. This schedule is executed and validated each time the task is invoked on specialized embedded hardware. The work from Chapter 6 creates partitures and futures based on the analysis of timing graphs. Also, compared to them, this work is able to determine the levels of parallelism and potential problem spots in the application, which could prove beneficial to a large range of systems.

Previous work in timing analysis deals with either static or dynamic analysis. The CheckerMode concept presented in Chapters 2 – 4 [86, 87] presented a hybrid approach to performing timing analysis. Chapter 6 is similar in that it is also a hybrid approach which uses information for a variety of sources. The difference is that the latter is focused on finding the properties of interactions among threads in concurrent programs (analysis of complex software) while CheckerMode is focused on obtaining worst-case execution time results for modern, out-of-order processors. In fact, the two techniques are complementary. The results from that framework (the WCETs) can be plugged in to the temporal timing analyzer to obtain more precise results for applications running on modern processors.

Chapter 8

Future Work

Since this dissertation was loosely split into three parts, ideas for future research are also presented along those lines. Section 8.1 details potential research ideas for tackling the complexities of modern architectures. Sections 8.2 and 8.3 explain ideas for improved analysis techniques to handle complexities in embedded software. Section 8.4 discusses some interesting ideas that utilize combinations of all the analyses presented here.

8.1 CheckerMode Future Work

Chapters 2 – 4 presented techniques to analyze and bound the worst-case behavior of modern architectural features with a focus on *out-of-order (OOO) pipelines*. While the material presented here tackled most major issues dealing with OOO pipelines, further analysis could help reduce the pessimism and overheads of the analysis. Currently, snapshots are captured at *every* branch instruction as well as before *every* join point in the control flow graph (CFG). This greatly increases the analysis complexity, especially if many branches occur very close to each other, or in case of a large nesting depth for branches. A static analysis of the CFG could help in capturing snapshots at a *coarser* granularity by skipping some intermediate branches. The paths that then fall between the snapshots must be examined along all alternating combinations of branches/joins. Perhaps some annotations from the programmer could help guide the analysis towards certain branches while avoiding others.

A simplifying assumption was made that all *other* processor features are absent and that the pipeline could be analyzed in isolation. The increased performance of OOO processors is due to other processor features as much as it is due to the pipeline. Processor features, such as *dynamic*

branch prediction, instruction and data caches, prefetching, etc., go a long way in increasing the performance of these processors. While the current analysis precludes these features, including them in a future version will definitely help in making modern processors more acceptable for use in embedded and real-time systems.

The *branch predictor* is definitely a feature that is worth examining. Unlike the pipeline, though, the branch predictor is *not stateless*. Every branch instruction that is encountered influences and is influenced by the predictor. Hence, any attempt at capturing snapshots for a dynamic branch predictor like "G-share" [83] involves the daunting task of capturing and managing a large amount of state. This is especially problematic if snapshots occur close to each other. Another issue while dealing with branch predictors is related to "merging" snapshots. Since branch predictors are typically bit patterns and/or counters, a strategy for merge cannot be as simplistic as the a *max* function of two snapshots, which was what was used while dealing with pipelines. Another significant research challenge has to do with the Not-A-Number (NaN) values for input-dependent branches. How must the branch predictor be updated when the branch is input-dependent?

Caches (both instruction and data) are similar to the branch predictor in that they contain a large amount of state that must be captured for a comprehensive snapshot policy. NaN values present similar challenges: How must an access to the cache with a NaN address be treated? The pessimistic approach is to assume that *all* NaN accesses *miss* in cache and are sent to memory. This could lead to serious overestimations since the number of NaN-based references will increase as the program execution proceeds resulting in huge WCET overestimations, especially for larger, more complex programs.

Perhaps both of the above (branch predictors and caches) can be analyzed by capturing *incremental state* at each successive snapshot. The state of the entire component can perhaps be captured at coarser intervals, thus speeding up the analysis significantly. But the issue of how to deal with input-dependent values is still a significant hurdle in obtaining accurate WCET estimates for processors with these features.

8.2 ParaScale Future Work

The work in Chapter 5 illustrated the use of parametric timing analysis in achieving power savings. This work can be carried further to study the benefits of ParaScale with other dynamic voltage algorithms. These techniques, along with the associated run-time information, could also be used for admitting new (sporadic [77]) tasks into the system. Parametric analysis can also be

applied to calculate bounds on recursive functions.

8.3 Future Work for Analysis of Distributed Embedded Systems

Chapter 6 presented analysis techniques to understand the behavior of complex embedded systems, *i.e.*, those that are distributed in nature. The aim was to analyze and eventually transform existing multi-threaded applications to the partiture-future model so that the application can be adapted to a given hardware configuration ranging from small microcontrollers to modern multi-core architectures. The focus in this work was to adapt applications to *smaller* systems, *i.e.*, those with limitations on physical memory. This was achieved by decreasing the amount of parallelism in the application. An interesting extension would be to do the opposite, *i.e.*, study the effects of adapting the application to *larger*, more parallel systems (in particular multicore architectures). This would require *increasing* the parallelism of the application that would demand quite different trade-offs as compared to the analysis presented here.

Two techniques aimed to improve the scalability of the application were mentioned in Section 6.7.1, *viz.* to transform the application to get rid of interactions between threads or to change all sequential dependencies to be concurrent dependencies using the *future* construct. An interesting research challenge is to *automatically* determine which parts of the applications are targets for these transformations, if any, and then to actually carry out the transformations. The latter will aid in the process of automatically *adapting* the application to varying levels of hardware resources, such as parallelism, memory, *etc.*

8.4 Combination of Hardware and Software Analysis Techniques

The various techniques presented in this dissertation can actually be combined to provide for better analysis of modern embedded, real-time and cyber-physical systems. CheckerMode and ParaScale could be utilized in the analysis for distributed embedded systems to obtain accurate WCETs for code within single threads. Parametric analysis techniques could be used to calculate the effects of function pointers and synchronization constructs, *i.e.*, to provide formulae to describe the bounds on the number of *potential callees.* ParaScale techniques could also be used to estimate the power consumption for the target platforms. It could be used in combination with dynamic voltage scaling (DVS) techniques for smaller distributed embedded systems. For more complex and more powerful systems, ParaScale could be used with more comprehensive DVS schemes, such as

Lookahead [100], Greedy DVS [88], *etc.*

CheckerMode techniques could be enhanced to analyze multi-core architectures so that correct WCET information is available when trying to adapt the application to the high-end domain. Hence, a large amount of potential exists when trying to combine the analysis techniques presented in this dissertation.

Chapter 9

Conclusion

The original aim of this dissertation (Section 1.8) was to show that while modern embedded systems prove to be too complex for any single analysis technique, they can be dissected, and their worst-case behavior can be captured using a combination of the very same techniques. The work presented in Chapters 2 – 6, has shown this hypothesis to be true, both on the hardware as well as the software fronts. The following sections discuss this in more detail before delving into the correctness of the dissertation hypothesis in Section 9.4.

9.1 Analysis Techniques for Modern Processors

The *CheckerMode* infrastructure presented in Chapters 2 – 4 was developed to analyze contemporary processors with the aim of calculating worst-case execution times (WCETs) for code executing on them. It provides the foundation to make contemporary processors predictable and analyzable so that they may be safely used in embedded and real-time systems.

Chapter 2 presents a high-level overview of, the motivation for, and the design choices behind CheckerMode. The main idea is that interactions between hardware and software (a *hybrid* timing analysis technique) can be utilized to obtain safe and tight WCET values for embedded systems with modern processors. Sequences of code are extracted on the software side and dispatched to execute on the actual processor. Minor enhancements to the microarchitecture of modern processors is suggested to aid in the process of capturing information (“state”) during the execution of the given program fragments.

Capturing and restoring state (known as “snapshots”) in CheckerMode is a non-trivial task, especially in the presence of timing anomalies. CheckerMode is able to correctly deal with

timing anomalies in that they are preserved during the analysis. This is particularly important as the task of detecting a timing anomaly is quite difficult, and completely ignoring anomalies could lead to incorrect WCET estimates, even leading to underestimations. A correct handling of structural dependencies and data dependencies is also presented with the aim of preserving the worst-case behavior of the program.

Analysis of loops, especially those with input-dependent bounds, is problematic mainly due to the halting problem, *i.e.*, how many iterations must be timed to obtained the WCET for the loop? This was solved by use of a fixed point technique that only needs to analyze the loop for a few iterations and is then able to extrapolate for the remaining iterations. This is achieved via a combination of traditional fixed point timing analysis techniques and the snapshot scheme from CheckerMode. This analysis shows that the process of trying to capture the behavior of loops through an OOO pipeline demands that a significant amount of architectural state (retire stage and the issue/execute stages) be captured. Hence, any attempt to perform such an analysis cannot be oblivious or transparent to all internal details of the processor microarchitecture. Finally, the WCET for the loop and the benchmark as a whole can be presented as a formula if the upper bounds on the number of loop iterations is unknown.

Hence, CheckerMode has the ability to provide worst-case guarantees for *out-of-order pipelines* using a combination of analysis techniques by utilizing interactions and passing of information between the hardware and software. This moves forward the state-of-the-art in the design of embedded systems as OOO processors can now be made available to designers of such applications.

9.2 Reducing Constraints on Embedded Software

The requirement that loop bounds must be statically determined is relaxed in this part of the dissertation, presented in Chapter 5. Parametric formulae are integrated into the process of timing analysis. This is carried out without sacrificing safety or tightness of WCET bounds. The parametric formulae are calculated using a fixed point approach and embedded into the task code prior to entry into the parametric loop. The formulae are *evaluated at run-time* when actual loop bounds are available. This information is then exploited to reduce the voltage and frequency of the processor with the aim of achieving *energy savings*. The process involves the use of *two* schedulers, one inter-task and one *intra-task* scheduler. The latter evaluates the parametric formulae at run-time and then invokes the dynamic voltage scaling (DVS) technique to save power. The framework is referred to as *ParaScale*. Also presented is a new DVS algorithm named “Greedy DVS”.

The benefit of ParaScale is that it is able to *reduce voltage and frequency levels as execution proceeds*. This is in sharp contrast to existing DVS techniques, which increase voltage/frequency values as deadlines approach, thus resulting in losing some of the gains achieved through DVS. Power savings as high as 66% – 80% are observed while using ParaScale in combination with Greedy DVS compared to DVS-oblivious techniques. These savings closely match those obtained by dynamic, aggressive DVS algorithms while still maintaining a low time complexity and are easy to implement (as simple extensions of static DVS algorithms). These savings are in sharp contrast to those that can be achieved via conventional timing analysis since ParaScale is able to utilize knowledge about the *future* execution of the task.

Hence, parametric timing analysis expands the class of applications that can be analyzed and, hence, used on a real-time system. Programmers are now free to create more complex applications. ParaScale utilizes run-time information coupled with static analysis formulae to better characterize the worst-case behavior of modern embedded systems. This is in keeping with the theme that such systems, which could not be analyzed before, are now amenable to analysis due to the combination of techniques, both static and dynamic.

9.3 Analysis of Distributed Embedded Systems

Some embedded systems and many cyber-physical systems are often *distributed* in nature, *i.e.*, they have multiple threads of execution with synchronization/communication constructs passing information or forcing dependencies between them. Such systems are typically out of the reach of either static or dynamic analysis techniques, but not beyond a combination of the two. Chapter 6 illustrates the use of a combination of analysis techniques (static analysis, dynamic/run-time analysis, type information, domain knowledge, *etc.*) to accurately characterize the true nature of such applications.

Information from all of these analysis techniques feed into a “timing graph” on which transformations and reductions are carried out with the aim of trying to understand the underlying behavior and suggest changes/improvements to the application. The goal was to adapt a complex, distributed embedded system to a resource-constrained platform (especially constraints on physical memory).

One significant result obtained from the analysis was that *increasing the concurrency of an application also increased its sequentiality.* This will help in tailoring the application based on the hardware demands by increasing the sequentiality for resource-constrained systems while the

concurrency is increased for more powerful systems (such as multicore architectures).

This piece of work extends the reach of traditional static timing analysis. By use of a combination of analysis techniques and sources of information. It becomes possible to study classes of application that were previously considered to be "un-analyzable", such as the network stack used for the experiments in this work.

9.4 Correctness of the Dissertation Hypothesis

The aim of this dissertation (Section 1.8) was to show that hardware and software constructs that are complex and "un-analyzable" by any single analysis technique or information source, can now be studied and understood using a combination of techniques. This dissertation has provided the means to analyze each of the constructs mentioned in the hypothesis:

1. *Out-of-order processor pipelines* have shown to be analyzable using interactions between hardware and software through the *CheckerMode* framework [86, 87]. This framework has the ability to correctly preserve timing anomalies as well as handle loops without explicitly enumerating all loop iterations. These techniques can be extended to analyze other parts of the process (branch predictor, caches, *etc.*) in the future.

2. Embedded code with *statically indeterminate loop bounds* can now be analyzed by using static parametric timing analysis techniques coupled with run-time information about the actual loop bounds through the *ParaScale* framework [88, 89]. The savings (slack) from this technique were used to obtain a reduction in the energy consumption of the embedded system.

3. *Distributed embedded systems* can be analyzed by using information from static analysis, run-time/dynamic traces, type analysis and domain knowledge through the *Temporal Timing Analyzer (TTA)* [85]. Graph-based analysis techniques can help in adapting distributed embedded systems to a variety of hardware profiles.

Hence, the claims in the dissertation hypothesis have been shown to be correct.

Bibliography

[1] N. AbouGhazaleh, B. Childers, D. Mosse, R. Melhem, and Matthew Craven. Energy management for real-time embedded applications with compiler support. In *ACM SIGPLAN Conference on Language, Compiler, and Tool Support for Embedded Systems*, June 2003.

[2] N. AbouGhazaleh, D. Mosse, B. Childers, and R. Melhem. Toward the placement of power management points in real time applications. In *Workshop on Compilers and Operating Systems for Low Power*, September 2001.

[3] N. AbouGhazaleh, D. Mosse, B. Childers, R. Melhem, and Matthew Craven. Collaborative operating system and compiler power management for real-time applications. In *IEEE Real-Time Embedded Technology and Applications Symposium*, May 2003.

[4] Gagan Agrawal, Anurag Acharya, and Joel Saltz. An interprocedural framework for placement of asynchronous I/O operations. In *Proceedings of the 10th ACM International Conference on Supercomputing*, pages 358–365, Philadelphia, PA, 1996. ACM Press.

[5] A. V. Aho, R. Sethi, and J. D. Ullman. *Compilers – Principles, Techniques, and Tools*. Addison-Wesley, 1986.

[6] N. Al-Yaqoubi. Reducing timing analysis complexity by partitioning control flow. Master's thesis, Florida State University, 1997. Master's Project.

[7] A. Anantaraman, K. Seth, K. Patil, E. Rotenberg, and F. Mueller. Virtual simple architecture (VISA): Exceeding the complexity limit in safe real-time systems. In *International Symposium on Computer Architecture*, pages 250–261, June 2003.

[8] A. Anantaraman, K. Seth, K. Patil, E. Rotenberg, and F. Mueller. Enforcing safety of real-time schedules on contemporary processors using a virtual simple architecture (visa). In *IEEE Real-Time Systems Symposium*, pages 114–125, December 2004.

[9] Johan Andersson. Modeling the temporal behavior of complex embedded systems - a reverse engineering approach. Licentiate thesis, June 2005.

[10] R. Arnold, F. Mueller, D. B. Whalley, and M. Harmon. Bounding worst-case instruction cache performance. In *IEEE Real-Time Systems Symposium*, pages 172–181, December 1994.

[11] H. Aydin, R. Melhem, D. Mosse, and P. Mejia-Alvarez. Dynamic and agressive scheduling techniques for power-aware real-time systems. In *IEEE Real-Time Systems Symposium*, December 2001.

[12] Iain Bate and Ralf Reutemann. Worst-case execution time analysis for dynamic branch predictors. In *Euromicro Conference on Real-Time Systems*, pages 215–222, 2004.

[13] Christoph Berg. Plru cache domino effects. In Frank Mueller, editor, *6th Intl. Workshop on Worst-Case Execution Time (WCET) Analysis*, number 06902 in Dagstuhl Seminar Proceedings. Internationales Begegnungs- und Forschungszentrum fuer Informatik (IBFI), Schloss Dagstuhl, Germany, 2006. <http://drops.dagstuhl.de/opus/volltexte/2006/672> [date of citation: 2006-01-01].

[14] G. Bernat and A. Burns. An approach to symbolic worst-case execution time analysis. In *25th IFAC Workshop on Real-Time Programming*, May 2000.

[15] G. Bernat, A. Colin, and S. Petters. Wcet analysis of probabilistic hard real-time systems. In *IEEE Real-Time Systems Symposium*, December 2002.

[16] S. Borkar. Designing reliable systems from unreliable components: The challenges of transistor variability and degradation. *IEEE Micro*, 25(6):10–16, Nov/Dec 2005.

[17] S. Borkar, T. Karnik, S. Narendra, J. Tschanz, A. Keshavarzi, and V. De. Parameter variations and impact on circuits and microarchitecture. In *Design Automation Conference*, pages 338–342, 2003.

[18] Shekhar Borkar, Tanay Karnik, Siva Narendra, Jim Tschanz, Ali Keshavarzi, and Vivek De. Parameter variations and impact on circuits and microarchitecture. In *Design Automation Conference*, pages 338–342, 2003.

[19] V. Braberman, M. Felder, and M. Marre. Testing timing behavior of real-time software. 1997.

[20] David Brooks, Vivek Tiwari, and Margaret Martonosi. Wattch: A framework for architectural-level power analysis and optimizations. In *Proceedings of the 27th Annual International Symposium on Computer Architecture*, pages 83–94, Vancouver, British Columbia, June 2000. IEEE Computer Society and ACM SIGARCH.

[21] D. Burger, T. Austin, and S. Bennett. Evaluating future microprocessors: The simplescalar toolset. Technical Report CS-TR-96-1308, University of Wisconsin - Madison, CS Dept., July 1996.

[22] Doug Burger, Todd M. Austin, and Steve Bennett. Evaluating future microprocessors: The simplescalar tool set. Technical Report CS-TR-1996-1308, University of Wisconsin, Madison, July 1996.

[23] Claire Burguiere and Christine Rochange. A contribution to branch prediction modeling in wcet analysis. In *Design, Automation and Test in Europe*, pages 612–617, 2005.

[24] Susana Byhlin, Andreas Ermedahl, Jan Gustafsson, and Bjrn Lis per. Applying static wcet analysis to automotive communication software. In *ECRTS (Euromicro Conference on Real-Time Systems)*, 2005.

[25] C-Lab. Wcet benchmarks. Available from http://www.c-lab.de/home/en/download.html.

[26] R. Chapman, A. Burns, and A. Wellings. Combining static worst-case timing analysis and program proof. *Real-Time Systems*, 11(2):145–171, 1996.

[27] Kaiyu Chen, Sharad Malik, and David I. August. Retargetable static timing analysis for embedded software. In *Proceedings of the International Symposium on System Synthesis (ISSS)*, October 2001.

[28] David Cormie. The ARM11 microarchitecture. 2002.

[29] A. Cristal, O. Santana, M. Valero, and J. Martinez. Toward kilo-instruction processors. *ACM Trans. Archit. Code Optim.*, 1(4):389–417, 2004.

[30] A. Cristal, M. Valero, J. Llosa, , and A. Gonzlez. Large virtual robs by processor checkpointing. Technical Report UPC-DAC-2002-39, Universitat Politcnica de Catalunya, July 2002.

[31] Gianpaolo Cugola and Carlo Ghezzi. CJava: Introducing concurrent objects in java. In *Object Oriented Information Systems*, pages 504–514, 1997.

[32] A Dunkels, O Schmidt, T Voigt, and M Ali. Protothreads: simplifying event-driven programming of memory-constrained embedded systems. In *SenSys '06: Proceedings of the 4th international conference on Embedded networked sensor systems*, pages 29–42, New York, NY, USA, 2006. ACM.

[33] S. Edgar and A. Burns. Statistical analysis of WCET for scheduling. In *22nd IEEE Real-Time Systems Symposium*, pages 215–224, 2001.

[34] J. Engblom. *Processor Pipelines and Static Worst-Case Execution Time Analysis*. PhD thesis, Dept. of Information Technology, Uppsala University, 2002.

[35] Jakob Engblom. Analysis of the execution time unpredictability caused by dynamic branch prediction. In *IEEE Real-Time Embedded Technology and Applications Symposium*, page 152, 2003.

[36] Jakob Engblom, Andreas Ermedahl, Mikael Sjdin, Jan Gustafsson, , and Hans Hansson. Execution-time analysis for embedded real-time systems. In *STTT (Software Tools for Technology Transfer) special issue on ASTEC.*, 2001.

[37] Alessandro Forin. *Futures, in Advanced Language Implementation, Peter Lee editor*. MIT Press, Cambridge MA, 1990.

[38] Alessandro Forin, Benham Neekzad, and Nathaniel L. Lynch. Giano: The two-headed system simulator. Technical report vol. msr-tr-2006-130, Microsoft Research, One Microsoft Way, Redmond, WA 98052, 2006.

[39] D.P Friedman and D.S Wise. CONS should not evaluate its parameters. In *Michaelson and Milner (editors), Automata, Languages, and Programming*, pages 257–284. Edinburgh University Press, 1976.

[40] David Gay, Philip Levis, Robert von Behren, Matt Welsh, Eric Brewer, and David Culler. The NesC language: A holistic approach to networked embedded systems. In Jr. James B. Fenwick and Cindy Norris, editors, *Proceedings of the ACM SIGPLAN 2003 Conference on Programming Language Design and Implementation (PLDI-03)*, volume 38, 5 of *ACM SIGPLAN Notices*, pages 1–11, New York, June 9–11 2003. ACM Press.

[41] Valentin S. Gheorghita, Sander Stuijk, Twan Basten, and Henk Corporaal. Automatic scenario detection for improved wcet estimation. In *Design Automation Conference*, June 2005.

[42] John B. Goodenough and Lui Sha. The priority ceiling protocol: A method for minimizing the blocking of high priority Ada tasks. In *Proceedings of the 2nd International Workshop on Real-Time Ada Issues*, May 1988.

[43] K. Govil, E. Chan, and H. Wasserman. Comparing algorithms for dynamic speed-setting of a low-power cpu. In *1st Int'l Conference on Mobile Computing and Networking*, Nov 1995.

[44] Ronald L. Graham. Bounds on multiprocessing timing anomalies. In *IAM Journal of Applied Mathematics*, 1969.

[45] F. Gruian. Hard real-time scheduling for low energy using stochastic data and dvs processors. In *Proceedings of the International Symposium on Low-Power Electronics and Design ISLPED'01*, Aug 2001.

[46] D. Grunwald, P. Levis, C. Morrey III, M. Neufeld, and K. Farkas. Policies for dynamic clock scheduling. In *Symp. on Operating Systems Design and Implementation*, Oct 2000.

[47] Robert Halstead. MULTILISP: a language for concurrent symbolic computation. *ACM Trans. Program. Lang. Syst.*, 7(4):501–538, 1985.

[48] A. Hamann, M. Jersak, K. Richter, and R. Ernst. Design space exploration and system optimization with symta/s - symbolic timing analysis for systems. In *IEEE Real-Time Systems Symposium*, pages 469–478, December 2004.

[49] M. Harmon, T. P. Baker, and D. B. Whalley. A retargetable technique for predicting execution time. In *IEEE Real-Time Systems Symposium*, pages 68–77, December 1992.

[50] C. Healy, M. Sjodin, V. Rustagi, D. Whalley, and R. van Engelen. Supporting timing analysis by automatic bounding of loop iterations. *Real-Time Systems*, 18(2/3):121–148, May 2000.

[51] C. A. Healy, R. D. Arnold, F. Mueller, D. Whalley, and M. G. Harmon. Bounding pipeline and instruction cache performance. *IEEE Transactions on Computers*, 48(1):53–70, January 1999.

[52] C. A. Healy, M . Sjödin, and D. B. Whalley. Bounding loop iterations for timing analysis. In *IEEE Real-Time Embedded Technology and Applications Symposium*, pages 12–21, June 1998.

[53] C. A. Healy, D. B. Whalley, and M. G. Harmon. Integrating the timing analysis of pipelining and instruction caching. In *IEEE Real-Time Systems Symposium*, pages 288–297, December 1995.

[54] Reinhold Heckmann, Marc Langenback, Stephan Thesing, and Reinhard Wilhelm. The influence of processor architecture on the design and the results of WCET tools. *Proceedings of the IEEE*, pages 1038–1054, July 2003.

[55] Johannes Helander. Deeply embedded XML communication: Towards an interoperable and seamless world. In *5th ACM Conference on Embedded Software*‘, September 2005.

[56] Johannes Helander and Alessandro Forin. MMLite: A highly componentized system architecture. In *Proceedings of the ACM SIGOPS European Workshop on Support for Composing Distributed Applications*, 1998.

[57] Johannes Helander, Risto Serg, Margus Veanes, and Pritam Roy. Adapting futures: Scalability for real-world computing. In *Real-Time Systems Symposium*, December 2007.

[58] Tom Henzinger, Christoph Kirsch, and Slobodan Matic. Schedule carrying code. In *Third International Conference on Embedded Software (EMSOFT)*, January 2003.

[59] André Hergenhan and Wolfgang Rosenstiel. Static timing analysis of embedded software on advanced processor architectures. In *DATE*, pages 552–559, 2000.

[60] X. S. Hu, Z. Tao, and E. H. M. Sha. Estimating probabilistic timing performance for real-time embedded systems. *Very Large Scale Integration (VLSI) Systems, IEEE Transactions on*, 9(6):833–844, 2001. 1063-8210.

[61] P. Hurat, Y.-T. Wang, and N.K. Vergese. Sub-90 nanometer variability is here to stay. *EDA Tech Forum*, 2(3):26–28, September 2005.

[62] Jonathan Jacky, Margus Veanes, Colin Campbell, and Wolfram Schulte. Model-based software testing and analysis with c#. In *Cmbridge Univeristy Press*, 2007.

[63] R. Jejurikar and R. Gupta. Dynamic slack reclemation with procrastination scheduling in real-time embedded systems. In *Design Automation Conference*, June 2005.

[64] R. Jejurikar, C. Pereira, and R. Gupta. Leakage aware dynamic voltage scaling for real-time embedded systems. In *Design Automation Conference*, June 2004.

[65] D. Kang, S. Crago, and J. Suh. A fast resource synthesis technique for energy-efficient real-time systems. In *IEEE Real-Time Systems Symposium*, December 2002.

[66] Alvin R. Lebeck, Jinson Koppanalil, Tong Li, Jaidev Patwardhan, and Eric Rotenberg. A large, fast instruction window for tolerating cache misses. In *ISCA '02: Proceedings of the 29th annual international symposium on Computer architecture*, pages 59–70, Washington, DC, USA, 2002. IEEE Computer Society.

[67] C. Lee, J. Hahn, Y. Seo, S. Min, R. Ha, S. Hong, C. Park, M. Lee, and C. Kim. Analysis of cache-related preemption delay in fixed-priority preemptive scheduling. In *IEEE Real-Time Systems Symposium*, December 1996.

[68] Cheol-Hoon Lee and Kang G. Shin. On-line dynamic voltage scaling for hard real-time systems using the edf algorithm. In *IEEE Real-Time Embedded Technology and Applications Symposium*, June 2004.

[69] Yann-Hang Lee and C. M. Krishna. Voltage-clock scaling for low energy consumption in fixed-priority real-time systems. *Real-Time Syst.*, 24(3):303–317, 2003.

[70] Joseph Y-T. Leung. A new algorithm for scheduling periodic, real-time tasks. to appear in *Journal of Algorithmica*.

[71] Xianfeng Li, Tulika Mitra, and Abhik Roychoudhary. Accurate timing analysis by modeling caches, speculation and their interaction. In *Proceedings of the Design Automation Conference*, 2003.

[72] Y.-T. S. Li, S. Malik, and A. Wolfe. Efficient microarchitecture modeling and path analysis for real-time software. In *IEEE Real-Time Systems Symposium*, pages 298–397, December 1995.

[73] Y.-T. S. Li, S. Malik, and A. Wolfe. Cache modeling for real-time software: Beyond direct mapped instruction caches. In *IEEE Real-Time Systems Symposium*, pages 254–263, December 1996.

[74] S.-S. Lim, Y. H. Bae, G. T. Jang, B.-D. Rhee, S. L. Min, C. Y. Park, H. Shin, and C. S. Kim. An accurate worst case timing analysis for RISC processors. In *IEEE Real-Time Systems Symposium*, pages 97–108, December 1994.

[75] Björn Lisper. Fully automatic, parametric worst-case execution time analysis. In *WCET*, pages 99–102, 2003.

[76] C. Liu and J. Layland. Scheduling algorithms for multiprogramming in a hard-real-time environment. *J. of the Association for Computing Machinery*, 20(1):46–61, January 1973.

[77] J. Liu. *Real-Time Systems*. Prentice Hall, 2000.

[78] Yanbin Liu and Aloysius K. Mok. An integrated approach for applying dynamic voltage scaling to hard real-time systems. In *Proceedings of the ninth IEEE Real-Time and Embedded Technology and Applications Symposium*, May 2003.

[79] T. Lundqvist and P. Stenström. An integrated path and timing analysis method based on cycle-level symbolic execution. *Real-Time Systems*, 17(2/3):183–208, November 1999.

[80] Thomas Lundqvist and Per Stenström. Timing anomalies in dynamically scheduled microprocessors. In *RTSS '99: Proceedings of the 20th IEEE Real-Time Systems Symposium*, page 12, Washington, DC, USA, 1999. IEEE Computer Society.

[81] Thomas Lunqvist. *A WCET Analysis Method for Pipelined Microprocessors with Cache Memories*. PhD thesis, Chalmers University, 2002.

[82] Sharad Malik, Margaret Martonosi, and Yau-Tsun Steven Li. Static timing analysis of embedded software. In *Proceedings of the 34th Conference on Design Automation (DAC-97)*, pages 147–152, NY, June 1997. ACM Press.

[83] Scott McFarling. Combining Branch Predictors. Technical Report TN-36, June 1993.

[84] S. Mohan, F. Mueller, D. Whalley, and C. Healy. Timing analysis for sensor network nodes of the atmega processor family. In *IEEE Real-Time Embedded Technology and Applications Symposium*, pages 405–414, March 2005.

[85] Sibin Mohan and Johannes Helander. Temporal analysis for adapting concurrent applications to embedded systems. In *Euromicro Conference on Real-Time Systems*, July 2008.

[86] Sibin Mohan and Frank Mueller. Hybrid timing analysis of modern processor pipelines via hardware/software interactions. In *IEEE Real-Time Embedded Technology and Applications Symposium*, April 2008.

[87] Sibin Mohan and Frank Mueller. Merging state and preserving timing anomalies in pipelines of high-end processor. In *IEEE Real-Time Systems Symposium*, (submitted to) 2008.

[88] Sibin Mohan, Frank Mueller, Will Hawkins, Michael Root, David Whalley, and Chris Healy. Parametric timing analysis and its application to dynamic voltage scaling. *ACM Transactions on Embedded Computing Systems (TECS)*, accepted in 2007.

[89] Sibin Mohan, Frank Mueller, William Hawkins, Michael Root, Christopher Healy, and David Whalley. Parascale: Expoliting parametric timing analysis for real-time schedulers and dynamic voltage scaling. In *IEEE Real-Time Systems Symposium*, pages 233–242, December 2005.

[90] D. Mosse, H. Aydin, B. Childers, and R. Melhem. Compiler-assisted dynamic power-aware scheduling for real-time applications. In *Workshop on Compilers and Operating Systems for Low Power*, October 2000.

[91] L. Motus, R. Kinksaar, T. Naks, and M. Pall. Enhancing object modelling technique with timing analysis capabilities. *iceccs*, 00:298, 1995.

[92] Leo Motus and Michael G. Rodd. *Timing Analysis of Real-Time Software: A Practical Approach to the Specification and Design of Real-Time*. Elsevier Science Inc., New York, NY, USA, 1994.

[93] T. Mowry and C.-K. Luk. Predicting data cache misses in non-numeric applications through correlation profiling. In *MICRO-30*, pages 314–320, December 1997.

[94] F. Mueller. Timing analysis for instruction caches. *Real-Time Systems*, 18(2/3):209–239, May 2000.

[95] Lev Nachmanson, George Robertson, and Bongshin Lee. Drawing graphs with GLEE. In *15th International Symposium on Graph Drawing*, September 2007.

[96] Subbarao Palacharla, Norman P. Jouppi, and James E. Smith. Complexity-effective superscalar processors. In *ISCA*, pages 206–218, 1997.

[97] C. Y. Park. Predicting program execution times by analyzing static and dynamic program paths. *Real-Time Systems*, 5(1):31–61, March 1993.

[98] T. Pering, T. Burd, and R. Brodersen. The simulation of dynamic voltage scaling algorithms. In *Symp. on Low Power Electronics*, 1995.

[99] Stefan Petters. *Worst Case Execution Time Estimation for Advanced Processor Architectures*. Technical University Munich Disserations, Technical University Munich, Germany, 2002.

[100] P. Pillai and K. Shin. Real-time dynamic voltage scaling for low-power embedded operating systems. In *Symposium on Operating Systems Principles*, 2001.

[101] H. Pohlheim, J. Wegener, and H. Sthamer. Testing the temporal behavior of real-time engine control software modules using extended evolutionary algorithms. 2000.

[102] Jurgo Preden and Johannes Helander. Auto-adapation driven by observed context histories. In *International Workshop on Exploiting Context Histories in Smart Environments*, September 2006.

[103] P. Puschner and C. Koza. Calculating the maximum execution time of real-time programs. *Real-Time Systems*, 1(2):159–176, September 1989.

[104] H. Ramaprasad and F. Mueller. Bounding preemption delay within data cache reference patterns for real-time tasks. In *IEEE Real-Time Embedded Technology and Applications Symposium*, pages 71–80, April 2006.

[105] H. Ramaprasad and F. Mueller. Tightening the bounds on feasible preemption points. In *IEEE Real-Time Systems Symposium*, pages 212–222, December 2006.

[106] Jan Reineke, Björn Wachter, Stephan Thesing, Reinhard Wilhelm, Ilia Polian, Jochen Eisinger, and Bernd Becker. A Definition and Classification of Timing Anomalies. In *Proceedings of 6th International Workshop on Worst-Case Execution Time (WCET) Analysis*, July 2006.

[107] Saowanee Saewong and Ragunathan Rajkumar. Practical voltage-scaling for fixed-priority rt-systems. In *Proceedings of the ninth IEEE Real-Time and Embedded Technology and Applications Symposium*, May 2003.

[108] J. Schneider. Cache and pipeline sensitive fixed priority scheduling for preemptive real-time systems. In *IEEE Real-Time Systems Symposium*, pages 195–204, December 2000.

[109] Joern Schneider. *Combined Schedulability and WCET Analysis for Real-Time Operating Systems*. PhD thesis, Universitaet des Saarlandes, 2002.

[110] K. Seth, A. Anantaraman, F. Mueller, and E. Rotenberg. Fast: Frequency-aware static timing analysis. In *IEEE Real-Time Systems Symposium*, pages 40–51, December 2003.

[111] D. Shin, J. Kim, and S. Lee. Intra-task voltage scheduling for low-energy hard real-time applications. In *IEEE Design and Test of Computers*, March 2001.

[112] Y. Shin, K. Choi, and T. Sakurai. Power optimization of real-time embedded systems on variable speed processors. In *Int'l Conf. on Computer-Aided Design*, 2000.

[113] Smith, J. E. A study of branch prediction strategies. In *Proc.* 8th *International Symposium on Computer Architecture*, pages 135–148, Minneapolis, 1981.

[114] Brinkley Sprunt. Pentium 4 performance monitoring features. 2002.

[115] Jan Staschulat and Rolf Ernst. Multiple process execution in cache related preemption delay analysis. In *International Conference on Embedded Sofware*, 2004.

[116] Jan Staschulat, Simon Schliecker, and Rolf Ernst. Scheduling analysis of real-time systems with precise modeling of cache related preemption delay. In *Euromicro Conference on Real-Time Systems*, 2005.

[117] H. Theiling and C. Ferdinand. Combining abstract interpretation and ilp for microarchitecture modelling and program path analysis. In *IEEE Real-Time Systems Symposium*, pages 144–153, December 1998.

[118] S. Thesing. *Safe and Precise WCET Determination by Abstract Interpretation of Pipeline Models*. PhD thesis, Saarland University, November 2004.

[119] S. Thesing, J. Souyris, R. Heckmann, F. Randimbivololona, M. Langenbach, R. Wilhelm, and C. Ferdinand. An Abstract Interpretation-Based Timing Validation of Hard Real-Time Avionics. In *Proceedings of the International Performance and Dependability Symposium (IPDS)*, June 2003.

[120] Jim Turley. Embedded processors by the numbers, 1999.

[121] S. Unger and F. Mueller. Handling irreducible loops: Optimized node splitting vs. dj-graphs. *ACM Transactions on Programming Languages and Systems*, 24(4):299–333, July 2002.

[122] G. D. Veciana, M. Jacome, and J.-H. Guo. Assessing probabilistic timing constraints on system performance. *Design Automation for Embedded Systems*, 5(1):61–81, 2000.

[123] X. Vera, B. Lisper, and J. Xue. Data caches in multitasking hard real-time systems. In *IEEE Real-Time Systems Symposium*, December 2003.

[124] E. Vivancos, C. Healy, F. Mueller, and D. Whalley. Parametric timing analysis. In *ACM SIGPLAN Workshop on Language, Compiler, and Tool Support for Embedded Systems*, volume 36 of *ACM SIGPLAN Notices*, pages 88–93, August 2001.

[125] J. Wegener. Verifying timing constraints of real-time systems by means of evolutionary testing. *Real-Time Systems*, 15:275–298(24), 1998.

[126] J. Wegener and F. Mueller. A comparison of static analysis and evolutionary testing for the verification of timing constraints. *Real-Time Systems*, 21(3):241–268, November 2001.

[127] J. Wegener, H. Sthamer, B. F. Jones, and D. E. Eyres. Testing real-time systems using genetic algorithms. *Software Quality Journal*, 6(2):127–135, June 1997.

[128] Joachim Wegener, Kerstin Buhr, and Hartmut Pohlheim. Automatic test data generation for structural testing of embedded software systems by evolutionary testing. In *GECCO ’02: Proceedings of the Genetic and Evolutionary Computation Conference*, pages 1233–1240, San Francisco, CA, USA, 2002. Morgan Kaufmann Publishers Inc.

[129] M. Weiser, B. Welch, A. Demers, and S. Shenker. Scheduling for reduced cpu energy. In *1st Symp. on Operating Systems Design and Implementation*, Nov 1994.

[130] Ingomar Wenzel, Raimund Kirner, Peter Puschner, and Bernhard Rieder. Principles of timing anomalies in superscalar processors. In *QSIC ’05: Proceedings of the Fifth International Conference on Quality Software*, pages 295–306, Washington, DC, USA, 2005. IEEE Computer Society.

[131] R. White. *Bounding Worst-Case Data Cache Performance*. PhD thesis, Dept. of Computer Science, Florida State University, April 1997.

[132] R. White, F. Mueller, C. Healy, D. Whalley, and M. Harmon. Timing analysis for data caches and set-associative caches. In *IEEE Real-Time Embedded Technology and Applications Symposium*, pages 192–202, June 1997.

[133] R. T. White, F. Mueller, C. Healy, D. Whalley, and M. G. Harmon. Timing analysis for data and wrap-around fill caches. *Real-Time Systems*, 17(2/3):209–233, November 1999.

[134] J. Whitham. *Real-time Processor Architectures for Worst Case Execution Time Reduction*. PhD thesis, University of York, May 2008.

[135] Wikipedia. Anti-lock Braking System (ABS), 2008.

[136] R. Wilhelm, J. Engblohm, A. Ermedahl, N. Holsti, S. Thesing, D. Whalley, G. Bernat, C. Ferdinand, R. Heckmann, T. Mitra, F. Mueller, I. Puaut, P. Puschner, J. Staschulat, and P. Stenstrom. The worst-case execution time problem — overview of methods and survey of tools. *ACM Transactions on Embedded Computing Systems*, page (accepted), January 2007.

[137] Fan Zhang and Samuel T. Chanson. Processor voltage scheduling for real-time tasks with non-preemptable sections. In *IEEE Real-Time Systems Symposium*, December 2002.

[138] Xiliang Zhong and Cheng-Zhong Xu. Energy-aware modeling and scheduling of real-time tasks for dynamic voltage scaling. In *IEEE Real-Time Systems Symposium*, December 2005.

[139] N. Zhu, J. Chen, and T.-C. Chiueh. TBBT: Scalable and accurate trace replay for file server evaluation. In *USENIX Conference on File and Storage Technologies*, pages 323–336, December 2005.

[140] Y. Zhu and F. Mueller. Feedback edf scheduling exploiting dynamic voltage scaling. In *IEEE Real-Time Embedded Technology and Applications Symposium*, pages 84–93, May 2004.